UM-HSRI-78-31

Final Report

THE STATE OF KNOWLEDGE RELATING TIRE DESIGN TO THOSE TRACTION PROPERTIES WHICH MAY INFLUENCE VEHICLE SAFETY

P. O. No. 6640

Robert D. Ervin

Highway Safety Research Institute
The University of Michigan

Prepared for:

Bolt, Beranek and Newman, Inc.

July, 1978

Technical Report Documentation Page

1. Report No.	2. Government Accession No.	3. Recipient's Catalog No.
UM-HSRI-78-31		

4. Title and Subtitle	5. Report Date
STATE OF KNOWLEDGE RELATING TIRE DESIGN TO THOSE TRACTION PROPERTIES WHICH MAY INFLUENCE VEHICLE SAFETY.	July 1978
	6. Performing Organization Code
7. Author(s) R. D. Ervin	8. Performing Organization Report No. UM-HSRI-78-31
9. Performing Organization Name and Address Highway Safety Research Institute The University of Michigan Ann Arbor, Michigan 48109	10. Work Unit No.
	11. Contract or Grant No. P.O. 6640-1
12. Sponsoring Agency Name and Address Bolt, Beranek, and Newman, Inc. 50 Moulton Street Cambridge, Massachusetts	13. Type of Report and Period Covered Final 10/77 - 6/78
	14. Sponsoring Agency Code

15. Supplementary Notes

16. Abstract

The various mechanical properties of pneumatic tires are reviewed in light of the influence of tires on vehicle maneuvering behavior.

The report serves as a primer in the phenomenology of tire force and moment production—providing a broad overview of existing tire measurements and interpreting tire behavior in terms of elementary vehicle dynamics considerations.

Example data are presented illustrating the basic responses of the tire to braking and cornering slip and the sensitivities of those responses to operating and design variables. The state of knowledge is summarized covering the conditions of braking, cornering, combined slip, and mobility on soil or snow. Sensitivities of tire performance to inflation pressure, load, velocity, surface texture, water depth, carcass design, tread design, and tread rubber compounding are discussed.

17. Key Words	18. Distribution Statement
tire mechanics, vehicle maneuvering, traffic safety, braking, cornering, combined slip, mobility	UNLIMITED

19. Security Classif. (of this report)	20. Security Classif. (of this page)	21. No. of Pages	22. Price
NONE	NONE	128	

TABLE OF CONTENTS

INTRODUCTION

This report is intended as a general discussion of the state of knowledge which may connect tire design to vehicle safety. It is primarily intended as a primer in tire mechanics, identifying the various mechanisms by which tires generate steering and braking forces and the sensitivities which those mechanisms have to design and operating variables. It is pertinent, then, before considering tire properties per se to reflect on the manner in which a connection might be made between tires and vehicle pre-crash safety.

Motor vehicle safety, or conversely, the occurrence of motor vehicle traffic accidents, is known to depend upon the interaction of a broad set of factors. These have been broken down in various investigations of vehicle safety into the factors constituting a complete description of the traffic system itself. Such diverse elements as roadway geometry, surface condition, road system signing, climatic variables, driver physiology, psychology, and driving history, vehicle braking and handling properties, and various mechanisms by which these properties interact with one another are believed to be all relevant to accident potential. The linking of any single factor to the accident record is, of course, a difficult exercise since the interaction mechanisms are so strong and since the factors of potential importance are so numerous.

Nevertheless, many researchers have studied the correlations between individual factors describing the highway, driver, vehicle, traffic environment and accident occurrence. Regarding the specific area of the relationship between vehicle dynamic performance and accident involvement, certain studies have been made to establish the extent of correlations which may be hypothesized as evidencing causal relationships. To a much larger degree, however, research which is intended to examine the vehicle's role in pre-crash safety is simply based upon notions of suspected relationships, such as the following:

1) High levels of braking capability should render a vehicle more capable of avoiding collisions or of minimizing the velocity prevailing upon impact.

2) High levels of cornering or lateral acceleration performance should render a vehicle more capable of obstacle avoidance.

3) The retention of yaw stability up to the cornering limits imposed by the saturation of tire shear forces should render the vehicle more likely to be successfully controlled throughout any obstacle avoidance maneuver.

Such hypotheses have underpinned most studies which have sought to expand vehicle dynamics technology in a direction benefiting vehicle safety. Thus it is largely on the basis of the link provided by intuitive hypothesis that we can presume to examine the state of knowledge relating tire design characteristics to vehicle safety. That is, we have a safety interest in tire design (putting aside structural integrity issues such as puncture and blowout resistance) only insofar as the design of a tire determines its traction qualities which, in turn, influence the braking and steering properties of the vehicle which, in turn, influence the accident avoidance potential of the driver/vehicle/highway system. Insofar as improper inflation pressures, improper application of a given tire size or type, excessive tread wear, or excessive tire loading may compromise the as-designed traction quality of a tire, the relationship between tire design and vehicle safety will be obscured. Insofar as other non-tire-related properties inherent to the vehicle tend to reduce accident avoidance potential (such as the low rollover immunity of certain heavy trucks), the safety importance of the tire's design characteristics is reduced. Nevertheless, there seems ample reason to believe that the relationship of tire design to traction properties and thence to vehicle dynamic behavior constitutes, to a significant degree, a connection between tire design and vehicle safety.

The discussion in this report is broken down into sections addressing different aspects of tire performance, as follows:

1) Braking properties

2) Cornering properties

3) Combined braking and cornering properties

4) Mobility (deformable surfaces) properties

Of these four areas, only the first three are seriously suggested to affect the safety quality of vehicles. Mobility properties are primarily seen as determining a vehicle's ability to "go" in snow or mud—the failure of which is not characteristically accident-producing.

The level of treatment of each subject is that of an overview. Readers interested in particular aspects of tire mechanics are advised to seek the referenced sources for detailed treatments of the various subjects. The discussion is not meant to represent a comprehensive review of the available literature on each subject area, but rather provides a condensed view of tire mechanics as is necessary to understand vehicle maneuvering behavior. The discussion is phenomenological rather than analytical in nature. It addresses the question "What does the tire do and what is its performance sensitive to?" At the conclusion of each of the first three discussion sections on tire properties, the general influence of the respective tire characteristics on vehicle maneuvering performance is discussed.

By way of introducing the discussion on tire mechanics, it is convenient here to reference the SAE tire axis system shown below in Figure 1.1 [1]. This diagram establishes the conventions for locating the wheel plane and the ground plane, and for orienting the three tire forces and three moments.

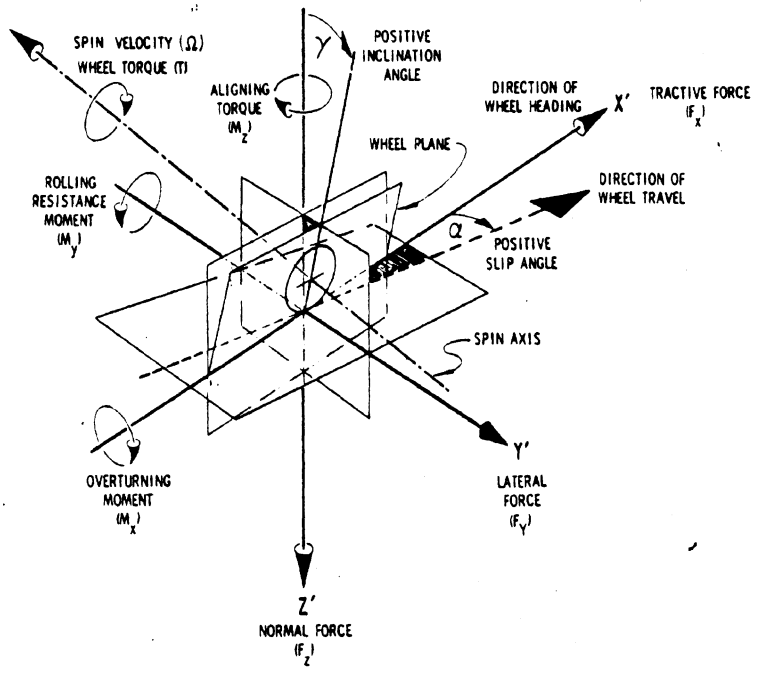

Figure 1.1 SAE Tire Axis System

1.0 BRAKING PROPERTIES

The tires on a motor vehicle are mounted such that their plane of rotation is nominally aligned with the direction of motion of the vehicle. Thus, when brakes are applied, the wheel is caused to slow down below its free-running speed and a "slip" condition is produced between the tire and road, resulting in a braking force which acts to decelerate the vehicle. The role played by the tire in this process can be examined by reducing the generation of the braking force into two stages. In the first stage, the application of brake torque causes the tire to produce an increasing level of longitudinal shear force or "brake" force, F_x, as wheel speed, ω, drops off. The rate at which this force is produced, per unit of wheel slip, s, is defined as the longitudinal stiffness, C_s, viz.,

$$C_s = \left.\frac{\partial F_x}{\partial s}\right|_{s=0}$$

where

F_x = braking force

s = longitudinal slip, defined by the relation

$$s = (1 - \frac{R_e\omega}{V} \times 100\%$$

with R_e = effective rolling radius

ω = wheel angular velocity

and V = vehicle velocity

Thus, C_s is merely the initial slope in the brake force response to slip.

Under typical braking conditions, the tire will become limited in brake force capability at a rather low level of slip, in the vicinity of 20%. Thus, while the tire is still rolling at approximately

80% of its free-rolling speed, brake force will arrive at a peak value and then characteristically decline as wheel speed reduces toward the "lockup" condition, at 100% slip. Accordingly, we shall also discuss this second stage in which braking force is limited by the prevailing frictional coupling, thereby determining the peak longitudinal traction coefficient, μ_p, and the locked wheel, or slide traction coefficient, μ_s, viz.,

$$\mu_p = \left.\frac{F_x}{F_z}\right|_{peak}$$

and

$$\mu_s = \left.\frac{F_x}{F_z}\right|_{slide}$$

where F_z = vertical load.

It is convenient to consider these traction limits as a fraction of the vertical load on the tire because load is the primary tire operating variable determining the magnitude of the F_x response. We see, however, that the simple "coulomb" relationship of elementary physics, by which "friction coefficient," μ, has one value for all load levels, does not apply to the pneumatic tire. Indeed, the tire is comprised of both viscous and elastic type materials which together produce a complex nonlinear relationship between limit shear forces and vertical load.

In the two structured discussions which follow, concerning longitudinal stiffness, C_s, and longitudinal traction limits, μ_p and μ_s, a set of eight performance sensitivities will be cited, as follows:

Sensitivity to:

1. inflation pressure
2. vertical load
3. velocity
4. surface texture
5. water depth
6. carcass design
7. tread design
8. tread rubber compounding

The section on each tire property is concluded with a statement on the relevance of each property to vehicle maneuvering behavior.

1.1 Longitudinal Stiffness, C_S.

The tire can be considered as a type of spring element in its initial development of braking, or longitudinal, force. This "spring rate" function of a tire depends primarily upon the length of the footprint of the tire's contact with the road. As contact length increases, each tread element must spend a longer time interval in contact with the pavement during each revolution, thereby accumulating a larger net rearward deflection due to the slip condition, and generating an accordingly greater braking force.

1.1.1 Sensitivity to Inflation Pressure.

Two opposing mechanisms accompany inflation pressure changes—one tending to increase C_S, the other tending to decrease C_S. As inflation pressure increases, the contact length reduces, thus tending to reduce the longitudinal stiffness. Also, however, as inflation pressure increases, tire cords become more heavily preloaded and the overall carcass stiffens, thus tending to increase C_S. Thus, the net sensitivity of C_S to inflation pressure for any specific tire will be determined by the design characteristics influencing the relative strength of these two mechanisms.

1.1.2 Sensitivity to Vertical Load. Longitudinal stiffness categorically increases with increasing load over the normal range of loading. This result, of course, derives from the simple fact that adding load always increases contact length. The function is clearly a nonlinear one, however, since the rate of change in contact length with increasing load diminishes at higher levels of load. Thus, for example, we see a curvature in the C_s versus load function, as in Figure 1.2 [2].

Another way to view the influence of load on C_s is in the data of Figure 1.3 [3]. Here we see that the initial slope (i.e., C_s) of the F_x versus slip curve rises with increased load, but, on the other hand, the peak force limits rise also. Since the peak force values all occur at approximately the same value of slip, we see that longitudinal stiffness basically changes to establish consistent curve shape.

1.1.3 Sensitivity to Velocity. Since C_s is a property of the elastic makeup of the tire, it is known to be virtually insensitive to velocity.

1.1.4 Sensitivity to Surface Texture. Again, as an elastic characteristic, C_s is basically insensitive to either the textural or adhesive properties of the surface. Since the "spring constant" character of the C_s numeric applies to the operating regime in which no tread elements are slipping in the contact patch, the friction coupling level which prevails is immaterial.

1.1.5 Sensitivity to Water Depth. As water depth becomes large, say above .050 inches, and when vehicle velocity is high, above 50 mph, a certain degree of hydroplaning will prevail, tending to shorten the effective length of the contact patch. Since the hydroplaning phenomenon can be looked upon as a "penetration" from the leading edge of the contact patch by a water "wedge," the observed value of C_s will reduce under this condition. At small levels of water depth in which hydroplaning is negligible, C_s will be uninfluenced by the presence of water.

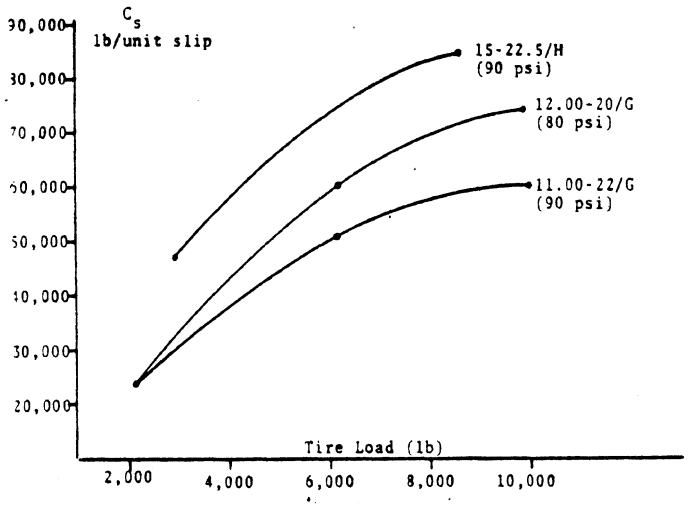

Figure 1.2 C_s vs F_z, for Truck Tires

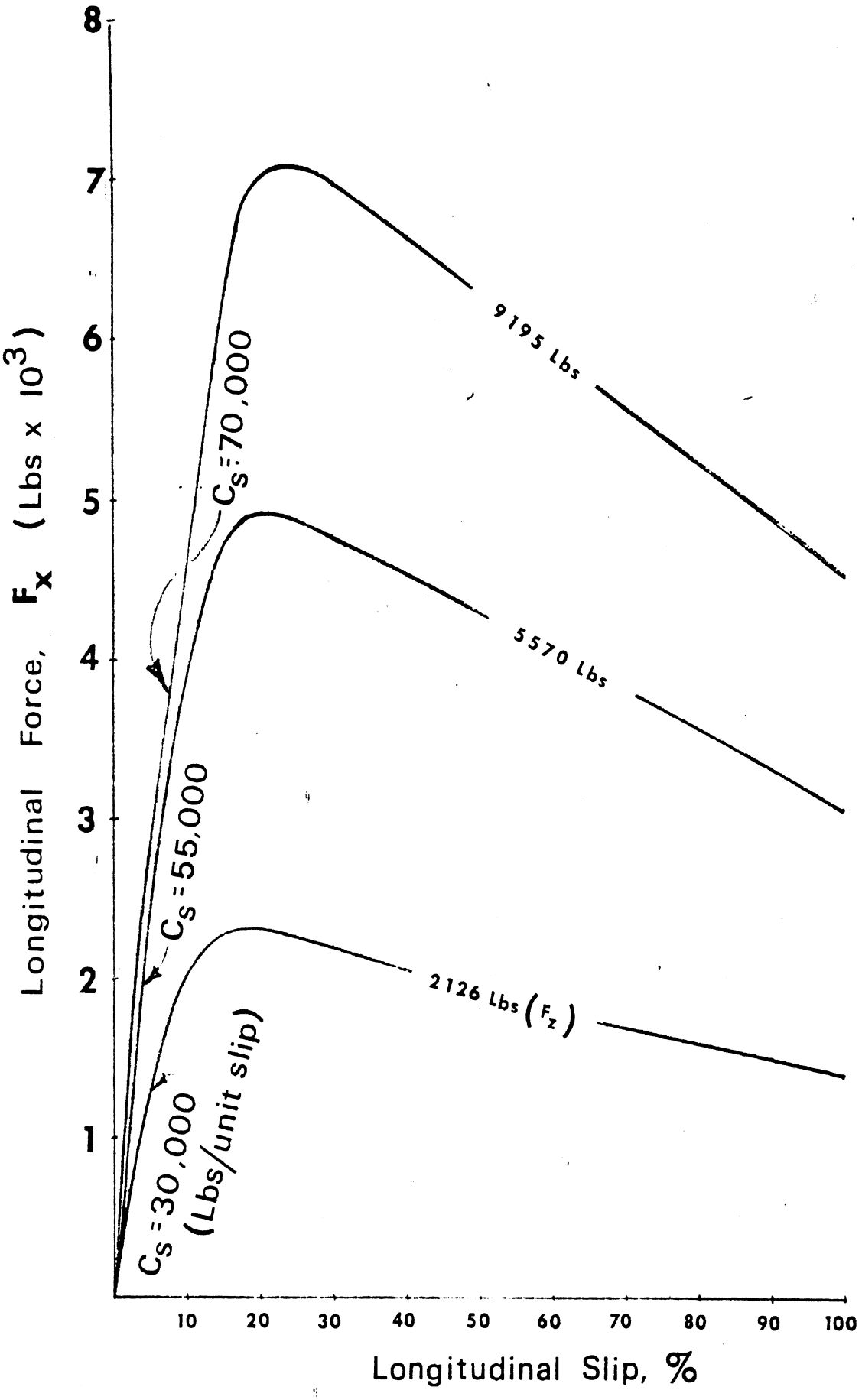

Figure 1.3 Influence of vertical load on the non-normalized (F_x) versus slip behavior of a Firestone 10.00x20/F on an asphalt surface."

1.1.6 Sensitivity to Carcass Design. Longitudinal stiffness is influenced by carcass design in two ways: Firstly, by the manner in which the carcass determines contact patch length, for a given load, and secondly, by the resulting circumferential stiffness of the carcass structure, itself. Shown in Figure 1.4 is a plot, not of C_s, but of the longitudinal force produced on a laboratory test machine as a function of longitudinal displacement of the tread, using a locked wheel [4]. It is seen that the bias-ply tire yields a higher level of circumferential stiffness than does a radial-ply tire. This result is simply explained by the influence of cord orientation on this structural deflection mode. Figure 1.4 also directly illustrates the advantage which the radial construction offers in isolating the vehicle from longitudinal disturbances arising from road irregularities. Combining the effects of circumferential stiffness and contact length in rolling experiments using heavy truck tires, Figure 1.5 shows a numeric closely proportional to C_s for a sample of bus and truck tires which differ in both tread and carcass type [5]. It is seen that radial constructions register substantially higher than the bias samples in this measure. Further, rib-type tread designs indicate higher values of longitudinal stiffness than do lug-type treads.

1.1.7 Sensitivity to Tread Design. Since the tread of a tire can be looked upon as an array of cantilever springs connecting the carcass and belt structures to the roadway, tread design influences the value of C_s in a fashion directly related to the effective "cantilever stiffness" of the tread elements. Thus, circumferential rib-type patterns are known to produce higher levels of C_s (for the same carcass construction), while discrete block patterns, such as with snow tires, are known to indicate lower levels of C_s. Further, as a tire tread wears, reducing the effective length of the tread element "cantilevers," C_s will rise markedly.

1.1.8 Tread Compound Variations. Tread compound is presumed to affect longitudinal stiffness simply as a reflection of the nominal durometer, or elastic modulus of the tread rubber. Shown in

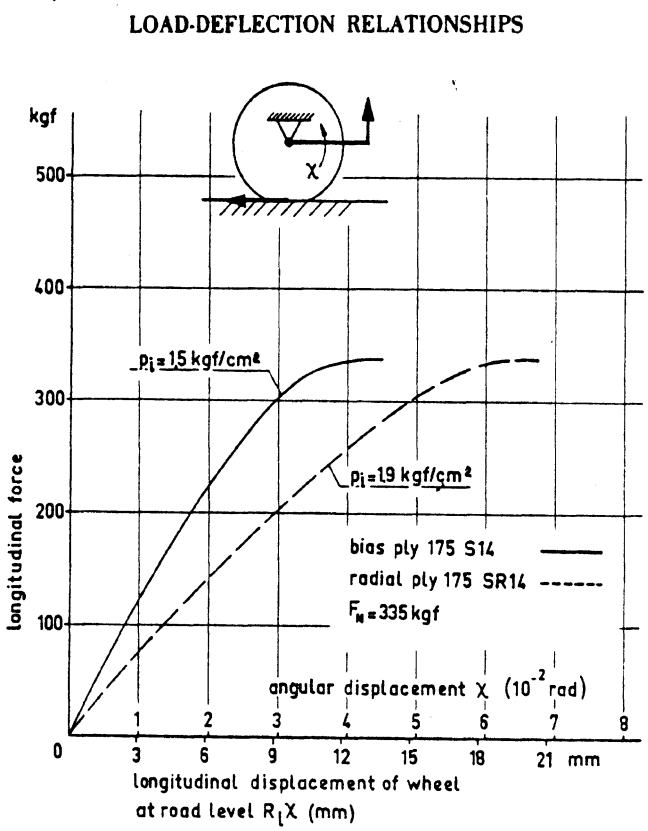

Figure 1.4 *The tangential stiffness of the radial ply tire is much lower than the bias ply tire.*

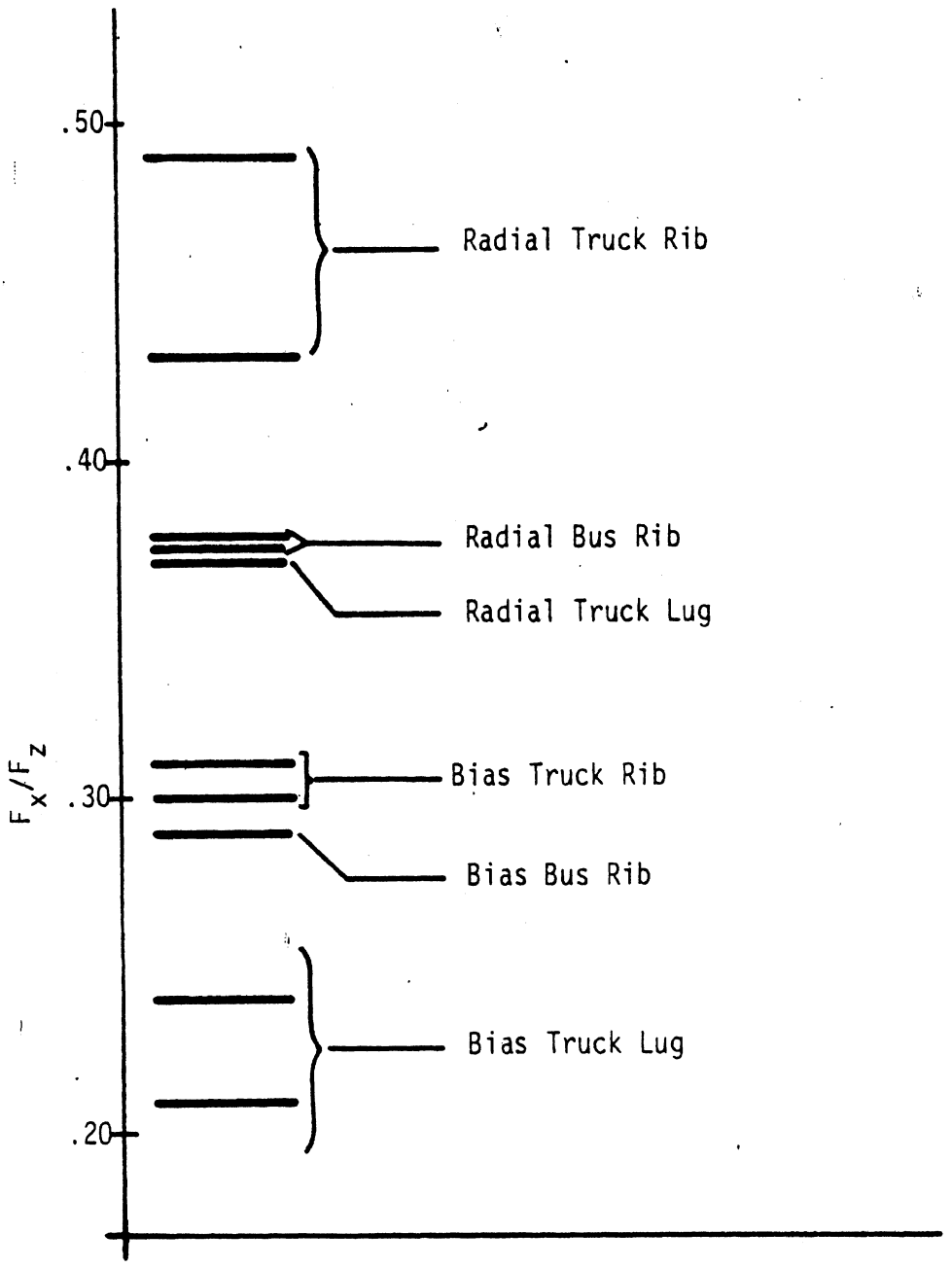

Figure 1.5 Distribution of F_x/F_z values measured at 4% slip, indicating relative longitudinal stiffnesses of various generic types of heavy tires, each tested at rated load.

Figure 1.6 is the relationship between μ_p and the value of slip at which the peak occurs, for each of the two tread compound formulas [6]. Taking the "slip at μ_p" numeric as roughly proportional to C_s, we see an approximate 2 to 1 difference between the levels attained with a high styrene, styrene butadiene copolymer (SBR) and the blended SBR copolymer with polybutadiene (BR).

1.1.9 Relevance of C_s to Maneuvering Behavior of Vehicles. Longitudinal stiffness is a property of negligible significance to vehicle maneuvering behavior, except, perhaps, insofar as it interacts with the cycling efficiency of antilock control systems. One other circumstance indirectly relating to the level of C_s regards braking in a turn. In this case, since longitudinal slip rapidly reduces tire side force capability (as will be discussed in Section 3), the tire with a higher value of C_s will be beneficial. The benefit derives from the fact that higher levels of braking force can be attained with the high-C_s tire at lower levels of longitudinal slip. Thus, a given braking application in a turn will produce less of a lateral disturbance to the vehicle outfitted with the higher C_s tire, all other things being equal. This interactive aspect of the C_s property is presumed to be of low overall significance to traffic safety, however.

1.2 Peak and Slide Braking Traction Limits

Perhaps the most safety-relevant characteristic of a pneumatic tire is its ability to maximize longitudinal traction limits over the range of surface conditions which are encountered. Both peak and slide limits of braking traction will be discussed here, since both have similar sensitivities to operational and design variables.

1.2.1 Sensitivity to Inflation Pressure. Longitudinal traction limits are influenced by inflation pressure in different degrees on dry and wet surfaces. Three changes in the operating state of the tire serve to explain sensitivities to inflation pressure.

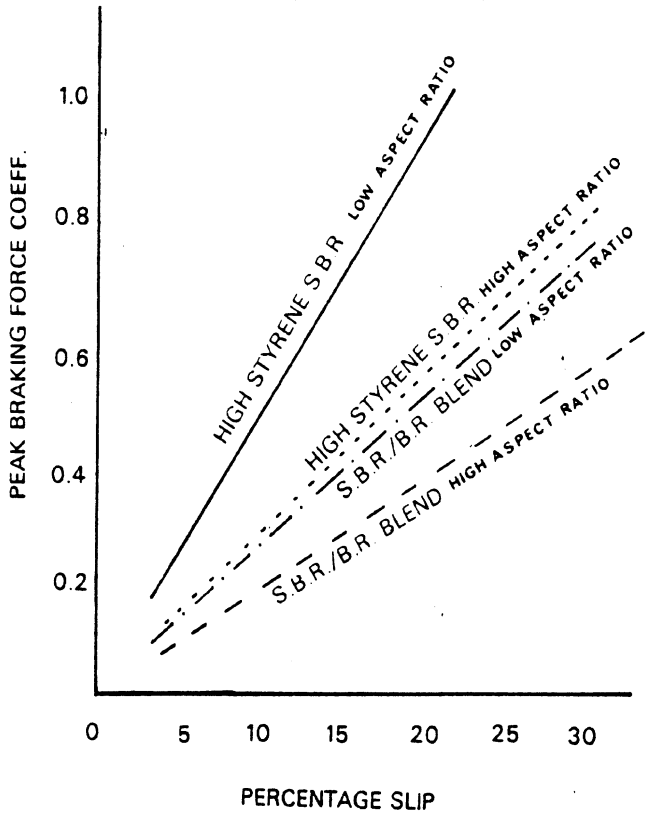

Figure 1.6 The influence of longitudinal stiffness, tread compound, and speed on percentage slip at peak braking force.

Firstly, the increased inflation pressure will cause an increase in the tread/road contact pressure—predominantly increasing the contact stress at the inner rib positions across the tread face. Secondly, the contact length of the tire decreases with increasing inflation pressure. Thirdly, the lateral "shrinkage" of the tread face, producing closure of the tread grooves on low friction, wetted surfaces, will decrease as inflation pressure increases.. This decreased shrinkage is a result of changes in the structural properties of the tire as they determine tread stresses during the rolling process.

For the case of braking on dry pavements, inflation pressure increases are seen to result in mild improvements in both μ_p and μ_s traction levels. For example, Table 1.1 illustrates traction level changes which result from a threefold increase in inflation pressure [7].

For wet surfaces, inflation pressure increases are known to significantly improve μ_p and μ_s limits. Expressed in terms of hydroplaning speeds (that is, the vehicle velocity at which tires will become dynamically separated from road contact by a water film), it is reported that a three psi increase in inflation will add on the order of one mph to the hydroplaning speed of bias-ply tires [9]. Tire traction under the complex phenomenon of hydroplaning is seen to benefit from increased inflation pressure because of the reduced lateral shrinkage of the tread, thereby lessening the closure of the tread grooves which are the primary water drainage paths.

1.2.2 Sensitivity to Vertical Load. Increasing vertical load is known to categorically reduce normalized traction levels under all types of dry and wetted pavement conditions. As examples of this interaction on dry surfaces, it is typical with both passenger car and truck tires to see on the order of .01 reduction in μ_p or μ_s with each 10% increase in load, in the vicinity of the tire's rated load. Representative of these sensitivities are the data shown in Figure 1.7 [8].

Table 1.1 Peak and Slide Friction Coefficient (μ_p and μ_s) for the Firestone Deluxe Champion Sup-R-Belt H78-14, Dry Asphalt.

Inflation Pressure (psi)	Speed (mph)	Load (lbs) 800 μ_p	800 μ_s	1100 μ_p	1100 μ_s
12	40	.9	.88	.87	.76
	20			.83	.78
20	40	.92	.85	.90	.80
	20			.92	.79
28	40	.92	.85	.96	.79
	20			.92	.79
36	40	.97	.80	.92	.80
	20			.95	.79

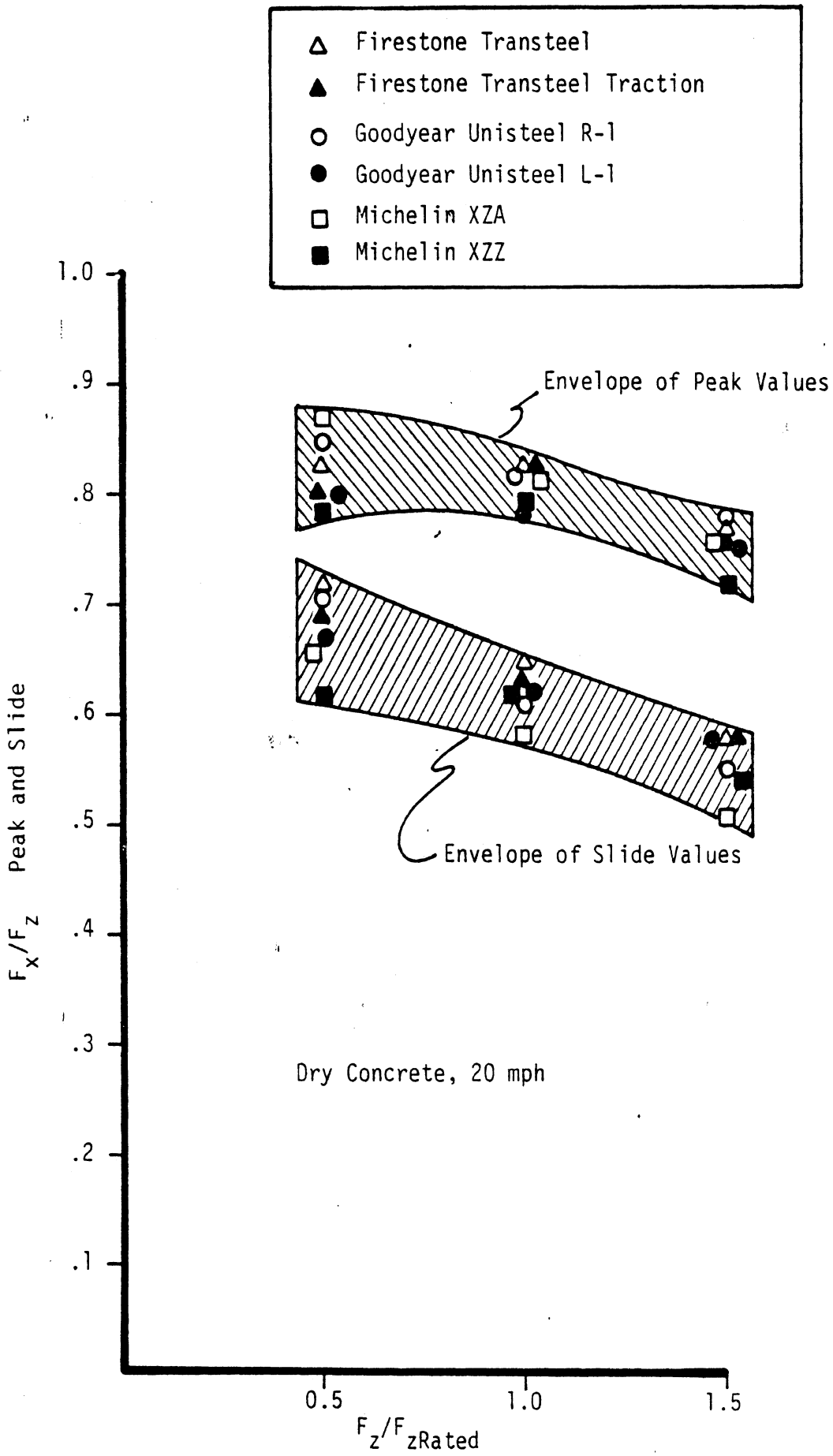

Figure 1.7 Peak and slide values versus load for radial Truck tires at 20 mph.

On wetted surfaces load is known to generally reduce limit traction capability, although with a less strong influence than is seen on dry surfaces. In the operating conditions in which hydroplaning is a problem, the influence of load on traction limits is reported to be a negligible improvement [9].

1.2.3 Sensitivity to Velocity. Beyond some very low creeping speed, it is generally established that increasing speed results in reduced levels of μ_p and μ_s. On dry surfaces, peak traction coefficient of car tires is somewhat sensitive to speed, as shown in the example data of Figure 1.8 [10]. Similarly, truck tires have been seen to exhibit only a small sensitivity of μ_p level to velocity, typically illustrating a -.002/mph gradient in μ_p [3].

Figure 1.8 also shows the influence of velocity on μ_s for heavy truck tires. In this case, it is typical to observe steep gradients (on the order of -.01 μ_s/mph) in the lower speed range and virtually no gradient in μ_s in the vicinity of highway speeds.

On wetted surfaces, of course, we know that hydrodynamic phenomena act to render velocity the crucial variable in determining traction limits. By one empirical formula, the minimum hydroplaning speed, given sufficient water depth, is related directly to the inflation pressure by the relationship, $V = 10\sqrt{p}$, where V is speed of total hydroplaning (mph), and p is inflation pressure. Of course, the actual speed of hydroplaning is modified very strongly by tire tread design.

For tires running at highway speeds and commonly-encountered water depths (in the vicinity of .020 inches), speed sensitivities in the peak and slide traction levels would typically fall in the ranges cited in Table 1.2 [11].

A range of velocity sensitivity data for truck tires on wet surfaces is shown in Figure 1.9, presenting both peak and slide sensitivities as contrasted against typical European passenger car tires [12]. It is seen that the steeper velocity sensitivities of the μ_p and μ_s values of truck tires is confined to lower speeds, below 40 mph.

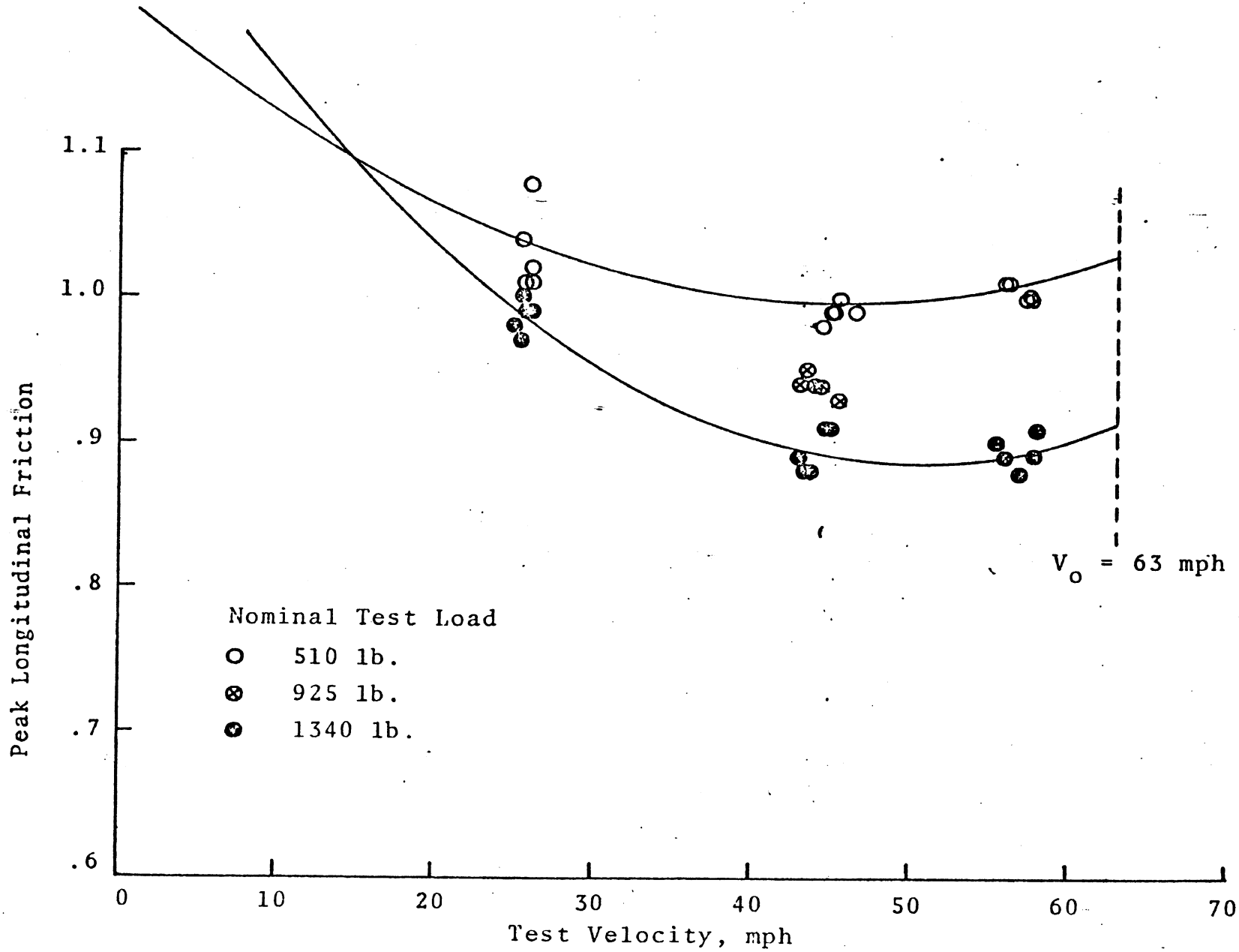

Figure 1.8 Reference tire data: Dry asphalt surface.

Table 1.2. Typical Velocity Sensitivity of Car Tires on Common Wet, Fine Texture Surface.

	μ_p/mph	μ_s/mph
Bias Ply	.04	.02
Bias Belted	.008	.012
Steel Belted Radial	less than .005	.010

1.2.4 Sensitivity to Surface Texture or Friction Potential. For tire properties which are fundamentally frictional in nature, the makeup of the pavement is, of course, an elementary determinant of the performance level. Accordingly, a broad area of the technology of pavement construction and maintenance has been built up around the interest in the frictional potential of road surfaces. Paved road surfaces commonly found around the U.S. could be expected to yield μ_p values for passenger car tires ranging from, perhaps, as low as 0.3 for wet, "bleeding" asphalt, to as high as 1.1 for dry asphalt having an aggressive texture. The low-end estimate, of course, is in the absence of hydroplaning.

Regarding texture, per se, it is generally accepted that coarse texture surfaces are preferable for enhancing the drainage of water from under the tire tread at high speed. Such coarseness, pertaining to the size of the aggregate used in the paving material, refers to the so-called "macrotexture" property. This characteristic is distinguished from a finer texture characterization, microtexture, which refers to the irregularity and sharpness of the surface on individual particles of aggregate. Shown in Figure 1.10, these features are crudely defined and their respective wet traction potentials are generalized by the μ_s versus speed relationship of a standard car tire [13]. As examples of both μ_p and μ_s performance on surfaces of grossly differing texture, Figures 1.11 and 1.12 show representative traction limits versus velocity for radial- and bias-ply tires on two surfaces [14]. In Figure 1.11, the surface is of the "fine, gritty" variety

Figure 1.9 Comparison of wet skid resistance of truck and car tires.

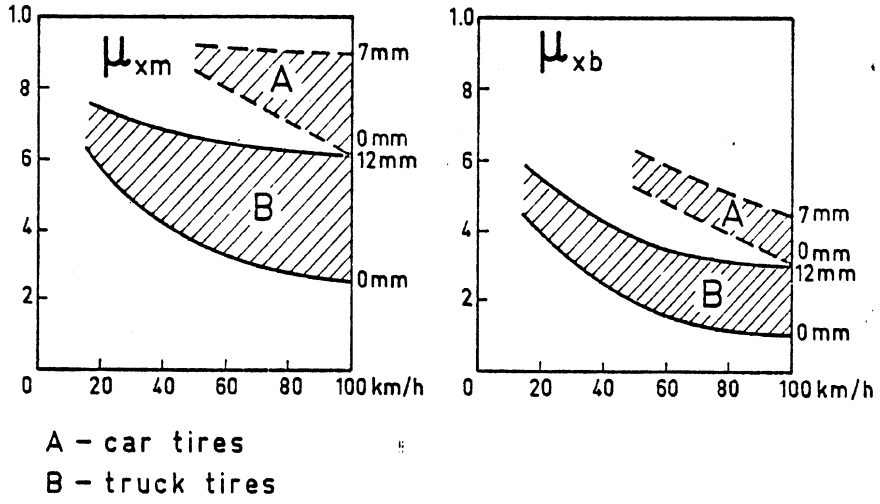

Figure 1.10 Classification of pavement surfaces according to their wet friction and drainage properties.

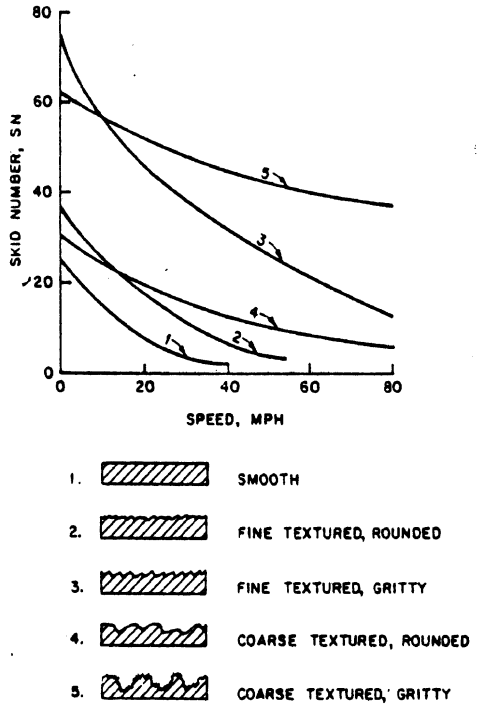

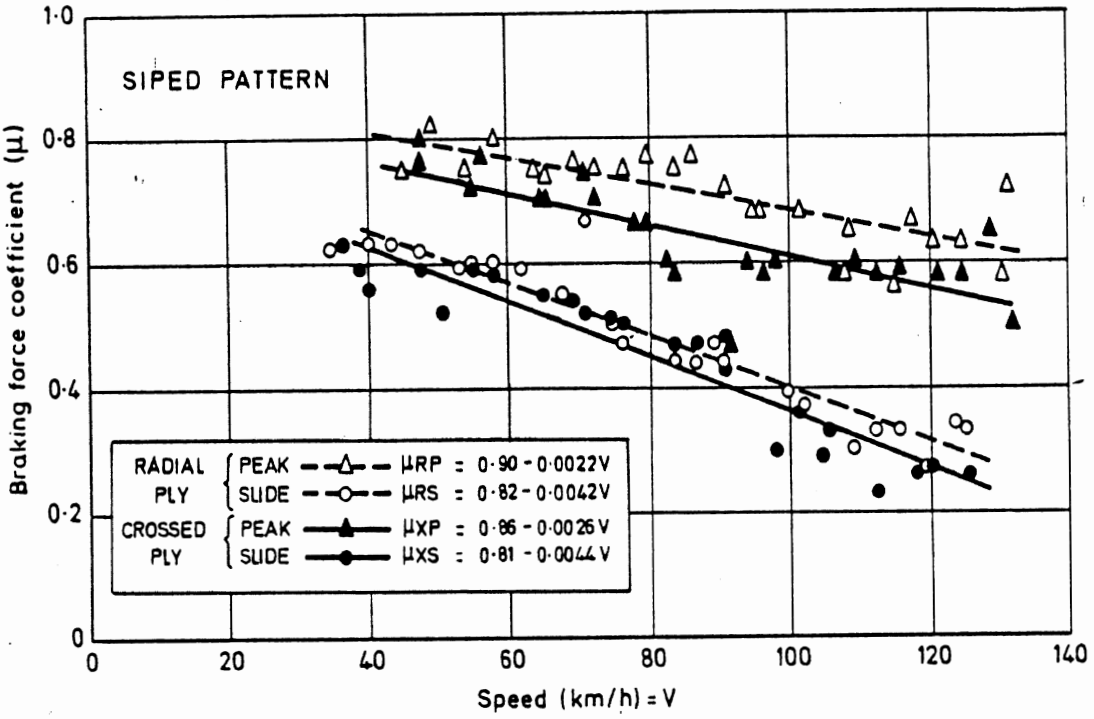

Figure 1.11 RESULTS OBTAINED ON SURFACE 3. (FINE COLD ASPHALT)

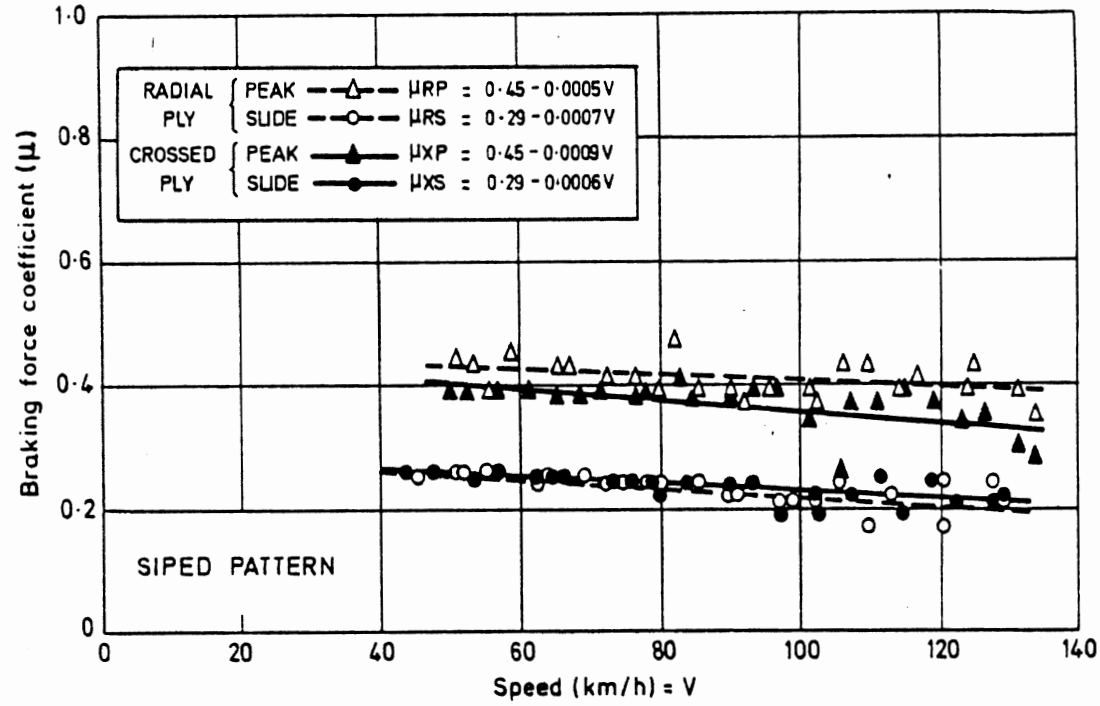

Figure 1.12 RESULTS OBTAINED ON SURFACE 4. (ROUNDED GRAVEL CARPET)

(as No. 3 in Fig. 1.10), while in Figure 1.12, the surface is of the "coarse textured, rounded" variety (as No. 4 in Fig. 1.10). The reader should note that while these examples serve to display the general significance of texture differences, a very large body of research literature has accumulated to deal with texture characterization and surface friction enhancement.

A principal quality of a paving aggregate is its ability to retain textural aggressiveness over extended use, and to resist polishing. Expressed in terms of minimum stopping distances, Figure 1.13 shows the effects of polishing of three aggregates in a Portland cement base [15]. In this dry stopping condition, we infer that peak traction levels can reduce by 40% as a result of polishing. It is also known that the friction loss resulting from polishing is somewhat dependent upon the base material, either asphaltic or Portland cement.

1.2.5 Sensitivity to Water Depth. The influence of water depth on μ_p and μ_s appears to involve at least two distinct modes of influence. At low levels of water depth, between 0 and 0.010 inches, the depth is both difficult to ascertain and strongly influential as a determinant of friction level. In this range of low depth values, the depth appears to be instrumental in determining the loss in "adhesive bonding" of tread rubber to aggregate. The steep sensitivity of traction level in this regime, as shown in Figure 1.14, is seen as resulting from a wetness/dryness property rather than to hydrodynamic phenomena relating to the dynamic fluid pressures [16].

We see that a zone of water film thickness exists, between .010 and .040 inches, in which little further influence on traction level is affected at the lower highway speeds. A broader view of the influence of water depth over the whole usable speed range is shown in Figure 1.15 [17]. We see, while water depth only lightly affects the "braking force coefficient" (μ_s) at lower speeds, the greater water depths produce dramatic reductions in traction level at elevated highway speeds.

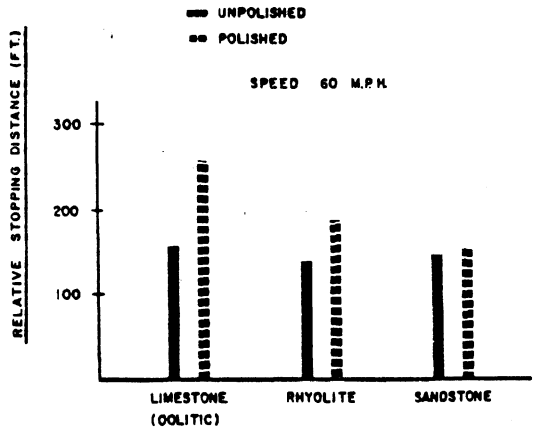

Figure 1.13 Effect of polished surface

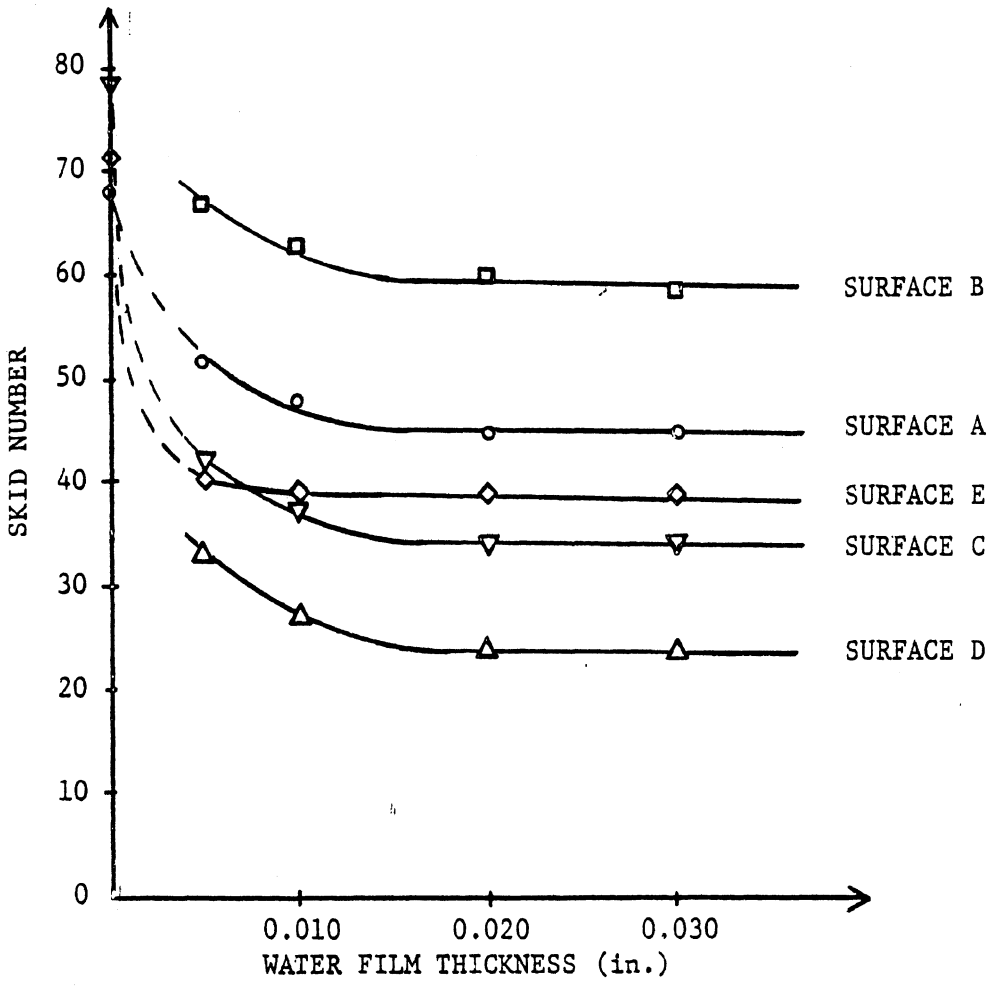

Figure 1.14 Effect of Water Film Thickness on Skid Number on Five Test Pavements; 40 mph

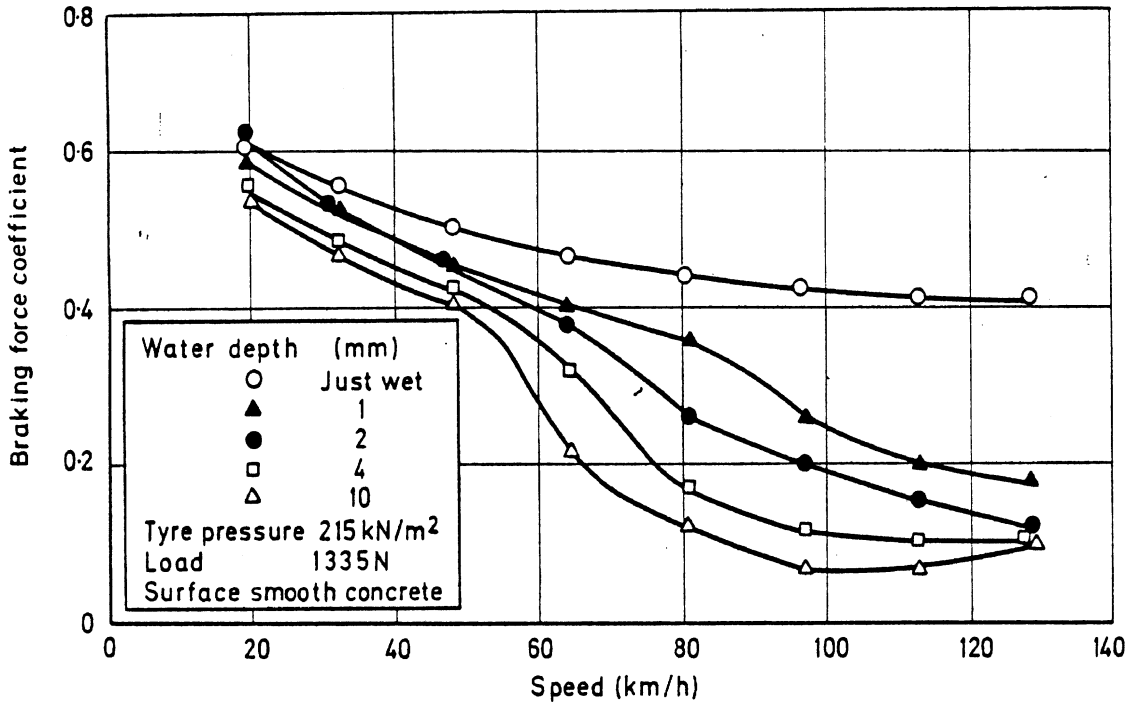

Figure 1.15 EFFECT OF WATER DEPTH ON THE LOCKED WHEEL BRAKING FORCE COEFFICIENT TYRE No. 1 (FULLY PATTERNED RADIAL)

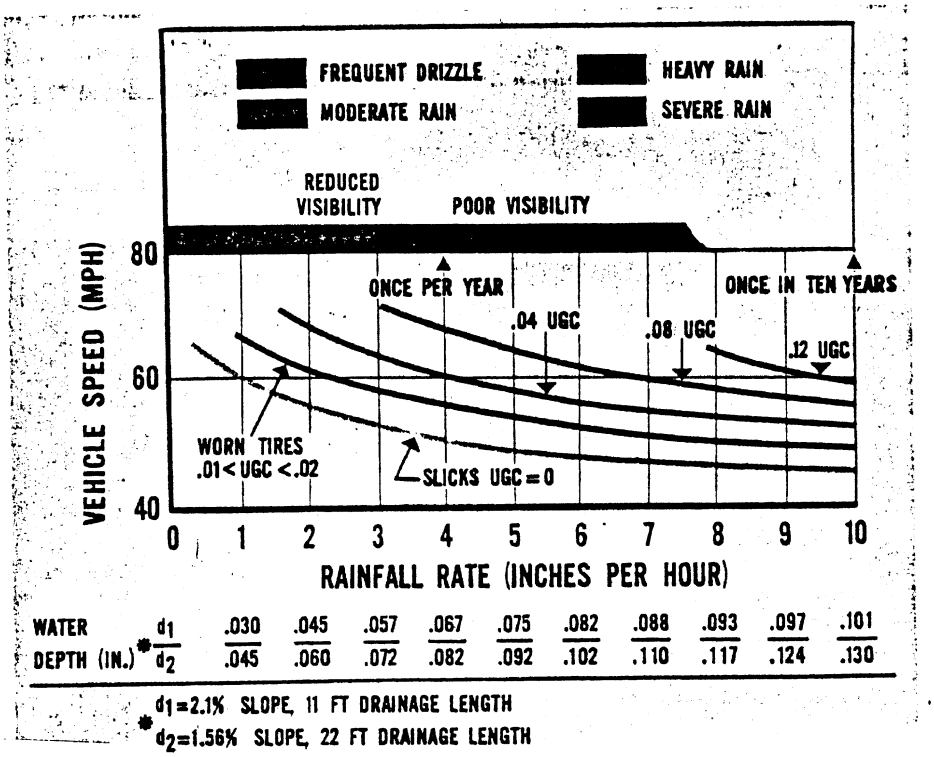

Figure 1.16 Estimated free rolling minimum full dynamic hydroplaning speed for passenger tires (conditions: relatively smooth surface, rounded footprint, and rated inflations and loads).

Relating water depth to the occurrence of full hydroplaning, we see in Figure 1.16 that a continuous "hydroplaning speed" relationship to water depth is established for tires of differing tread effectivenesses [9]. The UGC characterization, "unit groove capacity," identifies tires by the openness of their tread and other geometric characteristics. A modern, open-treaded radial tire would register a UGC of .08 on Figure 1.16.

Although no research is known to have been done relating truck tire traction limits to water depth, hydroplaning of such tires in normal service is accepted to be rare due to high contact pressures and characteristically open-type tread patterns [9].

1.2.6 Sensitivity to Carcass Design. The importance of carcass design, per se, in determining longitudinal traction limits is not great, but can easily be confused by the higher importance of tread patterns which are peculiarly employed with each of the generic carcass types. For example, it is known that the bias-ply tire suffers from high lateral stresses in the contact patch during the rolling process, giving rise to tread "squirm" which, in turn, encourages the use of continuous rib-type tread patterns. If open block-type tread patterns were to be used on bias-ply carcasses, very poor tire mileage would result. Also, it is known that radial-ply tires can be confidently constructed with rather rigid belt plies, reducing tread squirm by about two-thirds and permitting use of very open tread patterns. As a result of common design practices which have linked certain tread patterns with certain carcass types, we find that the typical passenger car radial tire is superior in wet traction performance to the typical bias-ply tire. Shown in Figure 1.17 are three tread designs typical of diagonal (or bias-ply) constructions, belted-bias-ply constructions, and radial-ply constructions [11]. Tables 1.3 and 1.4 present ratings of relative μ_s and μ_p performances (assigning to a standard tire's performance, the value 100) for tires of each carcass construction, each of which has been treaded (for purposes of demonstration) with each of the three indicated tread designs [11]. The "normal" carcass and

Figure 1.17 Typical tread designs.

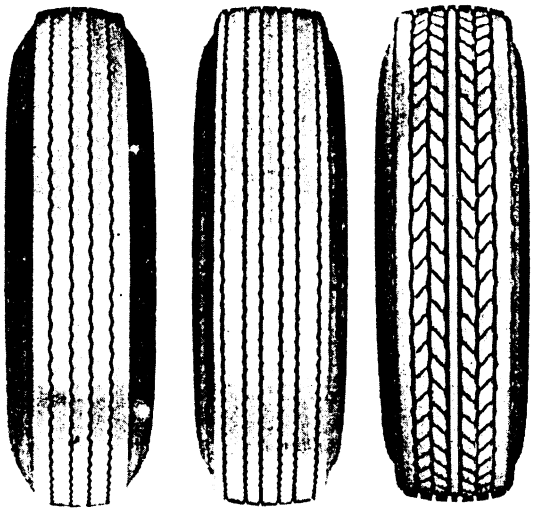

Diagonal Belted Radial

Table 1.3 Straight ahead slide traction ratings.

	μ = 0.3 Pad		μ = 0.5 Pad	
	64 km/h	97 km/h	64 km/h	97 km/h
Diagonal Design				
Diagonal Construction	96	82	103	104
Belted Construction	85	85	106	100
Radial Construction	85	73	103	91
Belted Design				
Diagonal Construction	98	88	100	102
Belted Construction	98	90	105	105
Radial Construction	95	80	100	94
Radial Design				
Diagonal Construction	112	113	112	112
Belted Construction	101	102	106	108
Radial Construction	109	102	106	109
Difference for 90% Confidence Level	5.2	4.9	4.1	3.2

Table 1.4 Straight ahead peak traction ratings.

	μ = 0.3 Pad		μ = 0.5 Pad	
	64 km/h	97 km/h	64 km/h	97 km/h
Diagonal Design				
Diagonal Construction	105	87	102	100
Belted Construction	106	91	103	98
Radial Construction	104	94	106	99
Belted Design				
Diagonal Construction	108	102	104	105
Belted Construction	106	103	109	104
Radial Construction	109	106	106	104
Radial Design				
Diagonal Construction	110	115	105	108
Belted Construction	107	105	109	105
Radial Construction	119	122	109	114
Difference for 90% Confidence level	3.2	4.2	1.8	3.1

tread combinations, such as diagonal tread design/diagonal carcass type, have been circled to identify the representative configurations which are actually produced for consumer use. We see that among the representative configurations, the radial tire is overall superior. Nevertheless, for the slide traction ratings, the radial tread design installed on a diagonal carcass construction provides the highest performance of all. Thus, it is clear that carcass type alone does not serve as a predictor of wet traction limits.

Shown in Figure 1.18 are μ_p data for a sample of eleven passenger car tires, covering a broad range of wet and dry surface and speed conditions [10]. We see that while the two tires with radial carcasses (dark symbols) register higher-than-average levels of μ_p on wet surfaces, they compare somewhat below average on the dry surfaces. Presumably, the reduced traction level of open-treaded radials on dry surfaces relates simply to the increased percentage void in such tread patterns—a characteristic which has been generally recognized as effecting a reduced dry traction level.

For the case of truck tires, no correlation has been seen between generic carcass type and longitudinal traction performance on either the wet or dry surfaces. Although only limited research work has been done in this area of truck tire mechanics, it appears that truck radials produce a narrower band of μ_p and μ_s performance levels than bias truck tires, but otherwise yield approximately the same average levels over the various designs available [8].

1.2.7 Sensitivity to Tread Design. As stated in the preceding section, it is known that increased void area in the tread pattern enhances wet traction performance of car tires and reduced tread void area enhances dry traction performance levels. As seen in Table 1.5, a tire with a "bald" tread produces an 8-10% higher value of μ_s than a ribbed tire on two different dry surfaces [18]. Similarly, since lug- or snow-type tread patterns have greater void area than tires of rib-tread design, lug tires are seen to register characteristically lower dry traction levels, as shown for passenger car tires in Table 1.6 [18]. Likewise, for truck tires, lug-type tread designs are seen

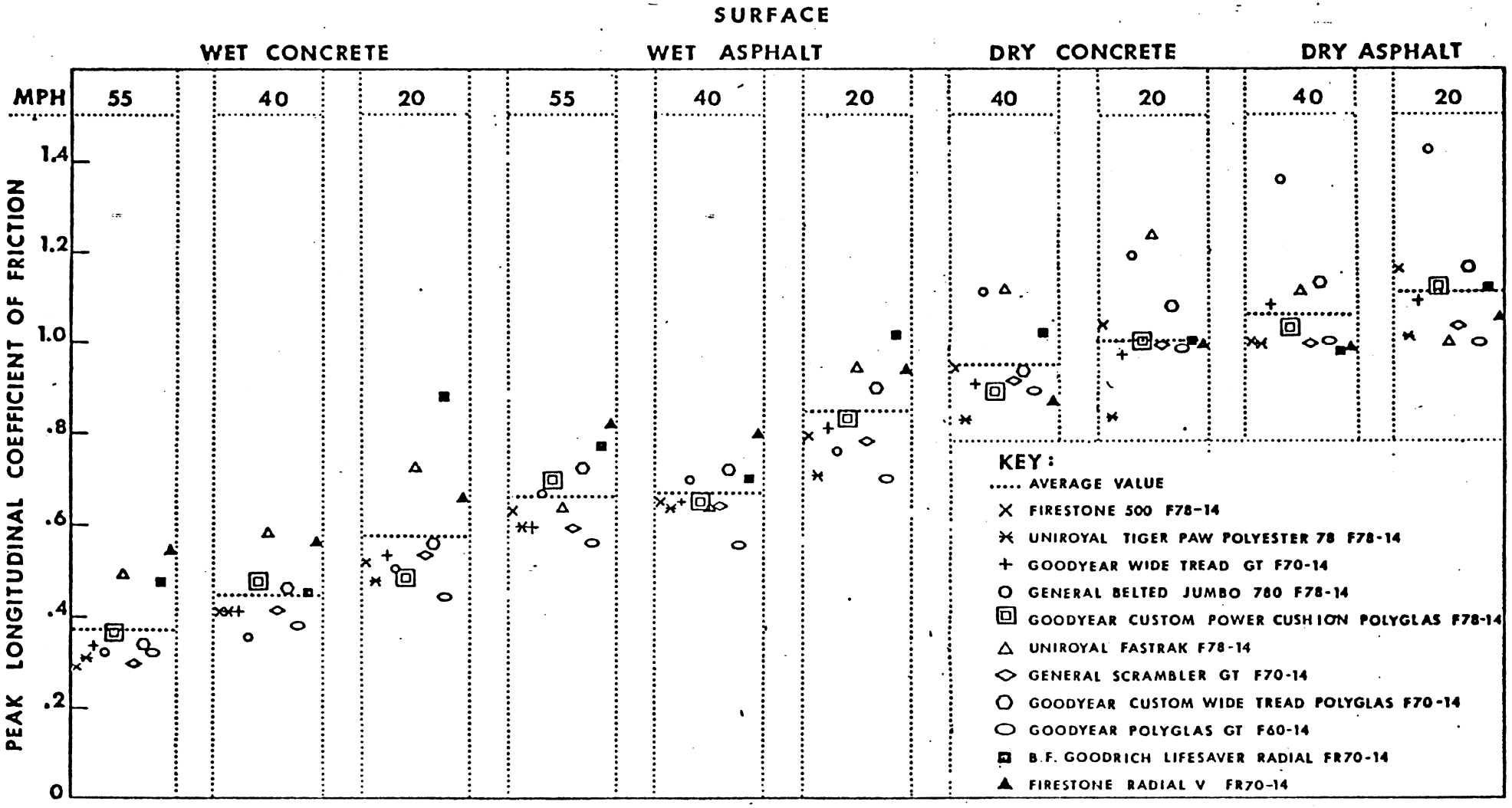

Figure 1.18 Peak Longitudinal Friction Coefficient Tire Data.

Table 1.5. Dry Coefficient of Friction Effect of Tread Design

Tire	Surface Coefficient	Tire Coefficient
Bald	0.87	0.91
	0.77	0.88
5 Straight Grooves	0.87	0.84
	0.77	0.79

Table 1.6. Dry Coefficient of Friction Effect of Groove Area (0.69 Coefficient Surface).

Tire	Mph	% Road Area In Contact Patch	Coefficient of Friction	
			Peak	Slide
Standard 7 Rib	20	0.83	0.76	0.66
	60	0.83	0.87	0.73
M&S Lug	20	0.65	0.73	0.66
	60	0.65	0.77	0.62

to produce substantially lower values of μ_p and μ_s on dry surfaces than do typical rib tread patterns; see Figure 1.19 [8].

On wetted surfaces, as was shown earlier, the μ_p and μ_s limits of passenger car tires show substantial sensitivity to tread pattern. It is known that not only tread "openness" but also the presence of sipes and diagonal cross grooves contribute to enhancing wet traction performance under certain road conditions. Further, the traction improvements deriving from details of tread pattern geometry are most significant on surfaces with very little macrotexture. It has been hypothesized that sipes in the tread can assist wet traction in three ways: as wipers, water reservoirs, and pressure points. Data which determine the generality of the traction improvements accompanying siping appear to conflict with one another. It suffices to say that, in certain circumstances, wet traction improvements may be large due to siping [18].

The advent of radial-ply tires has led to the common use of tread designs with cross grooves. Such grooves are seen to assist wet traction by equalizing the distribution of water between the circumferential grooves of the tread. The effectiveness of cross grooves is particularly noticeable in reducing loss of traction at high speeds. Measurements have revealed on the order of 20% improvement in μ_s level over that of a reference rib tire with no cross grooving—although this improvement is comparable to that expected simply from the additional void area represented by the grooves. It is also known that the angle at which cross grooves are applied has a substantial influence on μ_p values for wet, smooth surfaces. As shown in Figure 1.20, groove angle measured with respect to the circumferential line produces marked influence on μ_p, with an optimum value occurring near 50°.

Another tread design feature known to influence wet traction performance is the "zig-zag" circumferential groove whose pattern geometry is quantified by the "pitch" and "throw" dimensions. As shown in Figure 1.21, pitch refers to the circumferential distance

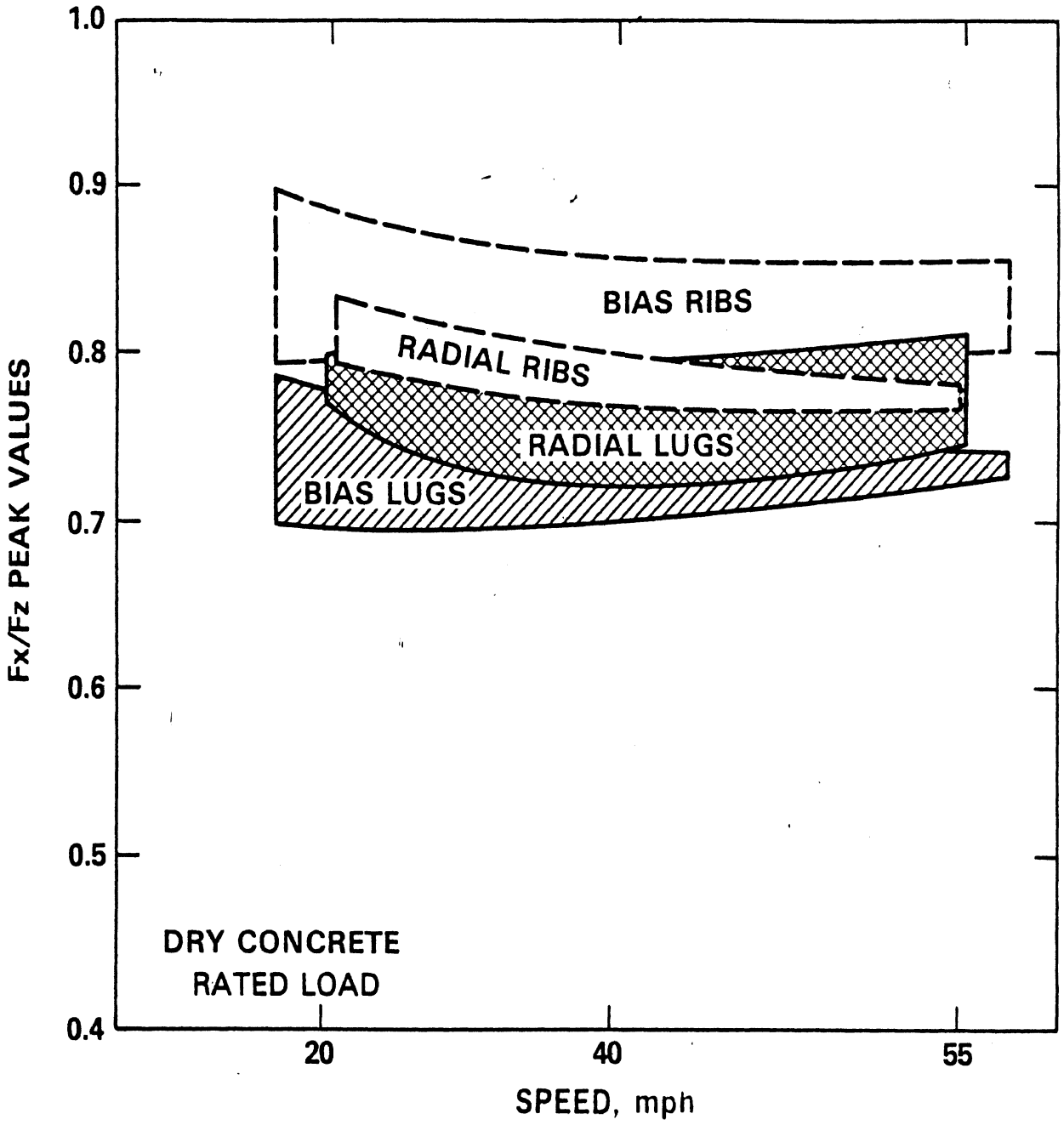

Figure 1.19 Envelopes of peak longitudinal traction values obtained on dry concrete.

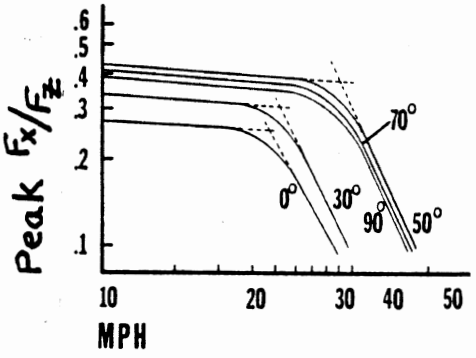

Figure 1.20 Effect of groove angle upon coefficient (μ) on wet concrete.

Figure 1.21 Illustrations Defining Pitch (P) and Throw (T)

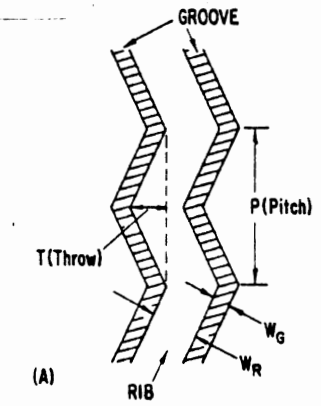

between peaks of the zig-zag, and throw refers to the zig-zag amplitude [19]. It has been found that decreasing the pitch of the zig-zag, making for a denser pattern and a longer effective channel length resisting front-to-back drainage in the contact area, reduces μ_s. It has been suggested that dense zig-zag patterns also suffer because the longitudinal braking force in the contact patch has a substantial shear component tending to fold down the angled walls of the zig-zag into the groove. This deflection of the rib material causes partial closure of the zig-zag groove and tends to further choke off water flow, front to rear [19].

While very little work on truck tire wet traction has been done, it is known that the higher tread contact pressures tend to heavily override the influences of tread pattern on wet traction level. As shown in Figure 1.22, we see that truck lug tires, despite their open tread patterns, yield lower values of μ_p on wetted concrete than do comparable tires of rib-type tread patterns [8]. It has been observed that, with contact pressures at levels which are three to five times that of passenger car tires, heavy truck tires tend to expel water so thoroughly as to render dry-like performance sensitivities even under large water depths.

1.2.8 Sensitivity to Tread Compound. The recipe used in formulation of the rubber used in tire treads can play a significant role in determining longitudinal traction limits. As shown in Table 1.7, six different tread rubber compounds are compared on the basis of locked-wheel stopping distances for a wet asphalt road [20]. We see typically that compounds producing high hysteresis (indicated by low values of Bashore resilience, "Rebound, 32°F") and low hardness (on the Shore A durometer scale) yield shorter stopping distances. It can be generalized that any compound change which will raise hysteresis or lower hardness will decrease stopping distance.

The explanation for these sensitivities is that the major mechanism of wet traction force generation is that of deformation, i.e., the deformation of rubber by large-scale asperities. A softer rubber

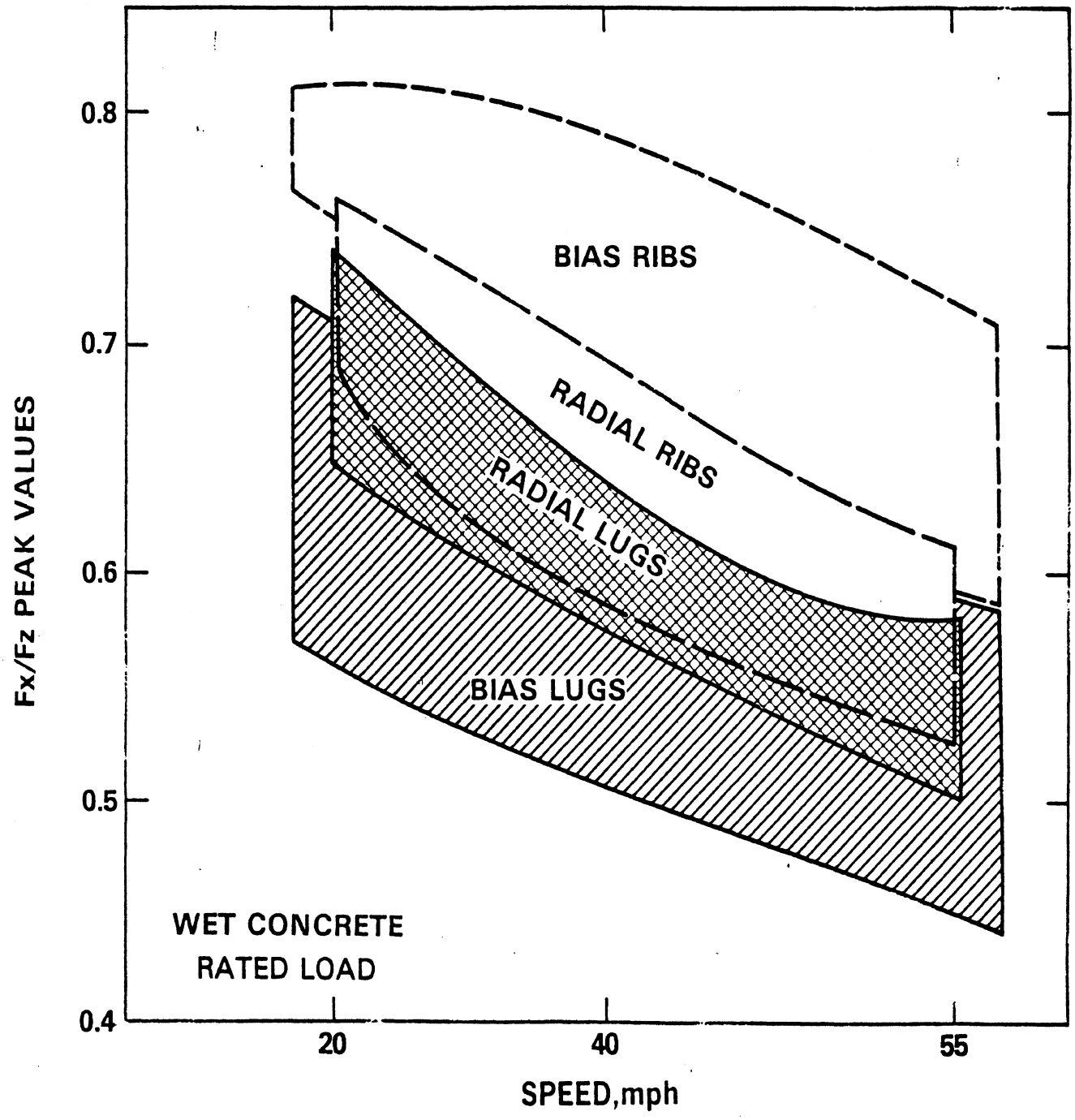

Figure 1.22 Envelopes of peak longitudinal traction values obtained on wet concrete.

will be deformed more by a given asperity, and a high-hysteresis rubber will be capable of absorbing a greater percentage of the energy produced in such deformations.

A typical tread recipe is given below:

Polymer	100
Extender Oil	40
Carbon Black	70
Zinc Oxide	3
Stearic Acid	2
Anti-Oxidants	1.5
Accelerators	1.5
Sulfur	2

Reviewing the major ingredients for influence on longitudinal traction potential, it is known that enhancement of skid resistance is in conflict with enhancement of wear resistance. Many polymers have been examined for suitability as tread stock material. For the most part, the so-called "glass transition temperature," Tg, of the polymer determines the modulus and hysteresis of a rubber at a given service temperature. The glass transition temperature merely orders polymers according to the temperature at which the polymer is changing most rapidly from a glassy to an elastomeric state. In the compound, however, improvements in wet skid resistance can be seen as directly following glass transition temperature while abrasion or wear resistance decline (see Fig. 1.23) [20]. As shown in Table 1.8, glass transition temperature is raised by increasing the styrene content of a butadiene-styrene copolymer [20]. We see that the relative "wet skid" rating (where higher number means higher μ_s) rises with Tg, while abrasion resistance declines. In general, the selection of the basic polymer determines hysteresis level, and thus wet skid resistance according to the glass transition temperature which results. A number of practical considerations affect the acceptability of a polymer, however, not the least of which is the need to provide good traction performance over a very wide range of in-service operating temperatures.

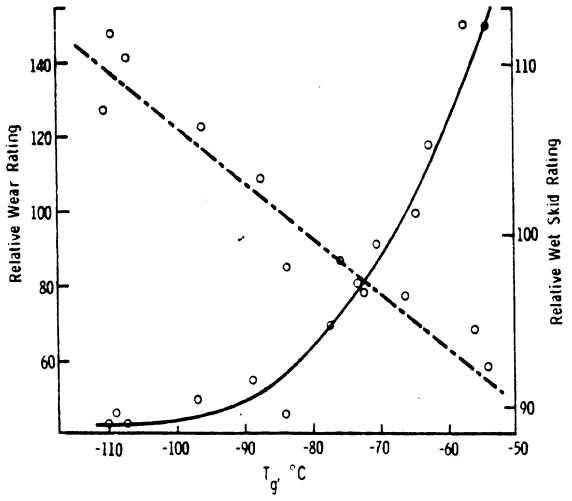

Figure 1.23 Dependence of skid resistance (solid line) and wear resistance (broken line) on polymer T_g.

When extender oils are used in a tread compound, more carbon black is usually also added to keep tensile strength and hardness at acceptable levels. Table 1.9 shows the effect of oil level on physical properties of a CIS-BR polymer as carbon black level is increased along with oil content [20]. We see hardness reducing and hysteresis increasing (i.e., lowering the rebound measure) as oil level is raised, thus producing higher wet skid ratings. It is known, however, that part of the hysteresis increase in Table 1.9 is due to the greater carbon black loading.

Carbon black is, in general, a reinforcing filler which greatly increases wear resistance and also raises hysteresis. Thus, carbon black is being studied as a component capable, by itself, of effecting improved wear resistance and longitudinal traction level.

The other ingredients in a tire tread compound are either anti-oxidants, which do not affect traction limits, or are substances connected in some way with the vulcanization reaction.

Regarding dry traction, little is available by way of tread rubber formulation to enhance shear force level under these conditions. Even drastic changes in tread recipe have been seen to effect no greater than a 15% change in dry traction limits. Certain changes in carbon black content or type of carbon black producing higher tensile strength or hysteresis have been seen to produce slight improvements in dry traction limits. Generally, however, tread rubber compounds cannot be clearly differentiated from one another at the very high temperatures which prevail under the conditions of limit shear force generation on dry roads.

1.2.9 The Relevance of Longitudinal Traction Limits to Vehicle Maneuvering Properties

Longitudinal traction peak, μ_p, is generally seen as the ultimate property of the tire/vehicle system limiting minimum wheels-unlocked stopping distance. This limitation does not typically constrain braking limits at each wheel of the vehicle simultaneously,

Table 1.7 Observed and Calculated Stopping Distance
Wet Asphalt Road

Rubber	Rebound, 32°F	Hardness	Stopping Distance, (ft.) Calculated	Stopping Distance, (ft.) Observed
BR	62	62	177	180
NR/BR	46	57	162	163
EPDM	32	63	160	160
SBR/BR	33	55	155	158
SBR	34	52	152	151
Butyl	9	40	132	130

Table 1.8 Effect of Styrene Content on T_g, Abrasion Resistance and Skid Resistance

Polymer	% Styrene	T_g	Rebound, 0°C	Wet Skid, Concrete	Abrasion Resistance
BR	0	−105	42	76	240
6:4 SBR:BR	14	− 76	26	94	122
SBR 1500	23.5	− 56	12	100	100
Solution SBR	25	− 50	10	102	97
SBR 1516	40	− 30	6	111	76

Table 1.9 Effect of Simultaneous Changes in Oil and Black Level on Physical Properties

Recipe:			
Polymer	100	100	100
Black	50	70	90
Oil	0	40	80
Properties:			
Rebound	60	36	23
Hardness	71	67	49
Tensile Strength	2160	2630	2040
Wet Skid	100	110	127

however, since at any braking level, certain wheels are bearing a disproportionate share of retardation torque for the vertical load which they are carrying. Because of this general problem of brake torque "proportioning," the μ_p limitation at the tire is only part of the effective limitation in a vehicle's minimum stopping distance without wheel locking.

Certain measures of vehicle minimum stopping capability have been employed using the tires' μ_p value as a normalizer. Termed "classical braking efficiency," such measures reveal that passenger cars may be only 60 to 65% efficient in utilizing the μ_p value that prevails on the installed tires [52].

On dry surfaces, deceleration levels can be high such that rear tires become very lightly loaded. Accordingly, the proportioning of the vehicle's brake system must avoid over-application at the rear for such high levels of brake actuation. On low friction surfaces, the converse constraint prevails, and over-actuation at the front must be avoided. Thus, while maximization of μ_p is certainly a high priority in assuring good limit braking performance, one should not assume that a given improvement in μ_p will be realized, one-for-one, in minimum wheels-unlocked stopping distance.

Regarding locked-wheel braking, it is generally found that the μ_s performance of the installed tires directly determines minimum stopping distance. Since rear-to-front load transfer places different loads on the rear- and front-mounted tires, however, load sensitivities in μ_s must be accounted in relating tire traction limits to vehicle braking performance. On wetted surfaces, also, certain complications arise due to front tires wiping water from the path to be traveled by rear tires. Thus, on wetted surfaces, for which front tires may be overbraked anyway, vehicle braking efficiency may be low because of the low front tire friction level compared to that available for rear tires.

For the case of heavy trucks, two peculiar sensitivities to longitudinal traction peaks should be noted. Since promulgation of Federal Motor Vehicle Safety Standard 121 for air-braked trucks, the

use of antilock braking systems has become common on heavy vehicles in the U.S. Examining the implications of μ_p level on one such antilock-equipped truck, it was found that a 10% reduction in μ_p produced 8% increase in stopping distance for the unloaded vehicle, and a 3% increase for the loaded vehicle [21].

For trucks produced without antilock systems, before FMVSS 121, the implication of μ_s appears more directly. Of special significance in this regard is the fact that such earlier-production trucks place their heavy braking effort on rear, drive axles which have been also characteristically outfitted with lug-type tires. Accordingly, the wheels-locked stopping distances of these vehicles have been somewhat degraded by the common use of a tire tread type which has been seen to be generally reduced in traction level. Also, with heavier braking torques being applied to the axles which are deficient in traction potential, the likelihood of rear tire lockup and the attendant loss in directional stability is seen to be greater.

2.0 CORNERING PROPERTIES

When the tire is rolling, it can generate a force normal to its wheel plane by one of two mechanisms. Referring again to the SAE tire axis system, shown earlier in Figure 1.1, the rolling tire will produce a lateral force, F_y, when a non-zero angle, α, is subtended between the direction of travel of the center of tire contact and the X' axis. This mechanism, termed lateral force due to slip angle, is the primary means by which cars and trucks obtain motion in a curved path. The linear portion of this lateral force response is described by the cornering stiffness, C_α, per the relation:

$$C_\alpha = \left.\frac{\partial F_y}{\partial \alpha}\right|_{\alpha=0}$$

This tire parameter is recognized as the single most important determinant of the tire's influence on car and truck handling behavior.

A second means of side force generation derives from rolling at a non-zero inclination, or camber angle, γ. When the tire is oriented to a positive camber angle, a positive lateral force, or "camber thrust," is produced. While lateral force due to inclination angle plays a secondary, or "trim," function in the dynamic response of passenger cars, this mechanism is the primary means by which two-wheeled motorcycles achieve motion in a curved path. The linear portion of the camber thrust function is described by the camber stiffness, C_γ, per the relation:

$$C_\gamma = \left.\frac{\partial F_y}{\partial \gamma}\right|_{\gamma=0}$$

By whichever mechanism side force is produced, the linear range of behavior is followed by a friction-determined saturation

level, $\mu_y = F_y/F_z$, which is directly analogous to the longitudinal saturation level, μ_p. Shown in Figure 2.1 is a typical profile of the F_y versus α relationship, illustrating both C_α and the saturation level which establishes μ_y.

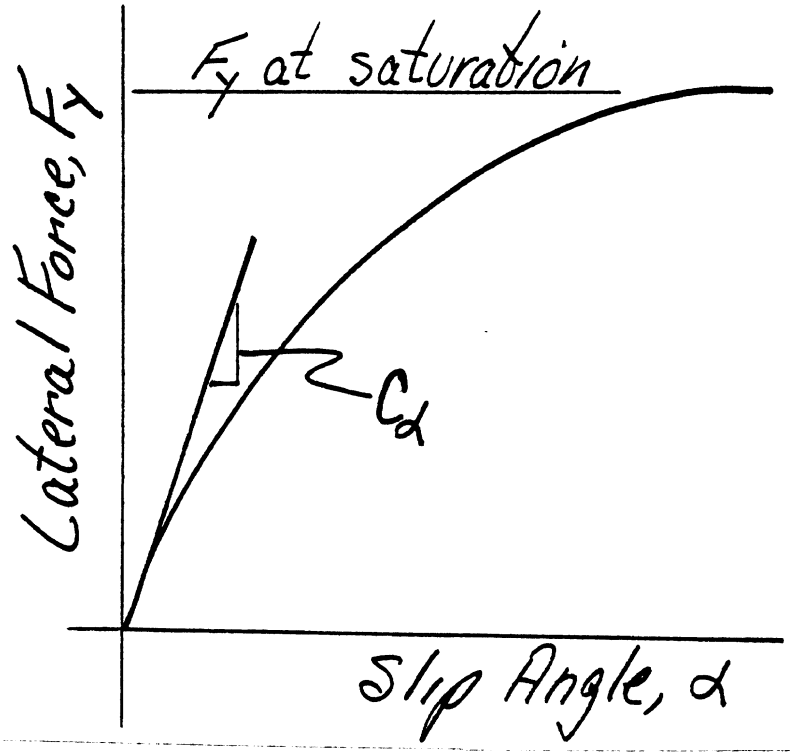

Figure 2.1

These three primary responses associated with lateral shear forces will be discussed in some detail in this section. Certain tire moment responses which are only obscurely related to vehicle controllability and thus to safety will be discussed first, however, in an introductory way. Although of minor significance to gross vehicle response, certain of these moment properties are known to be relevant to the subjective feel of a vehicle's handling behavior in the normal driving regime.

Because the tire is compliant in all three directions, the generation of lateral forces results in structural deflections of the tire which induce moments about each of the three principal axes. When the tire is operated at a slip angle, lateral shear stresses in the contact patch are initially developed with their centroid aft of the tire centerline. The resulting moment about the vertical axis, termed "aligning moment," contributes a reaction in the steering system assisting the driver's feel of the road. This moment contributes to the torque about the steering pivot which derives from tire lateral force and the effective lever arm due to caster geometry in the suspension. Together these "steering moments" act to deflect the steering linkage, thus effecting an incremental change in the steer angle of the front wheels. By this mechanism, aligning moment contributes to the total turning behavior of the vehicle. Aligning moment is also experienced as a small addition in the total summation of yaw moments on the vehicle.

A typical "carpet plot" of the influence of both slip angle and vertical load on aligning moment is shown in Figure 2.2 [22]. The plot shows aligning moment in lb-ft on the vertical axis for lines of constant load and slip angle.

Following the uppermost curve at 2400 lbs load, for example, we see that aligning moment rises steeply in the first few degrees of slip angle, peaking at 8° and 216 lb-ft aligning moment, and then declining for increasing slip angle. For low levels of load, aligning moment declines to the point of becoming slightly negative at high slip angles.

Radial- and bias-ply tires possess rather similar aligning moment response to slip angle.

Shown in Figure 2.3 [23] are distributions of "cornering aligning coefficient," N_α/p, for passenger car tires of differing carcass construction, where:

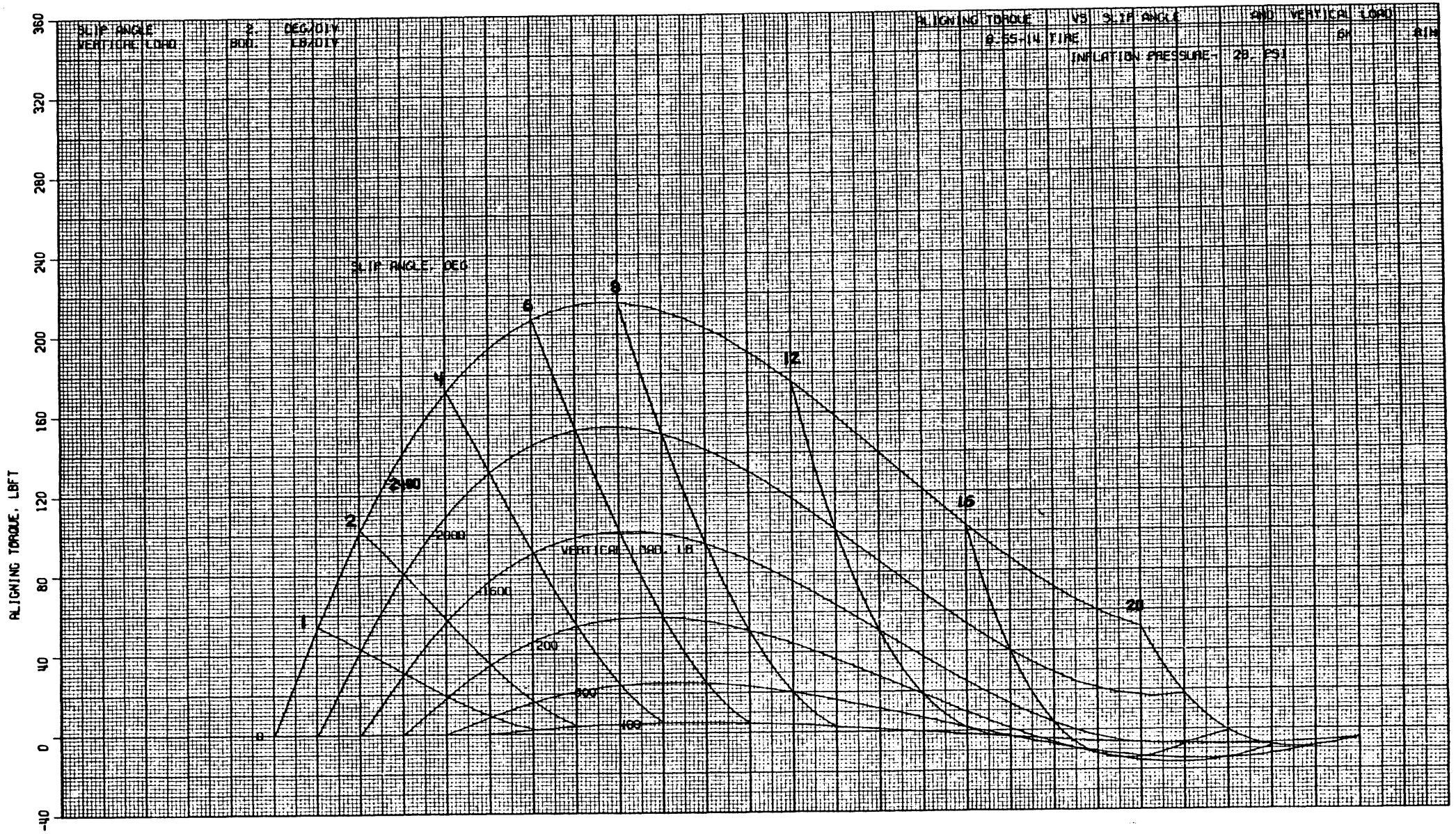

Figure 2.2 Effect of Slip Angle and Load on Aligning Torque

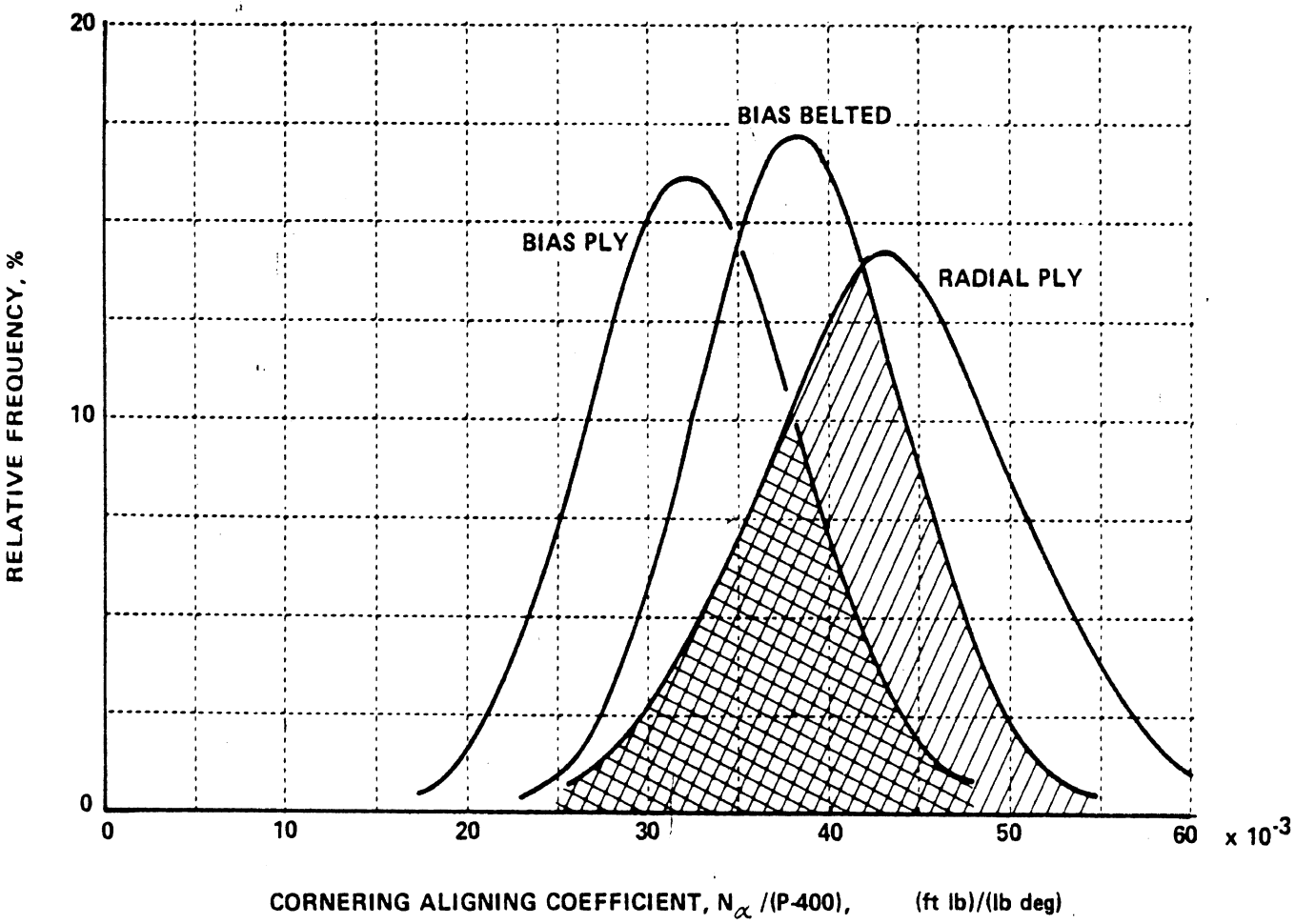

Figure 2.3 Distribution of cornering aligning coefficients of passenger car tires (aspect ratio 78; 24 and 28 psi)

$$N_\alpha = \partial M_z / \partial \alpha$$

and $$p = (\text{Design load} - 400\ \text{lb})$$

As seen in the figure, all tire constructions group closely together, with radials coming out the highest on the average. Road "feel" is generally reduced with radial tires, however, because the front tires operate at lower slip angles for a given maneuver (due to higher values of C_α, as will be discussed in Section 2.1), and thus generate proportionately less aligning moment. In some vehicles fitted with radial tires, front-wheel caster has been increased so as to provide a compensating increase in the total road feel moments [27].

An aligning moment is also produced when a tire rolls at a non-zero camber angle. As shown in Figure 2.4, a bias-ply car tire produces aligning moments due to camber which are on the order of 10% of the magnitude of aligning moments produced in response to slip angle [22]. For radial tires, aligning moments due to camber angle are substantially lower than those measured for bias tires. Shown in Figure 2.5 are distributions of "camber aligning coefficient," N_γ/p, for passenger car tires of differing carcass construction, where:

$$N_\gamma = \partial M_z / \partial \gamma$$

We see that radials produce aligning moment due to camber thrust at about 40% of the rate typical of bias-ply tires [23].

With regard to the various sensitivities of aligning moment to operating variables, it can be said that, in most cases, influences which increase side force level will also, in the small slip angle regime, tend to increase aligning moment output [28]. An exception to this rule is the case of inflation pressure increases which produce increased cornering stiffness in car tires, but reduced levels of aligning moment [29].

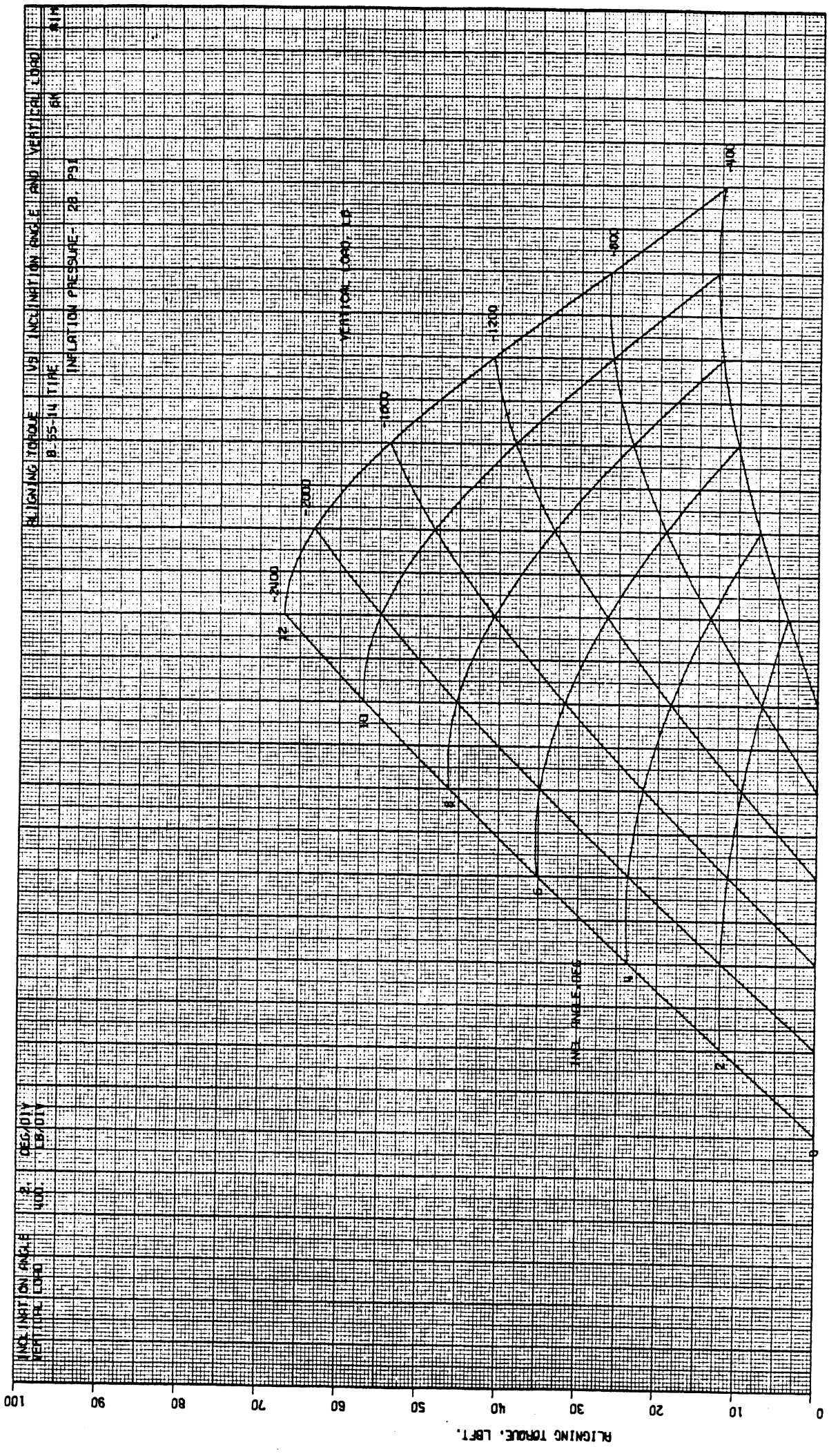

Figure 2.4 Effect of Inclination Angle and Load on Aligning Torque

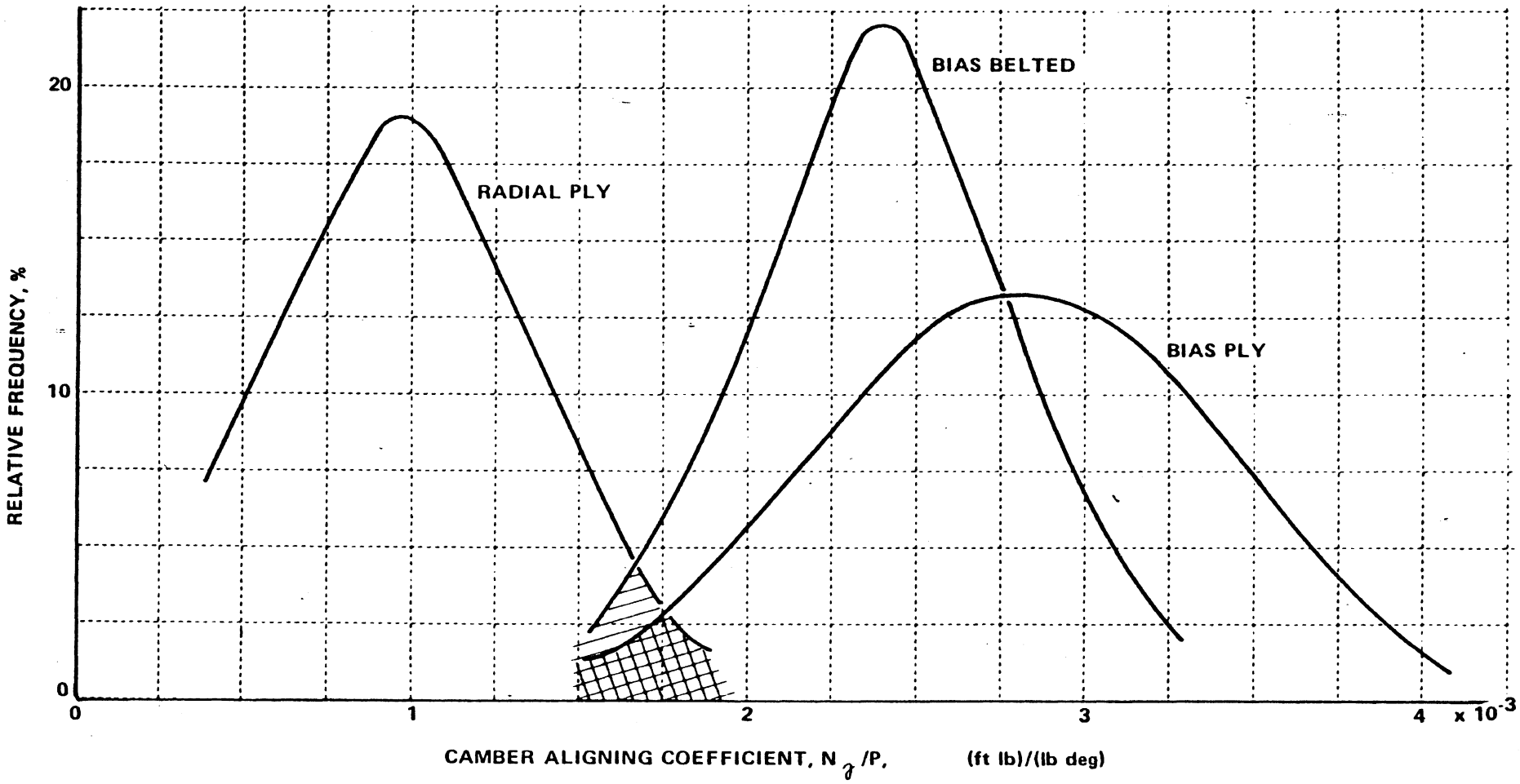

Figure 2.5 Distribution of camber aligning coefficients of passenger car tires (aspect ratio 78; 24 and 28 psi)

Two other moment responses of the tire which are of little or no consequence to vehicle controllability are the overturning moment, M_x, and the rolling resistance moment, M_y. The overturning moment derives from the lateral shift of the resultant vertical load which accrues from the tire distortion accompanying lateral force. This moment, involving as much as a two- to three-inch lateral shift of the load center, tends to reduce the overturning stability of the vehicle by reducing effective track width. Typical carpet plots of overturning moment response to slip angle and camber angle are shown for a bias-ply passenger car tire in Figures 2.6 and 2.7, respectively [22]. Again, as with aligning moments, this property exhibits sensitivities to design and operating variables that closely parallel the sensitivities in side force response, i.e., influences which tend to increase side force produced at a given condition will be expected to effect a proportionate change in overturning moment.

Rolling resistance moment, while of negligible significance to vehicle control, is of high interest, generally because of its connection to fuel consumption. Rolling resistance moment develops because of a longitudinal shift of the center of vertical load in the contact patch of the tire. The moment which results is non-zero even in the free rolling condition as a result of the characteristic deflection shape of the rolling tire. Rolling resistance moment is lower for tires with radial-ply constructions, and also for tread stocks incorporating low hysteresis rubber compounds. Rolling resistance moment is known to be influenced by vertical load and slip angle, as shown for a typical bias-ply tire in Figure 2.8 [22]. The influence of inclination angle on rolling resistance moment is known to be very small. During heavy braking, the tire deflects longitudinally so that the vertical load shifts aft of the centerline, producing a moment which is of the rolling "assistance" polarity rather than being rolling "resistant." In the case of passenger car tires, this moment can be of the order of 10% of the braking torque.

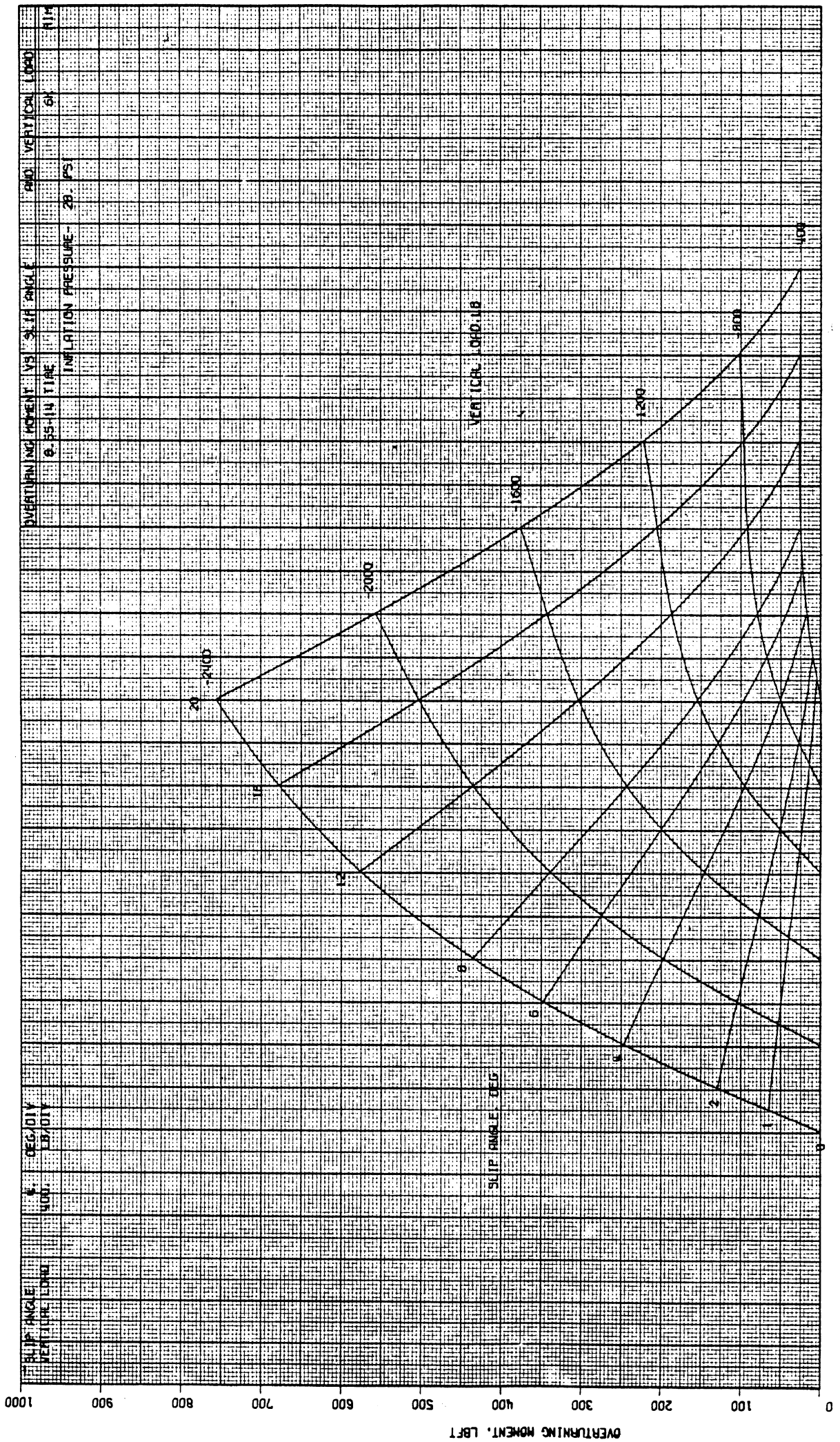

Figure 2.6 Effect of Slip Angle and Load on Overturning Moment

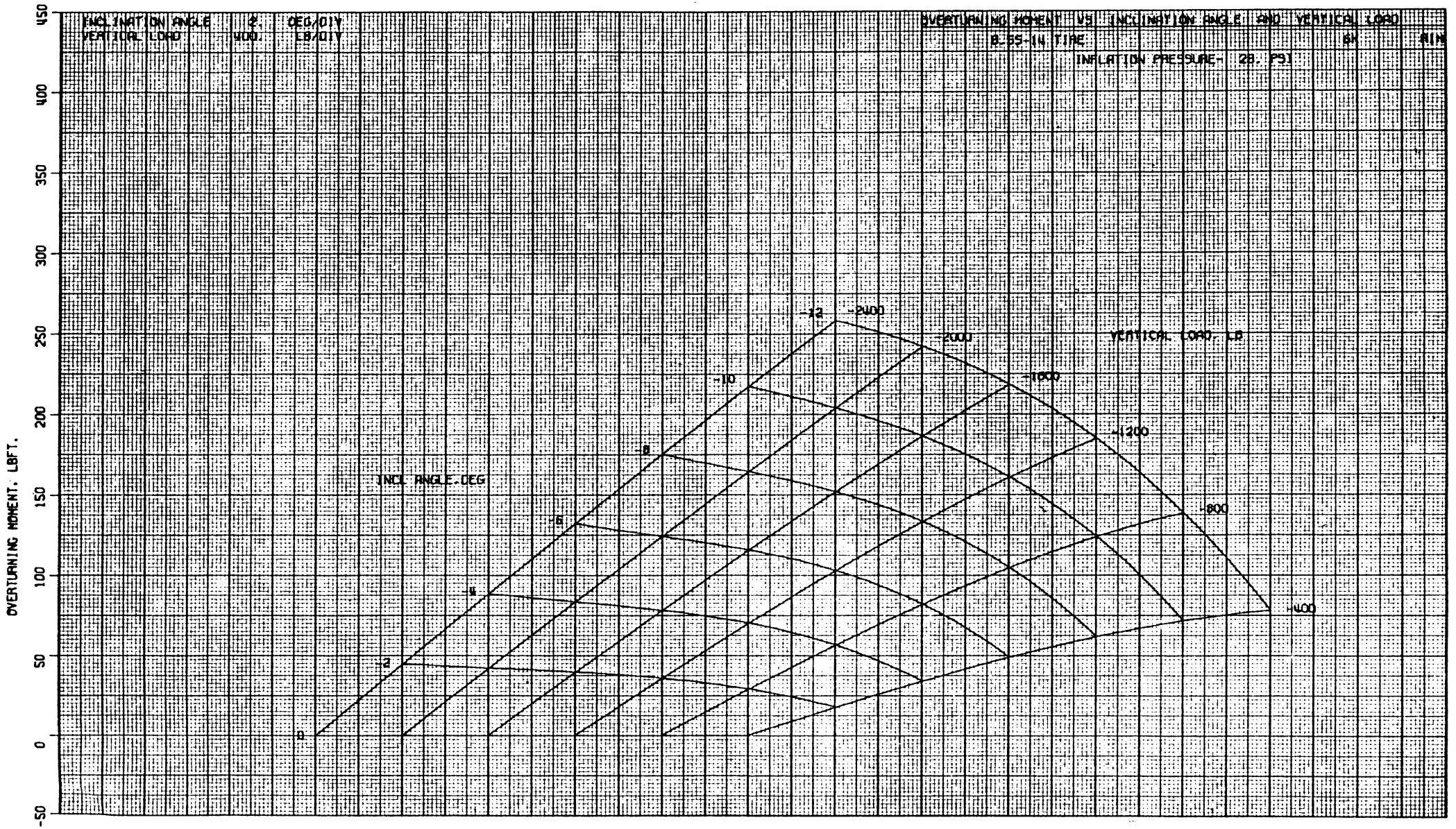

Figure 2.7 Effect of Inclination Angle and Load on Overturning Moment

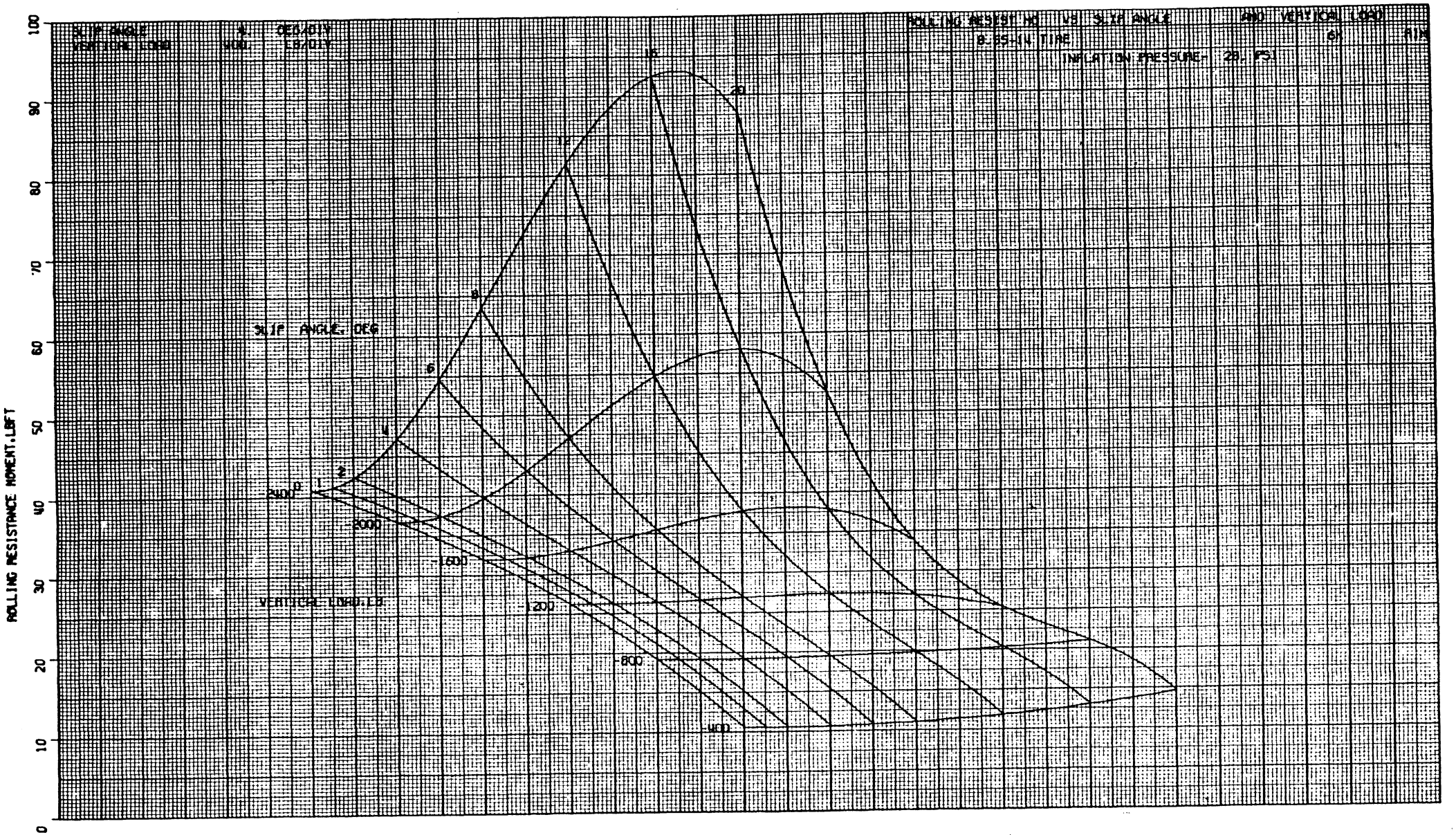

Figure 2.8 Effect of Slip Angle and Load on Rolling Resistance Moment

2.1 Cornering Stiffness, C_α

Tire cornering stiffness is the primary "spring rate" type property which determines the yaw or turning response dynamics of cars and trucks. Since it is an elastic characteristic of the tire, its significance to vehicle control is limited to the non-emergency regime of maneuvers, below 0.3 g level of lateral acceleration. In the following review of sensitivities to operating and design variables, we see that C_α is influenced by anything which affects structural stiffness or contact length, but uninfluenced by items affecting only the prevailing friction limits.

2.1.1 Sensitivity of C_α to Inflation Pressure. Since inflation pressure changes increase carcass stiffness but reduce contact length, the net influence on cornering stiffness cannot be generalized across all types of tires. It is generally accepted that increasing inflation pressure categorically results in increasing cornering stiffness for passenger car tires.

Typical data showing the sensitivity of cornering stiffness to inflation pressure for car tires is shown in Figure 2.9 [24]. An example of the change in this inflation sensitivity of cornering stiffness with increasing load is shown in Figure 2.10 [7]. We see that increasing load results in a steeper and more uniform sensitivity of C_α to inflation pressure.

Because of the monotonic and rather strong relationship between cornering stiffness and inflation pressure, the low-g steering behavior of passenger cars has long been controlled, at least in part, through the vehicle manufacturer's specification of distinct inflation pressures for front- and rear-mounted tires.

In the case of truck tires, it is known that the influence of inflation pressure on C_α is varied and dependent upon obscure sensitivities to details of the tire carcass design. Measurements have shown both steeply positive and steeply negative sensitivities with large dependence upon vertical load. It does appear, however, that similar to passenger car tires, increased load on a truck tire always

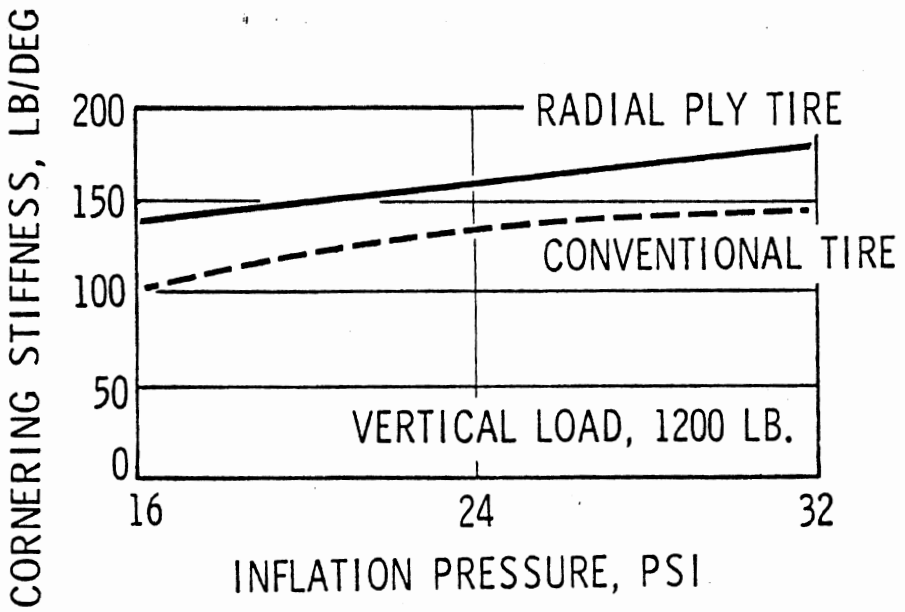

Figure 2.9 Cornering Stiffness-Inflation Pressure

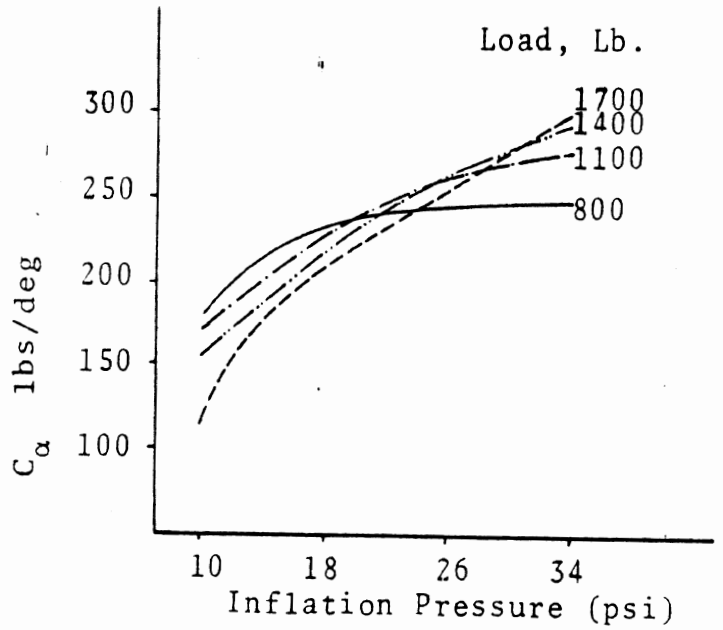

Figure 2.10 Cornering stiffness as a function of inflation pressure and load, Firestone 500 H78-14, 26 psi.

produces a more positive slope in the C_α sensitivity to inflation pressure. Examples of truck tire C_α sensitivity to inflation are shown in Figure 2.11.[5].

2.1.2 Sensitivity of C_α to Vertical Load. The sensitivity of cornering stiffness to vertical load is perhaps the single most important tire sensitivity function to the vehicle dynamicist. This sensitivity is important because it determines, in part, the influence on vehicle yaw behavior of adding payload. In addition, since tire load changes occur, side-to-side, on a vehicle during cornering, the nonlinearity of the C_α-F_z sensitivity will also influence yaw behavior. This latter characteristic of the tire is often termed the tire's "load transfer sensitivity."

Shown in Figure 2.12 are typical cornering stiffness versus load plots for two different passenger car tires.[25]. The typical nonlinearity shown in Figure 2.12, with cornering stiffness peaking in the vicinity of the tire's rated load, is significant in the determination of vehicle handling sensitivities to payload. For passenger car tires which are statically loaded at the peak of the C_α versus F_z curve, load changes can only result in a reduced level of C_α—thus introducing the potential for degrading the vehicle's response to steering when payload or passengers are added.

By way of contrast, truck tires show a rather steep slope in their C_α versus F_z relationship at rated load, as shown in Figure 2.13 [8]. Thus, with the large payload changes which commercial vehicles must bear, the typical C_α versus F_z behavior of commercial vehicle tires is a distinct advantage. This "advantage" can be understood by considering that much of a vehicle's yaw behavior is ultimately determined by the front and rear ratios of vertical load to cornering stiffness. Indeed, the most broadly applicable measure of vehicle yaw behavior in low level maneuvers is the understeer coefficient, u, which is based simply on the F_z/C_α ratios per the relation:

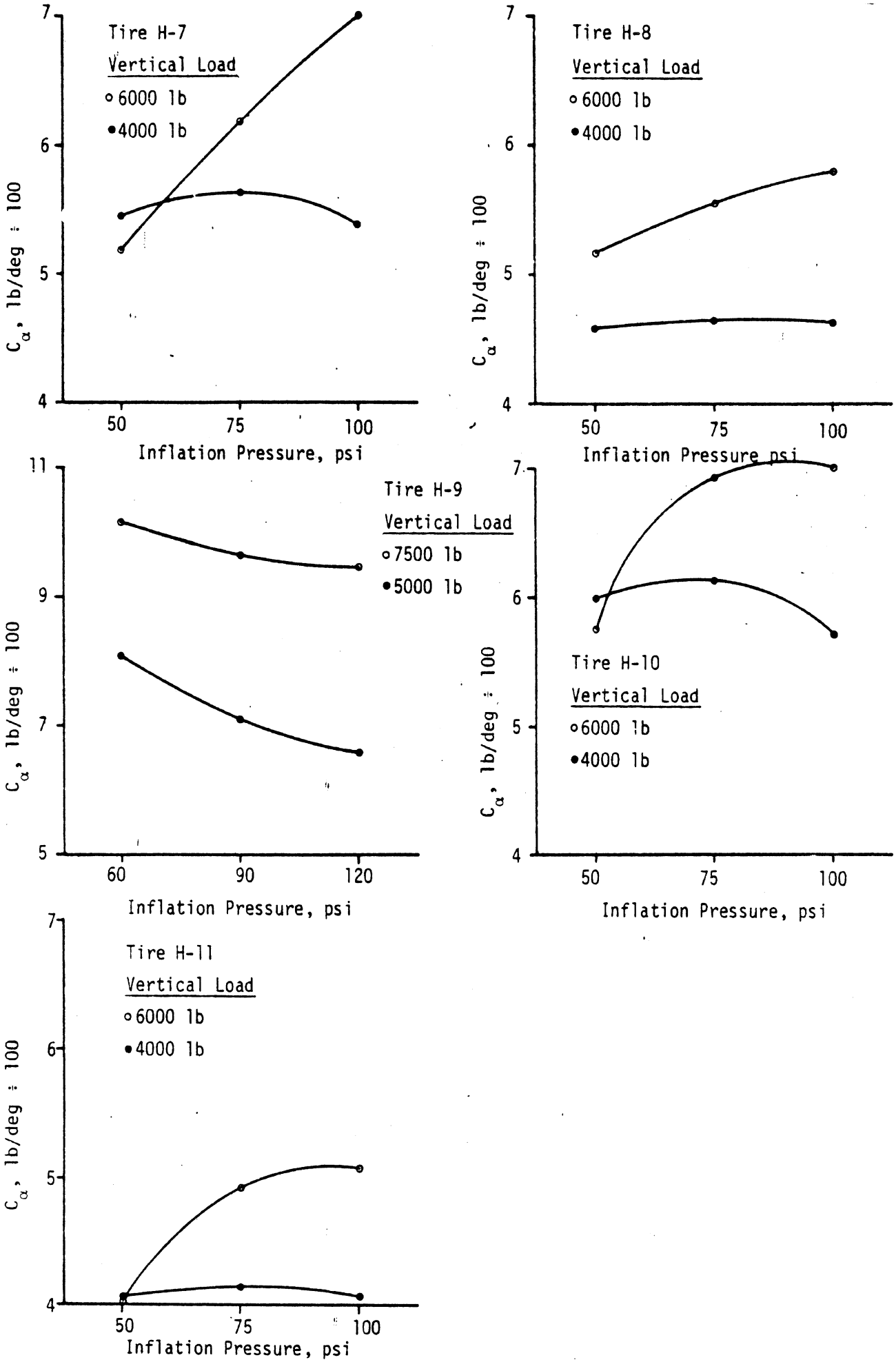

Figure 2.11 The effects of inflation pressure on cornering stiffness: heavy truck tires

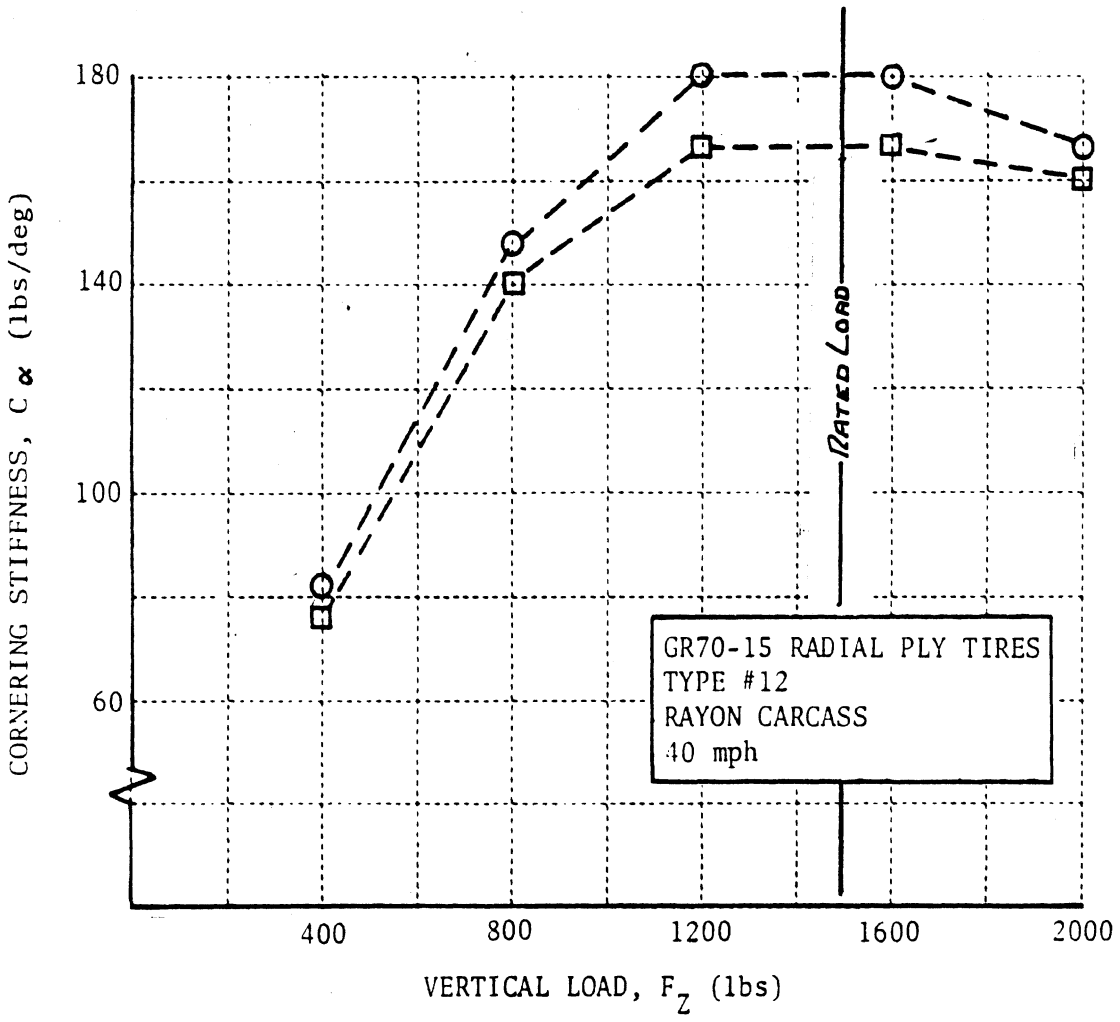

Figure 2.12 Vertical Load Influence on Cornering Stiffness of Radial Ply Tires.

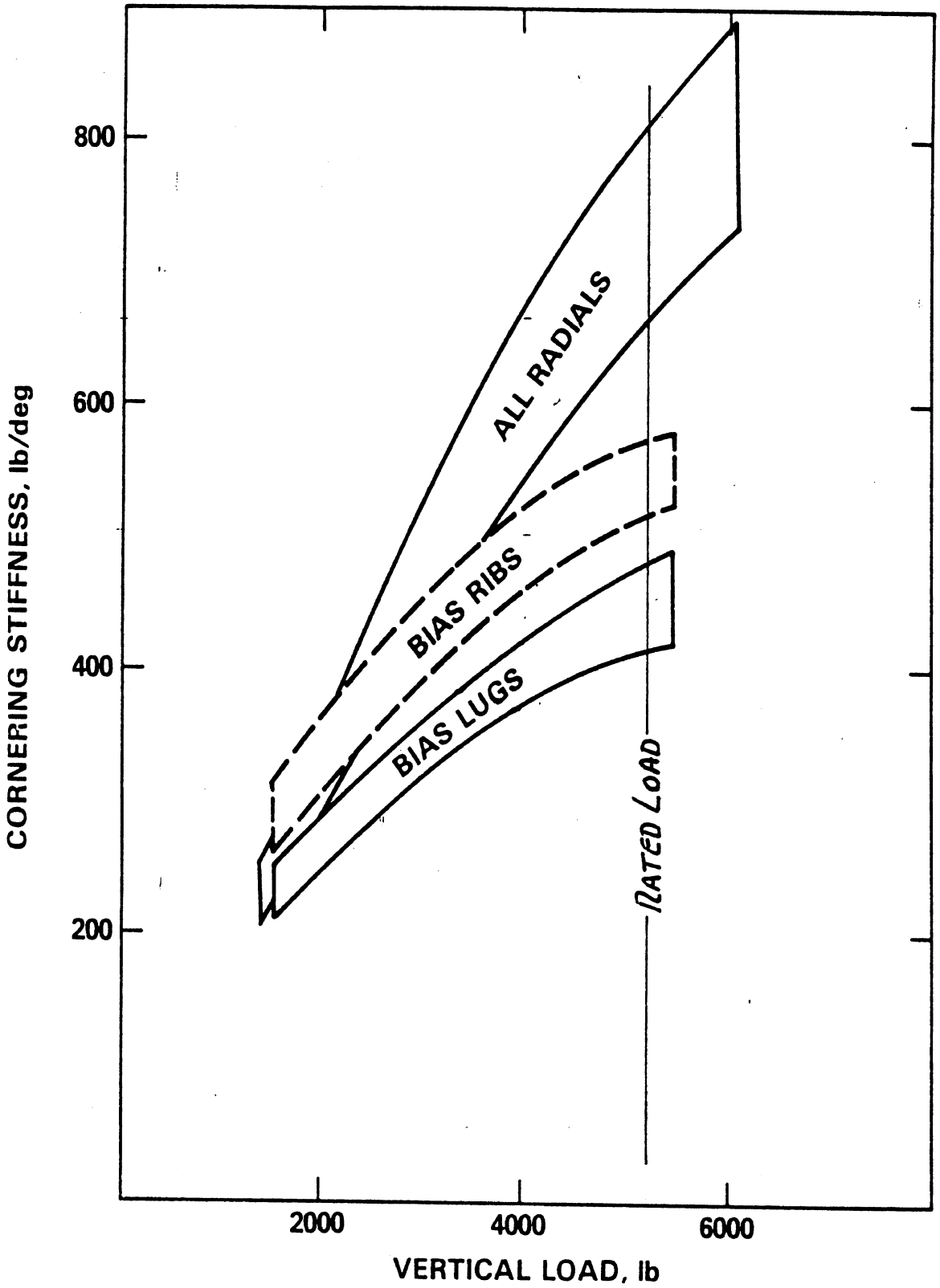

Figure 2.13 Envelopes of the cornering stiffness parameter measured over a range of vertical loads.

$$u = \left[\frac{F_{z_f}}{C_{\alpha_f}} - \frac{F_{z_r}}{C_{\alpha_r}} \right] \quad \text{deg/g}$$

where load and cornering stiffness values apply to single front (f) and rear (r) tires on the vehicle.

By this measure, tires whose C_α parameter rather linearly follows F_z (such as over most of the load range for many truck tires) provide little change in the vehicle's understeer level with addition in payload.

2.1.3 Sensitivity of C_α to Velocity. It is generally known that velocity does not significantly affect cornering stiffness of tires in the normal range of highway speeds. This basic insensitivity is due to the kinematic (rather than dynamic or inertial) nature of the mechanisms determining cornering stiffness. There may be rather academic exception to this rule for the case of partial hydroplaning during which the effective contact length is shortened and cornering stiffness is thereby decreased.

2.1.4 Sensitivity of C_α to Surface Texture or Friction. Cornering stiffness is basically unaffected by surface properties, as long as the surface itself is sufficiently rigid to react the developed shear forces without appreciable shear deflection of its own.

2.1.5 Sensitivity of C_α to Water Depth. Aside from the mentioned case of partial hydroplaning, cornering stiffness is insensitive to water depth.

2.1.6 Sensitivity of C_α to Carcass Construction. Cornering stiffness varies widely as a function of carcass construction variables. Looking at the three construction varieties of passenger car tires, Figure 2.14 illustrates the distributions of cornering coefficient, C_α/P where (P) is the design load for each tire [23]. We see that,

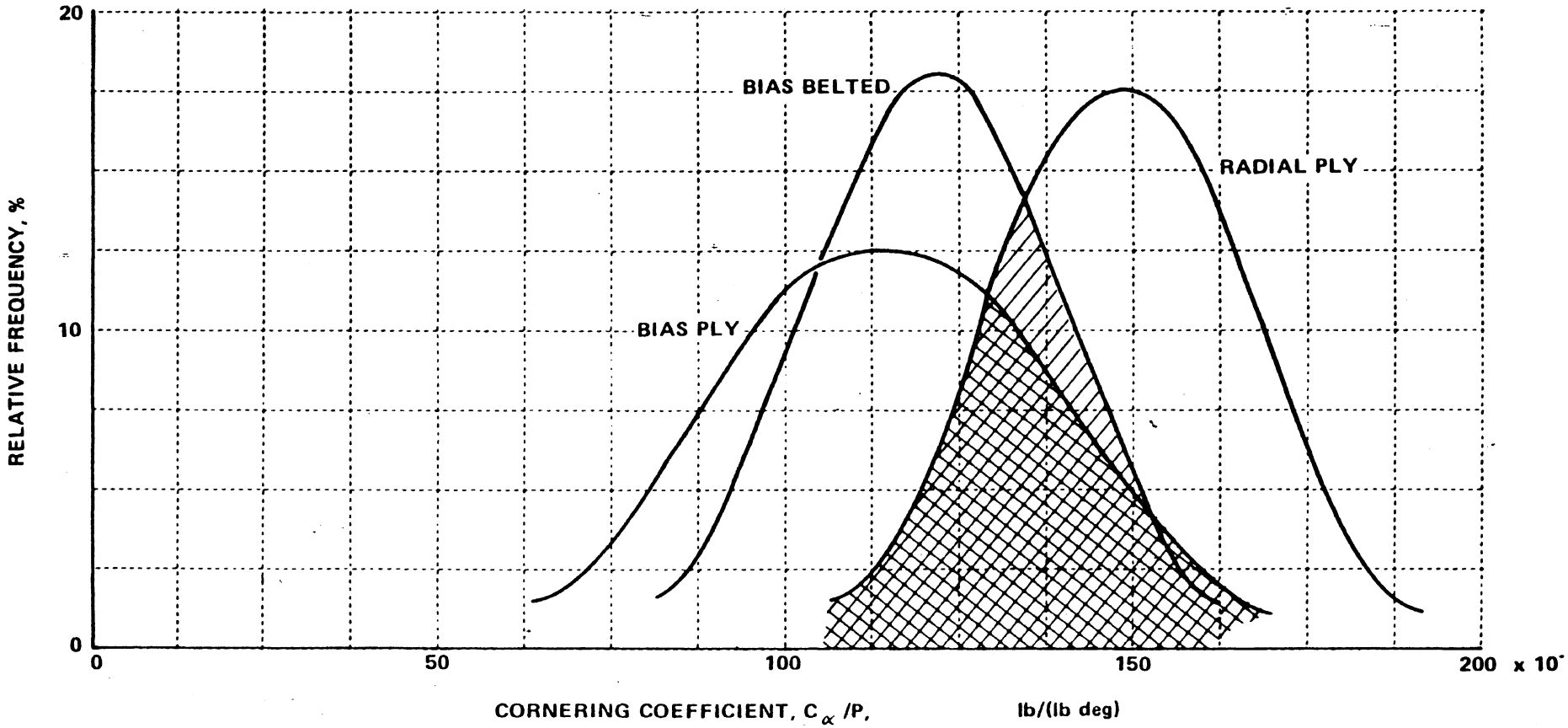

Figure 2.14 Distribution of cornering coefficients of passenger car tires (aspect ratio 78; 24 and 28 psi)

although radial tires indicate a mean level of cornering stiffness which is approximately 20% above that of bias-belted tires and 30% above that of bias-ply constructions, a large amount of overlap exists. Data shown earlier for truck tires (Fig. 2.13) showed that, for a more limited sample, heavy truck radials exhibit a mean level of C_α at rated load which is 42% higher than that of bias-ply tires. Regarding carcass details, information has been obtained which relates aspect ratio, belting material, and rim diameter to C_α. As seen in Figure 2.15, since aspect ratio number is connected to section width, a very large increase in cornering stiffness accompanies aspect ratio for tires of the same size designation [25]. While this figure also reveals a relationship between C_α and tire size designation, it should be noted that normalization of C_α by the design load accounts for the C_α versus tire size relationship. Accordingly, the data of Figure 2.15, all measured at one load, indicate that tires are commonly constructed to provide cornering stiffness levels proportional to their size designation and, thus, design loads.

Carcass ply materials and belting materials are known to markedly affect cornering stiffness. Examples of these effects are shown in Figures 2.16 and 2.17 [25]. Further, it is seen that belt plies, per se, generally contribute additional cornering stiffness over that provided without belting. Tempering these observations, however, is the fact that substantial differences in cornering stiffness can be seen between tires of similar generic construction but different manufacturer. Thus, a number of other pertinent construction parameters influence cornering stiffness, but have not been clearly quantified in the existing open literature. Shown in Figure 2.18, limited data also show a relationship between cornering stiffness and rim diameter [25].

2.1.7 Sensitivity of C_α to Tread Design. Insofar as the lateral compliance of the tread rubber constitutes a serial spring in the generation of a lateral force response to slip angle, tread design

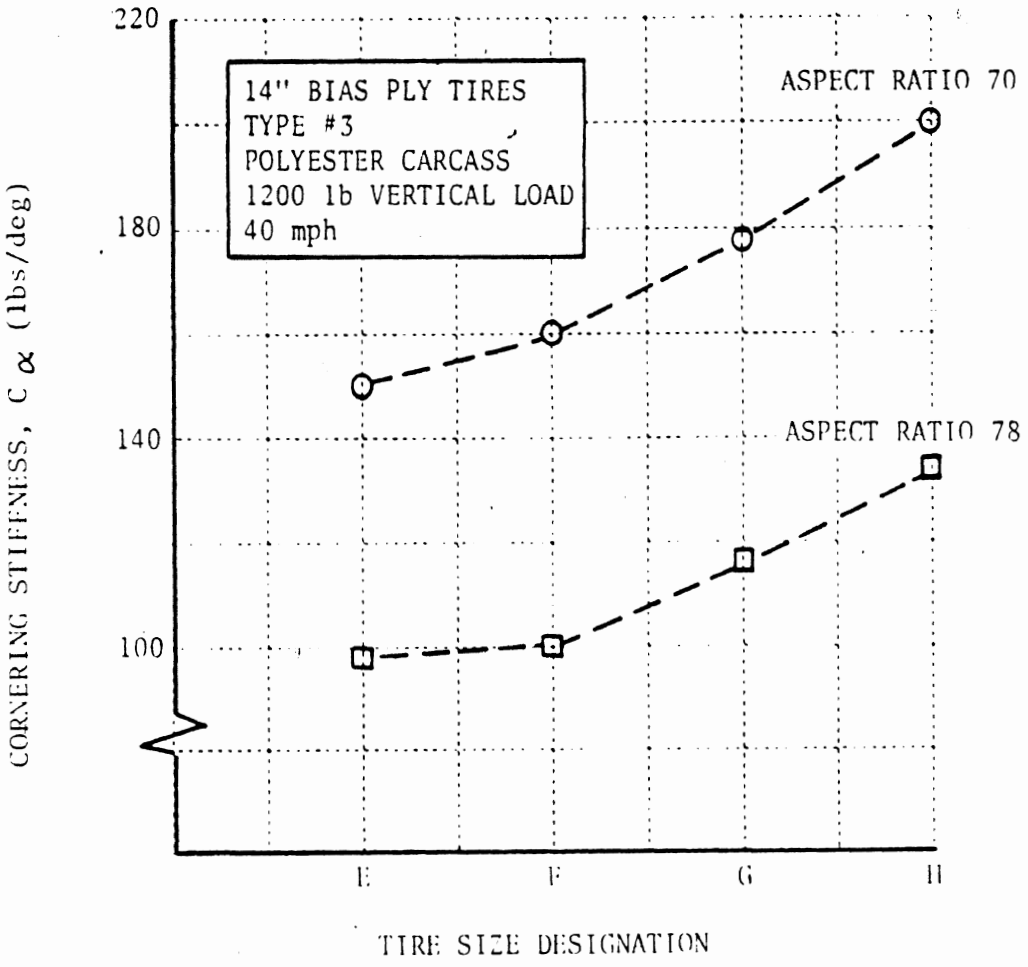

Figure 2.15 SIZE AND ASPECT RATIO EFFECTS ON CORNERING STIFFNESS OF BIAS PLY TIRES

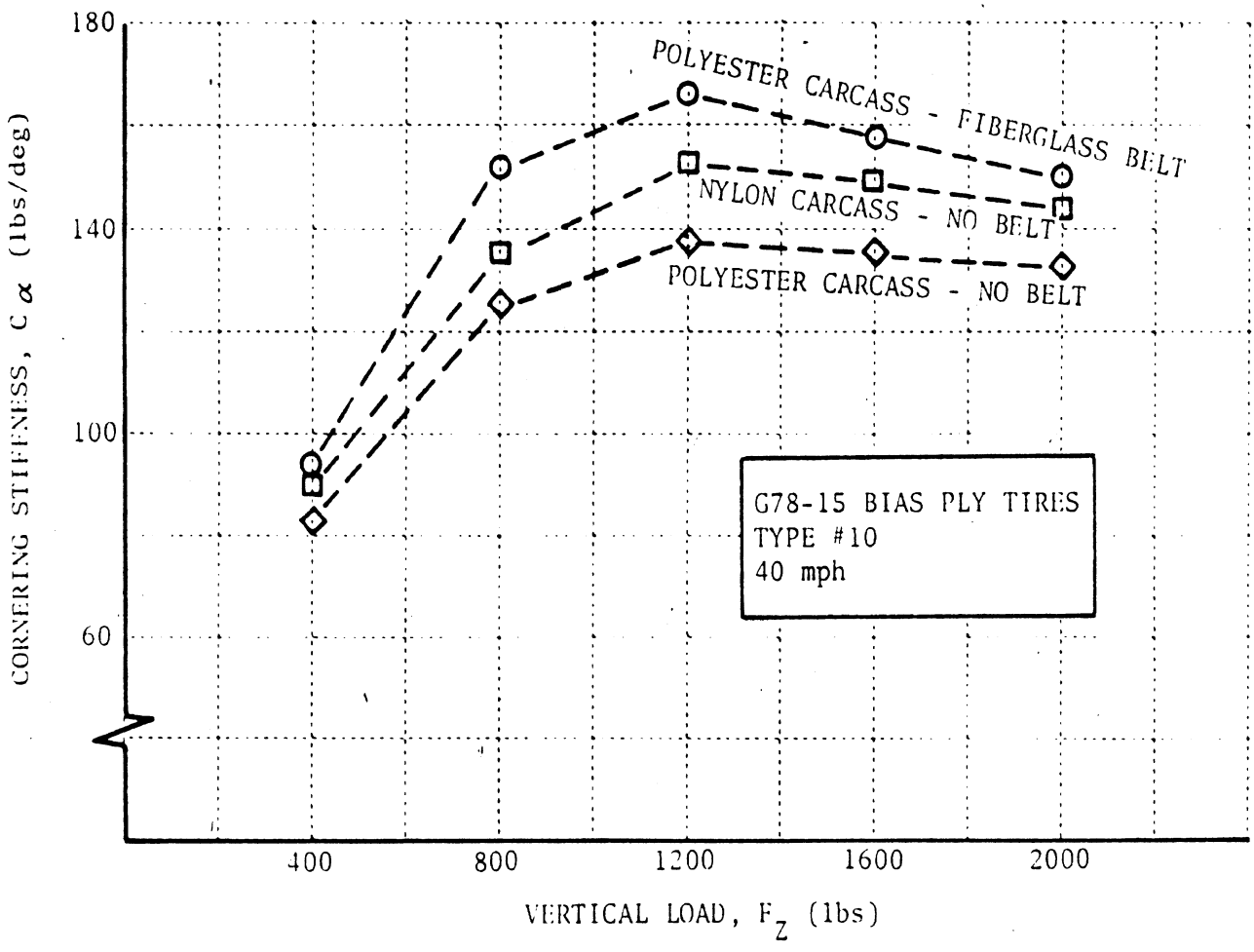

Figure 2.16 CARCASS MATERIAL AND BELTING EFFECTS ON CORNERING STIFFNESS OF BIAS PLY TIRES

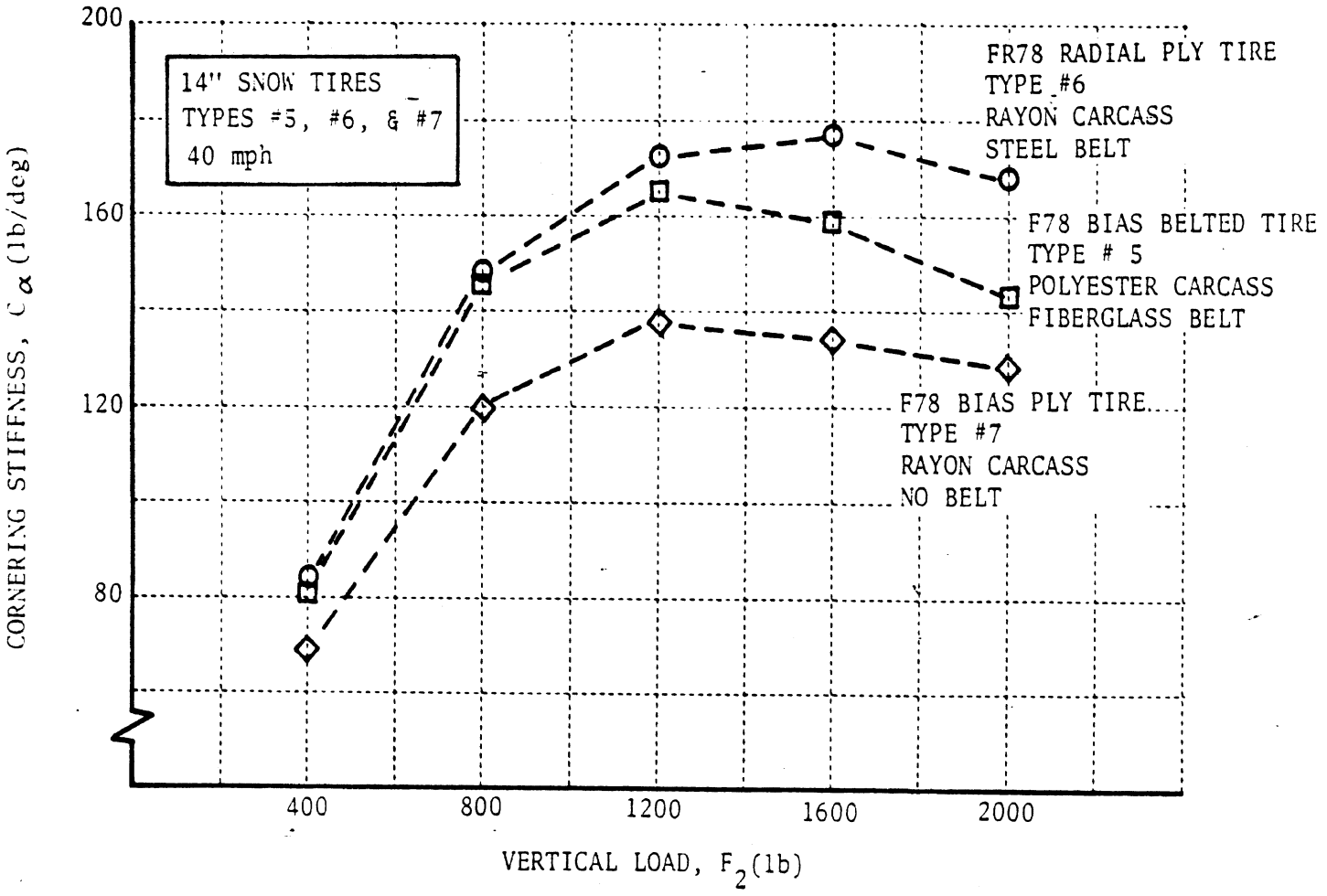

Figure 2.17 CONSTRUCTION AND MATERIAL EFFECTS ON CORNERING STIFFNESS OF SNOW TIRES

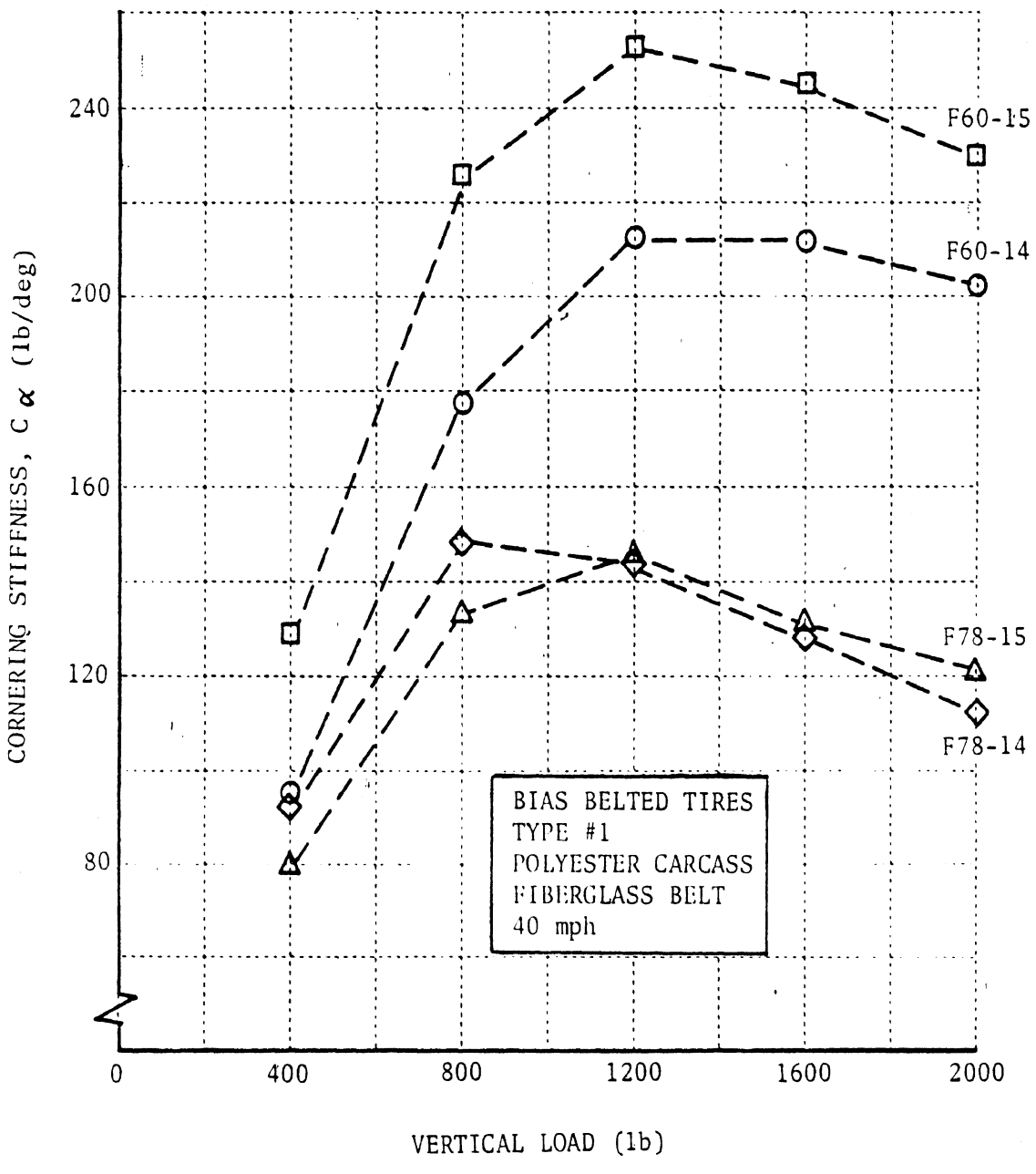

Figure 2.18 RIM DIAMETER EFFECT ON CORNERING STIFFNESS OF BIAS BELTED TIRES

is broadly recognized as a potential influence on cornering stiffness. It is generally known, for example, that bias-ply passenger car tires with snow-type tread patterns pproduce lower cornering stiffness levels than their respective rib tread counterparts. As shown in Figure 2.19 for a large sample of rib-tread and snow-tread tires of both bias and radial construction, however, the typical bias-ply snow-tread tire is approximately 5% lower, while the radial-type snow tread is approximately 10% higher in C_α than the corresponding rib-tread tires. This finding, while confirmed by other data sets which include a more confusing array of size variables [7, 25], is somewhat in conflict with the traditional notion that snow tires are categorically lower in cornering stiffness than rib-tread tires. It would appear that the traditional view was formulated in the era of bias tire dominance, for which the generalization was valid.

One should be cautious, however, to note that "survey data," such as that of Figure 2.19 which was taken on differing tire brands in the market, do not constitute a clear means of illustrating the relationship of two variables, exclusive of others. Thus, while generally lower values of C_α are not uniformly seen to accompany snow-type treads in these data, we must not conclude that compliant tread designs do not act to reduce cornering stiffness. Rather, we can be confident that, all other things being held fixed, changes in tread design producing more open patterns with deeper grooves and less support from one tread block or rib element to another will effect greater lateral compliance in the tread, and thus a reduction in cornering stiffness.

It is also well known that increasing tread wear produces an increase in cornering stiffness. Typical changes in C_α occurring due to a total wearing of the tread rubber down to a 2/32" depth condition are from 20% to 40% [e.g., see 2, 7].

2.1.8 Sensitivity of C_α to Tread Compound. It is not known that sensitivities of C_α to tread compound have been demonstrated. Presumably, increases in durometer (such as typically accompany increases

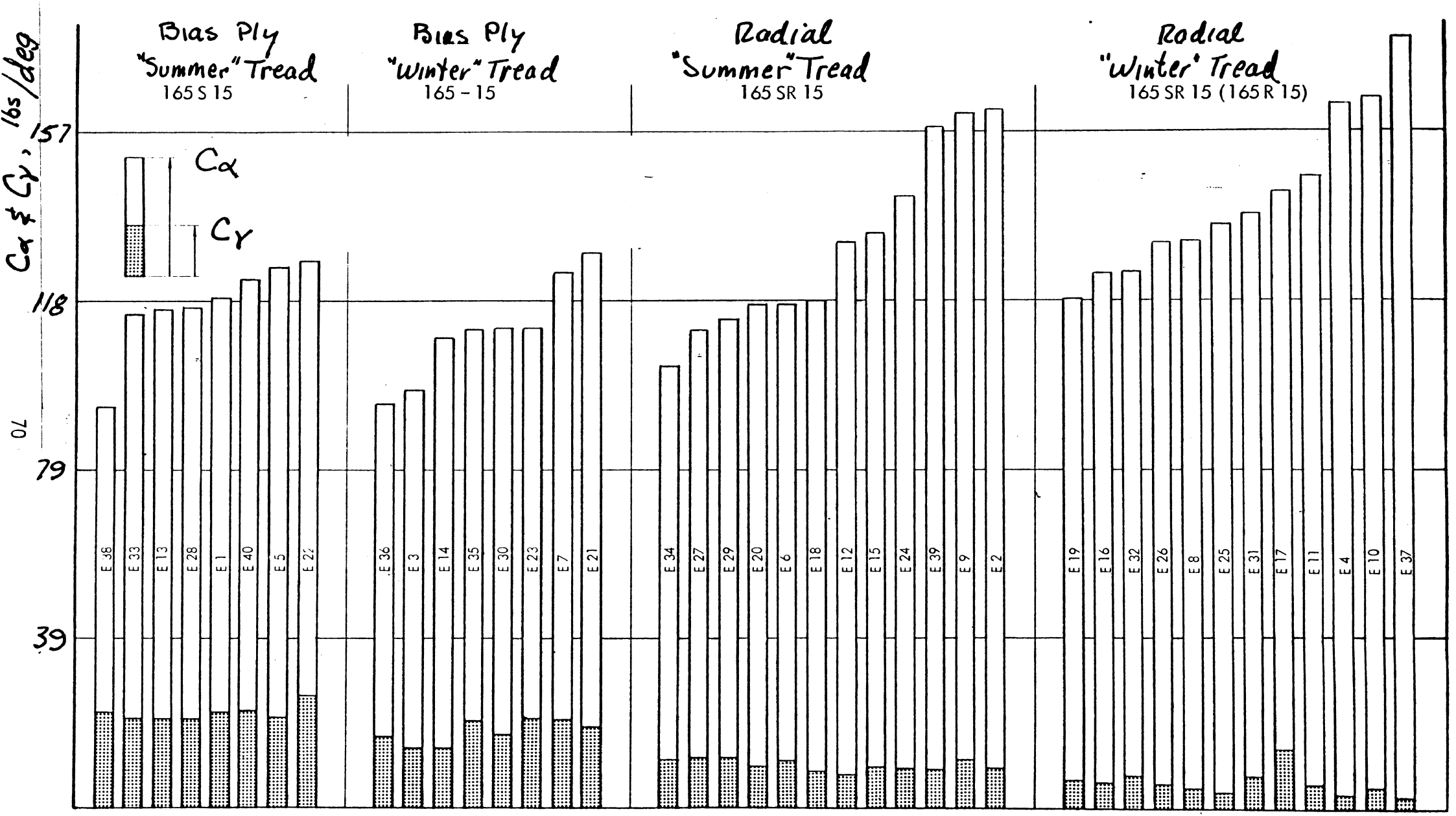

Figure 2.19 Cornering stiffness and camber stiffness levels at 1122 lbs load and 26 psi inflation.

in carbon black, for example) produce higher effective tread stiffnesses in all directions of loading. Accordingly, we could expect C_α to increase with increases in tread rubber durometer, or hardness. Such sensitivities would be expected to be rather small, however, especially in reflection on the small level of C_α sensitivities to tread pattern.

2.1.9 The Involvement of Cornering Stiffness in Determining the Maneuvering Properties of Vehicles. Cornering stiffness is a primary variable influencing the steady-state and transient cornering properties of vehicles in the normal driving regime. The most commonly cited maneuvering characteristic, understeer/oversteer level, is especially useful for quantifying the influence of C_α on steady turning behavior. As defined earlier, the understeer gradient, u, is determined by the balance of C_α values at front and rear tires, as ratioed to the respective front and rear loads. This measure relates to issues of steady-state "trim" by which, for example, increasing speed on a fixed radius turn will require either more or less steer input. If more steer input is required as speed is increased on a fixed radius turn, the vehicle is said to be understeer. Further, the value of the u parameter characterizes the number of additional degrees of front-wheel steer angle which will be needed to negotiate a turn at 1 g lateral acceleration, compared to the steer level needed in the limit 0 g condition. Thus the units of u are degrees/g.

For vehicles with oversteer (negative) values of u, the system becomes directionally or yaw unstable at some critical velocity. Thus it is generally desirable for u values to be positive, with most passenger cars designed to fall in the range of +3 to +7 deg/g. Shown in Figure 2.20 are the ranges in understeer coefficient, u, which might be expected with a typical compact sedan if outfitted with differing tire constructions [23]. The dark band adjacent to each vehicle sketch illustrates the range of understeer values which are possible, given ranges in C_α which are known to exist in the 1975-period tire market. Only small differences in u are observed when a single type of tire is distributed uniformly around the vehicle—whether the tire

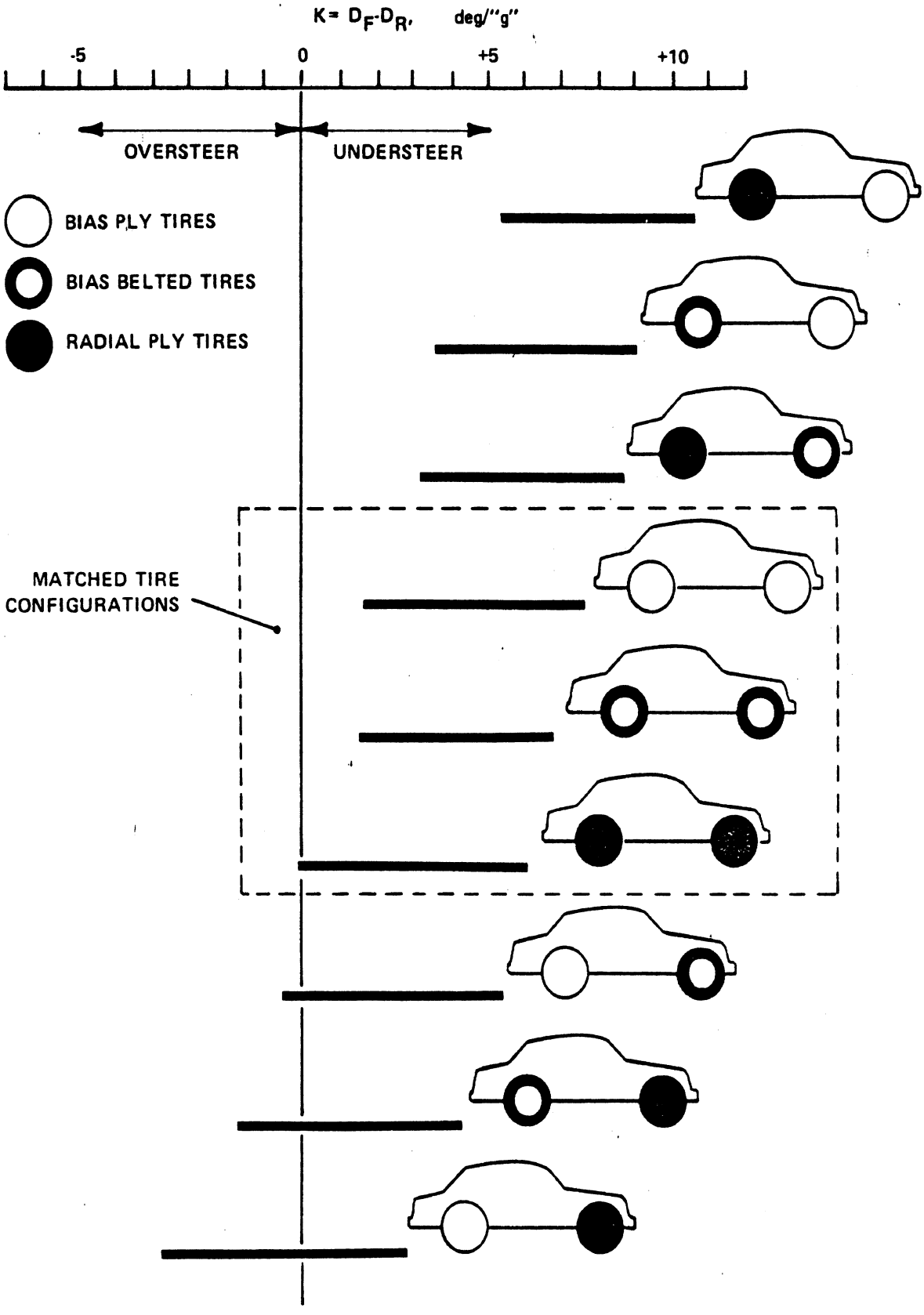

Figure 2.20 Cornering compliance ranges for various configurations of front/rear generic tire mix

is bias-, bias-belted-, or radial-ply construction. Large changes occur, however, when radial-ply tires are mixed with bias-ply tires.

Approximately the same level of sensitivity in u could be expected for heavy trucks if the tire "mixes" included bias-ply lug tires which exhibit especially low levels of C_α. Since many trucks and tractors employ lug tires on their drive axles, u factors of the oversteer polarity appear likely for certain vehicles [8].

Cornering stiffness is also a major determinant of vehicle transient yaw response in the low level maneuvering regime. Reducing the yaw response to a second-order motion, with damping ratio, ζ, and natural frequency, ω_n, [30] we find that C_α is involved through the understeer coefficient, u, and cornering compliances, D_f and D_r, per the relations:

$$\zeta^2 = \frac{1}{\left[1 + \frac{V^2 u}{\ell 57.3g}\right]}$$

and

$$\omega_n^2 = \frac{(57.3)^2}{D_f D_r V^2}\left[1 + \frac{V^2 u}{\ell 57.3g}\right]$$

where

V = forward velocity, ft/sec

ℓ = vehicle wheelbase, ft

g = gravitational constant, 32.2 ft/sec^2

D_f = front cornering compliance, deg/g (a summation of compliances including C_{α_f})

D_r = rear cornering compliance, deg/g

u = understeer coefficient, deg/g

Accordingly, we find that high values of understeer level produce small levels of yaw damping and high natural frequencies. Front and rear cornering compliance levels appear as a product in the denominator of the ω_n expression, reducing natural frequency as cornering compliance rises. Thus, while only the relative levels of front/rear cornering stiffness influence yaw damping, absolute levels of cornering stiffness influence yaw natural frequency.

2.2 Camber Stiffness, C_γ

The lateral force output per unit camber angle, termed camber stiffness, is a first-order mechanism influencing the cornering of motorcycles, a second-order mechanism for cars and other types of four-wheeled vehicles which have independent suspensions, and a generally insignificant mechanism in the case of heavy trucks. In absolute value, the C_γ value of a tire is typically in the range of 10% to 20% of its C_α value. In the case of the motorcycle, this low-stiffness function becomes the primary one because of the need to incline the motorcycle to achieve roll equilibrium in a turn. The inclination needed for roll stability results in lateral force due to camber—typically with such a close match to the side force needed for yaw equilibrium that negligible tire slip angle results.

Cars and other vehicles with independent suspensions produce wheel camber in one of three ways. At the independently-suspended wheels, camber is equal to the body roll angle plus the angle determined by the kinematic articulation of the suspension linkage.

For the solid axles on cars and for the all-solid axle configurations on heavy trucks, camber is produced only as a result of the difference in vertical deflection between left- and right-side tires.

2.2.1 Sensitivity of C_γ to Inflation Pressure.

There is no general rule concerning the sensitivity of camber stiffness to inflation pressure. As shown in Figure 2.21, passenger car tires of

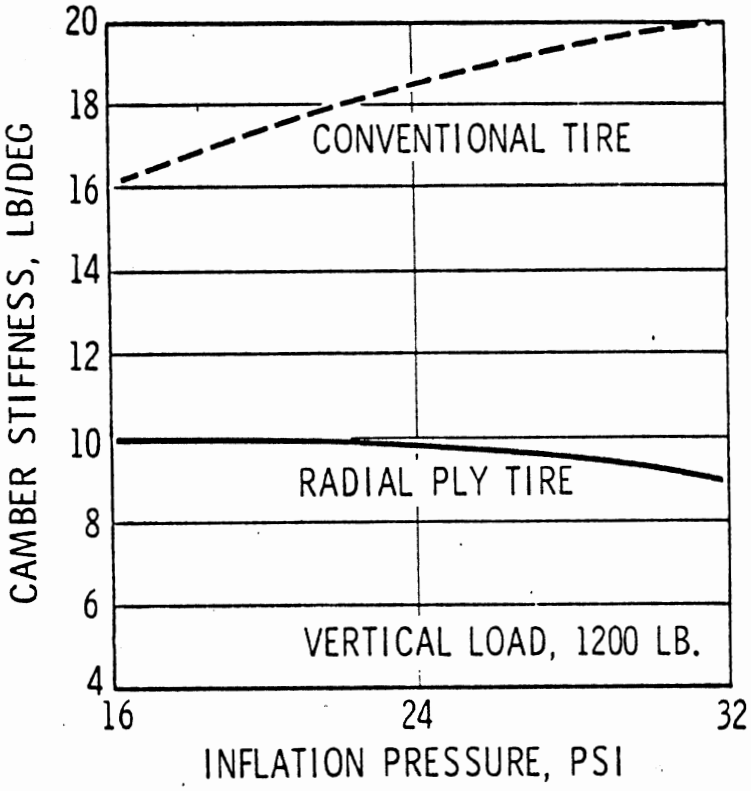

Figure 2.21 Camber Stiffness-Inflation Pressure

bias and radial construction show, respectively, increasing and decreasing sensitivities to inflation pressure [24]. Limited data available for motorcycle tires indicate no significant sensitivity of C_γ to inflation pressure [31].

2.2.2 Sensitivity of C_γ to Vertical Load. As indicated by a typical bias-ply car tire in Figure 2.22, camber stiffness is a mild function of vertical load, in the vicinity of the design load [25]. Looking at the slopes of the four (F_y) curves at their abscissa intercepts, we see that C_γ increases by 20% over the load interval 600 to 1800 lb. As seen in Figure 2.23, bias-ply heavy truck tires are known to exhibit at least at 200% increase in C_γ over the load range 2000 to 8000 lbs [2]. Camber thrust data from a typical motorcycle tire are shown in Figure 2.24, indicating that the initial slope, C_γ, is almost directly proportional to vertical load, increasing by a factor of 7 over the load range 100 to 700 lbs [31]. It should be noted, however, that since motorcycles experience virtually no dynamic load changes during pure cornering maneuvers, the load sensitivity behavior shown in Figure 2.24 is significant only to changes in the static loading conditions.

2.2.3 Sensitivity of C_γ to Velocity. Although the mechanisms of interaction are not known to have been explored, data taken on motorcycle tires do show a substantial interaction between camber coefficient, C_γ/F_z, and velocity, especially at speeds above legal highway levels. Shown in Figure 2.25 are C_γ/F_z data for eight motorcycle tires at speeds of 30, 60, and 90 mph [32]. Perhaps it is most generally useful to note that only small sensitivities are seen within the legal speed range on either wet or dry surfaces.

Generally speaking, since camber stiffness is a property primarily deriving from structural deflection properties of the tire, velocity should not influence behavior until speed levels are reached at which centrifugal loading acts to stiffen the tire.

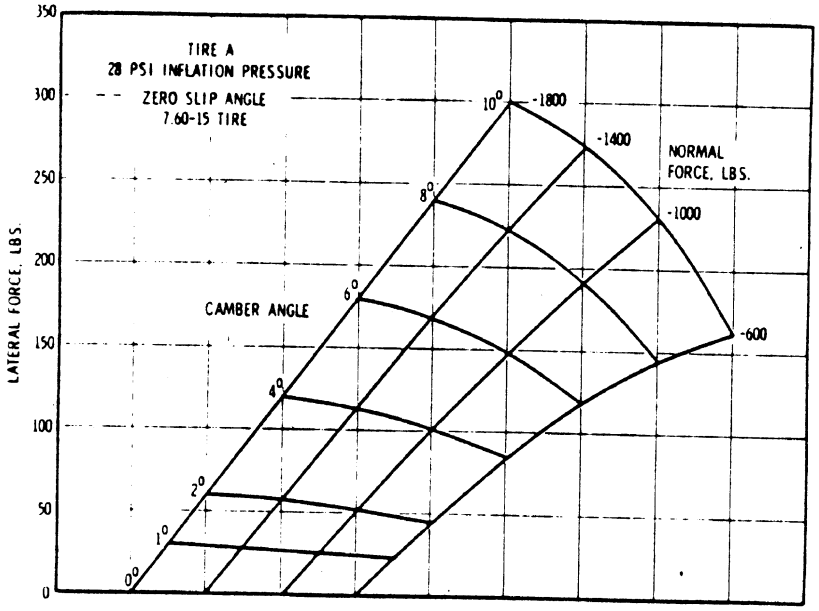

Figure 2.22 Carpet Plot of Camber Thrust vs Camber Angle and Load.

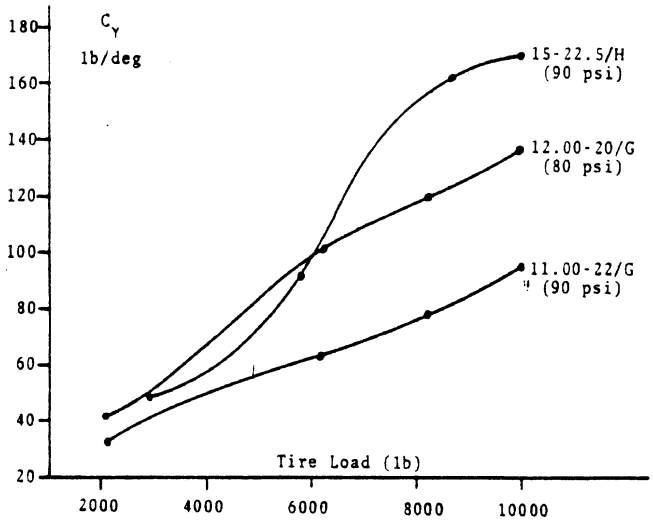

Figure 2.23 C_Y vs F_Z Relationship for Truck Tires.

Figure 2.24 *RIBBED-TREAD, 5.00-16, 18 psi, 40 mph, Dry, SN = 7580, TIRE DATA.*

CAMBER THRUST AT ZERO SLIP ANGLE vs CAMBER ANGLE.

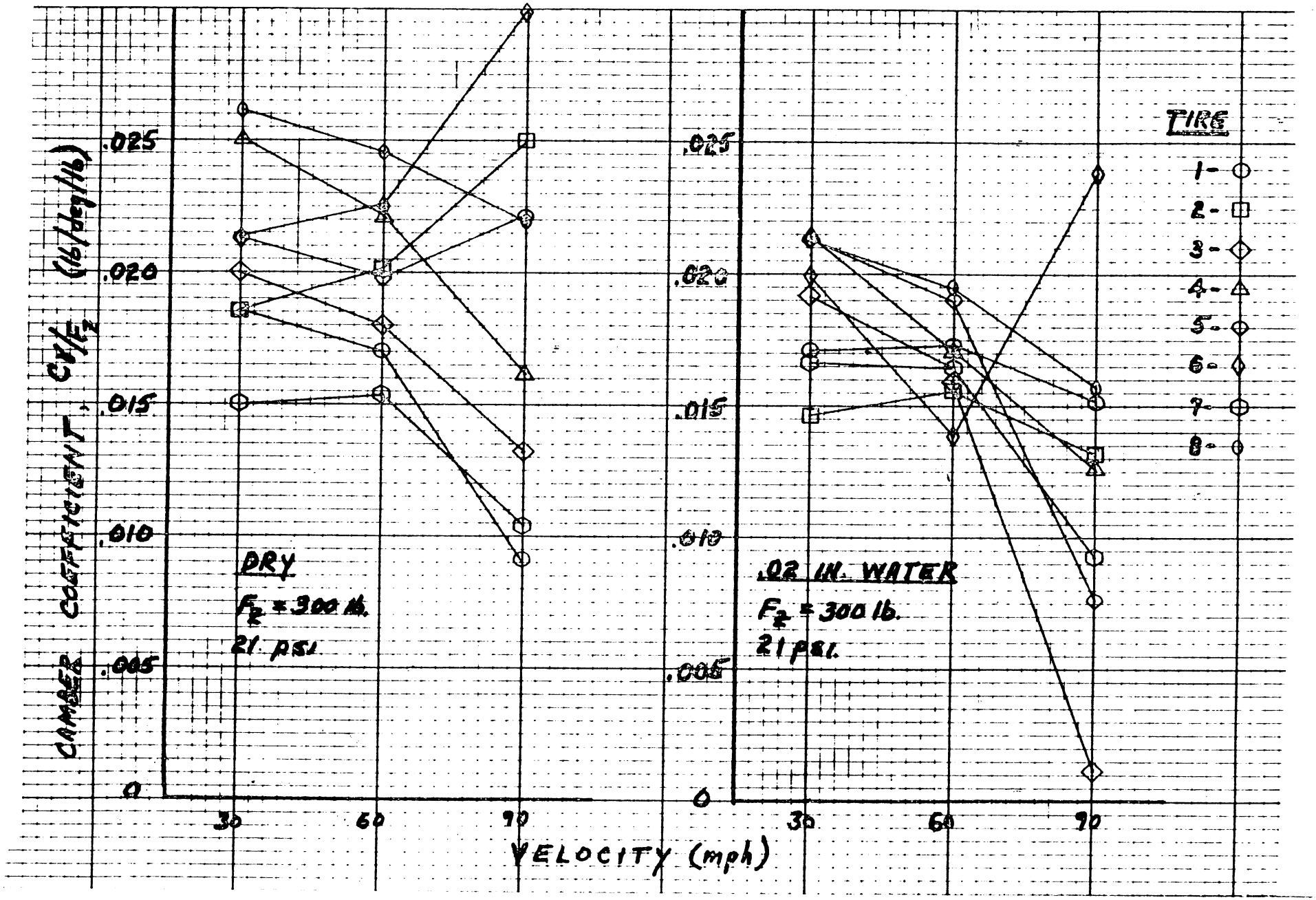

Figure 2.25 C_γ/F_z Values for Motorcycle Tires on Wet and Dry Surface.

2.2.4 Sensitivity of C_γ to Surface Texture. Insofar as the textural properties of paved surfaces only determine the limiting levels of frictional coupling, surface texture is unrelated to the determination of C_γ.

2.2.5 Sensitivity of C_γ to Water Depth. Except for cases of water film thicknesses which begin to reduce contact length due to partial hydroplaning, C_γ will be unaffected by water depth.

2.2.6 Sensitivity of C_γ to Carcass Construction. Large changes in C_γ are known to accompany differences in tire carcass construction. Shown in Figure 2.26 are distributions of C_γ for passenger car tires of radial, bias, and bias-belted construction [23]. As seen, radial passenger car tires are generally known to provide C_γ values which are in the range of 40-50% of the level exhibited by bias-ply and bias-belted tires. Looking at a large number of tires of identical size, the reader is referred back to Figure 2.19 to note C_γ values for bias- and radial-construction passenger car tires. These data confirm that the radial-ply tire provides C_γ values which are about 40% of the level seen in bias-ply tires.

Regarding truck tires, very limited data is available describing the camber stiffness changes which accompany carcass design. It has been generalized, however, that radial truck tires are less sensitive to inclination angle (than bias tires) by a "factor of two or three" [33].

Radial tires are not made for motorcycles because of the conflict between the low C_γ level of radials and the fact that motorcycles are primarily dependent upon the camber thrust mechanism for cornering force.

2.2.7 Sensitivity of C_γ to Tread Design. Camber stiffness is known to be sensitive to the gross compliance of the tire tread, increasing by a large fraction as a higher stiffness tread matrix is employed. Referring back again to the forty-tire sample of passenger

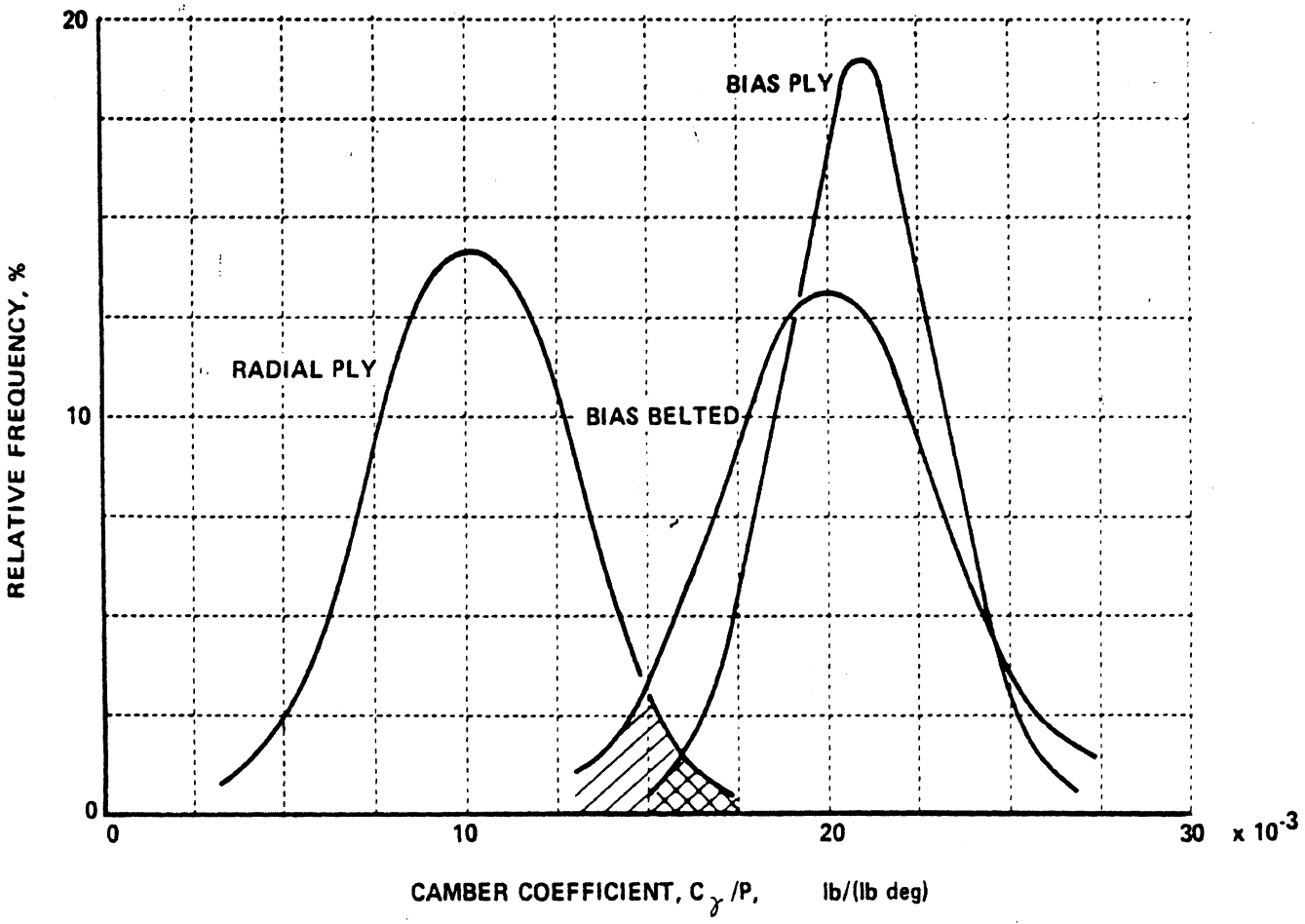

Figure 2.26 Distribution of camber coefficients of passenger car tires (aspect ratio 78; 24 and 28 psi)

car tires in Figure 2.19, it was seen that "winter-type" treads of bias- and radial-carcass construction yielded from 20 to 40% lower C_γ values than the denser "summer-type" tread patterns.

With truck tires, limited data show lug-type patterns producing a 30 to 40% lower C_γ value than that found with rib-type tread patterns. Also, when rib-type car and truck tires become worn, the resulting increase in tread stiffness is known to increase C_γ by 15% to 100% [7, 2].

Data available for motorcycle tires at light loads show that a fully-treaded rib tire can yield a C_γ level which is 50% below that provided by a "slick," or untreaded tire. At maximum load, however, no difference in C_γ is seen between the rib-treaded and smooth-type tread [31].

2.2.8 Sensitivity of C_γ to Tread Compound. It is not known that sensitivities of C_γ to tread rubber compound have been demonstrated. As stated earlier in regard to C_α sensitivities to compound, it is suspected that influences on C_γ are small within the range of commercially practicable tread rubber materials. Whatever C_γ sensitivities as do exist most probably relate to differences in the durometer reading which characterizes the tread.

2.2.9 Significance of C_γ to the Maneuvering Properties of Vehicles. As stated, the motorcycle and, indeed, any two-wheeled vehicle, employs camber thrust as its primary cornering force. For a given motorcycle, the vehicle is capable of "a perfect turn" when camber thrust is generated at each tire precisely at the level needed for side force equilibrium, without slip angle. The lateral force coefficient, F_y/F_z, needed for this "perfect turn" condition is equal to the tangent of the motorcycle roll angle, ϕ. Shown in Figure 2.27 are F_y versus γ data for differing values of slip angle, α, as measured on a typical motorcycle tire [31]. Overlaid on this plot is a dashed curve, $F_y = 291 \tan \phi$, showing the side force needed for equilibrium at each roll (or camber) angle for a vertical load of 291 lbs.

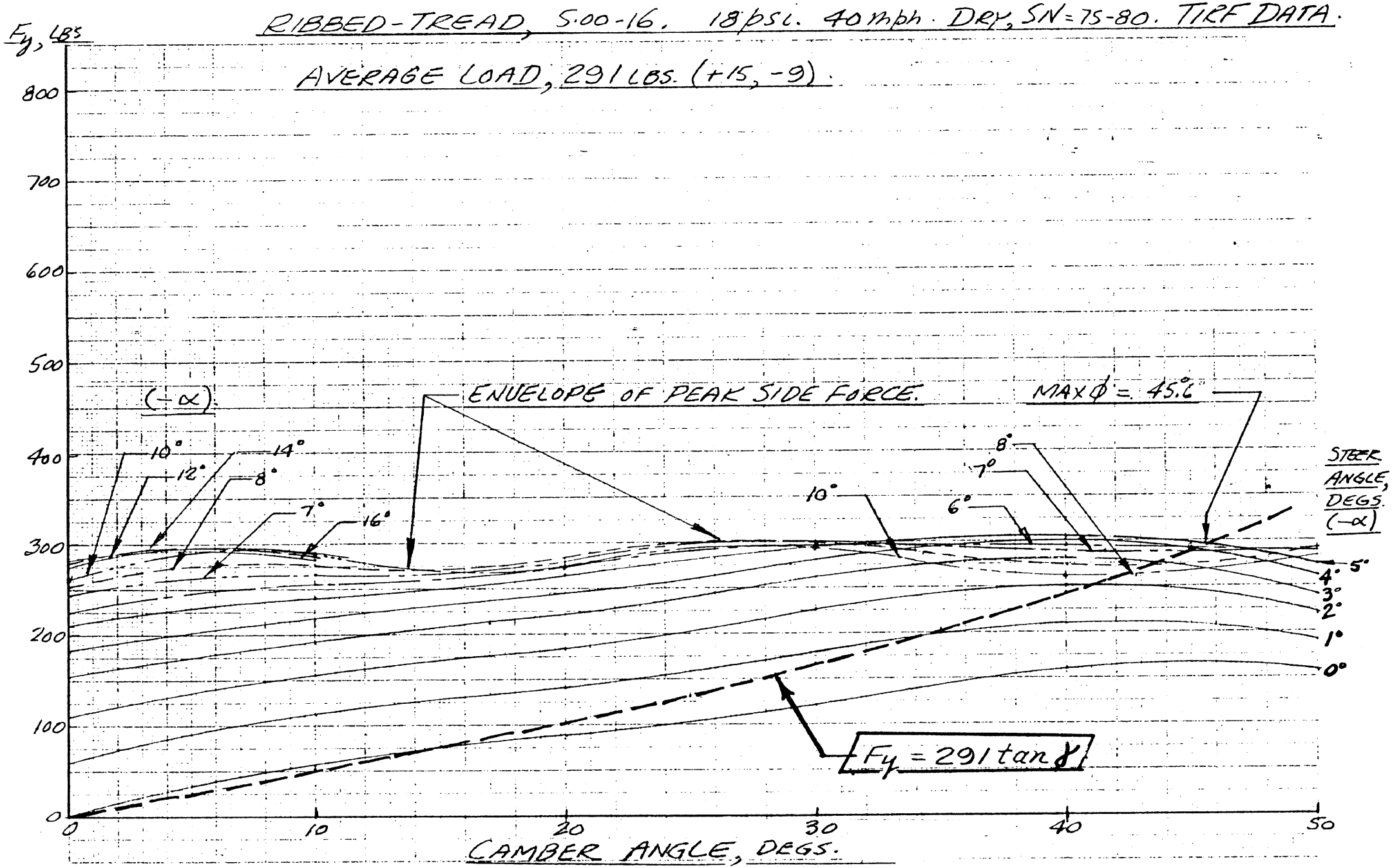

Figure 2.27 F_y vs γ for Different Values of Slip Angle, Showing the (F_z tan γ) Line.

Comparison of the 291 tan ϕ curve with the zero slip angle curve indicates that the tire/load combination permits a virtually perfect turn up to the 20° camber angle condition (.36 g's lateral acceleration). Beyond that condition, increasing slip angle is needed to obtain side force equilibrium. It can be seen that the perfect turn feature places the simple requirement that C_γ be equal to the slope of the F_z tan ϕ function, or, setting $\gamma = \phi$,

$$C_\gamma = \left.\frac{d(F_z \tan \gamma)}{d_\gamma}\right|_{\gamma=0} = .0175F_z \text{ lb/deg}$$

or, camber coefficient, $C_\gamma/F_z = 0.0175$. Looking at the sample of data for eight motorcycle tires which was shown in Figure 2.25, we see that when running in .02 inches of water, most of the tires are capable of producing a nearly perfect turn while much of the dry data shows C_γ/F_z values which are somewhat higher than the "perfect" value, indicating that opposing side force due to slip angle will be needed to maintain turn equilibrium. These data reveal, however, that motorcycle tires are commonly constructed to closely approximate the perfect turn capability. Nevertheless, the precision with which the perfect turn condition is achieved is of unknown significance to the actual controllability of motorcycles. At the present time, the perfect turn is at least of academic interest while serving as a useful reference in explaining the involvement of C_γ in the maneuvering behavior of two-wheeled vehicles.

Regarding the involvement of C_γ on passenger car handling, the most important influence concerns the additional understeer contribution which derives from roll camber of an independent front suspension. This effect, which most clearly distinguishes between radial- and bias-ply tires, accounts for approximately 25% of the understeer in a typical compact sedan [34].

Finally, as stated earlier, camber thrust plays a negligible role in the handling behavior of vehicles with solid-axle suspensions, such as heavy trucks.

2.3 Peak Lateral Traction Coefficient, μ_y

The peak side force, normalized to vertical load, is a tire property relevant to the cornering limits attainable in emergency conditions. Being of much lower overall significance to vehicle safety than longitudinal traction limits, it has been given less treatment by the technical community.

2.3.1 Sensitivity of μ_y to Inflation Pressure. Inflation pressure is known to have influences on μ_y which are similar to those discussed earlier for the longitudinal limits, μ_p and μ_s. As shown in Figure 2.28, data taken at three different pressures show a dramatic reduction in F_y at 15° slip angle and with increasing loads [35]. While one could assume that data shown in this figure for the 1000-lb and 1500-lb levels of F_z illustrate the true μ_y saturation levels, data taken at higher loads probably do not represent side force saturation because 15° is somewhat lower than the needed level of slip angle. Similar data shown in Figure 2.29 clearly show that inflation pressure most influences side force production at high loads, and that tires at lower inflation pressures arrive at side force saturation at substantially higher values of slip angle [7]. Shown in Figure 2.30 is the effect of inflation pressure on the speed sensitivity of μ_y for a cross-ply car tire running in .040 inches of water [36]. We see that inflation pressure has only a slight influence on μ_y in the range of normal highway speed. Shown in Figure 2.31, a truck tire at low speed produces a mixed picture of μ_y sensitivity to inflation pressure [2]. While it is clear that the slip angle value needed for side force saturation is increasing as pressure reduces, it would appear that the μ_y limits are also increasing—in contrast to data shown for passenger car tires. It is believed that the influence of inflation pressure on μ_y has not been reported for either truck or motorcycle tires running at highway speeds.

2.3.2 Sensitivity of μ_y to load. There is known to be a rather strong dependence of μ_y on load for all types of tires. Data

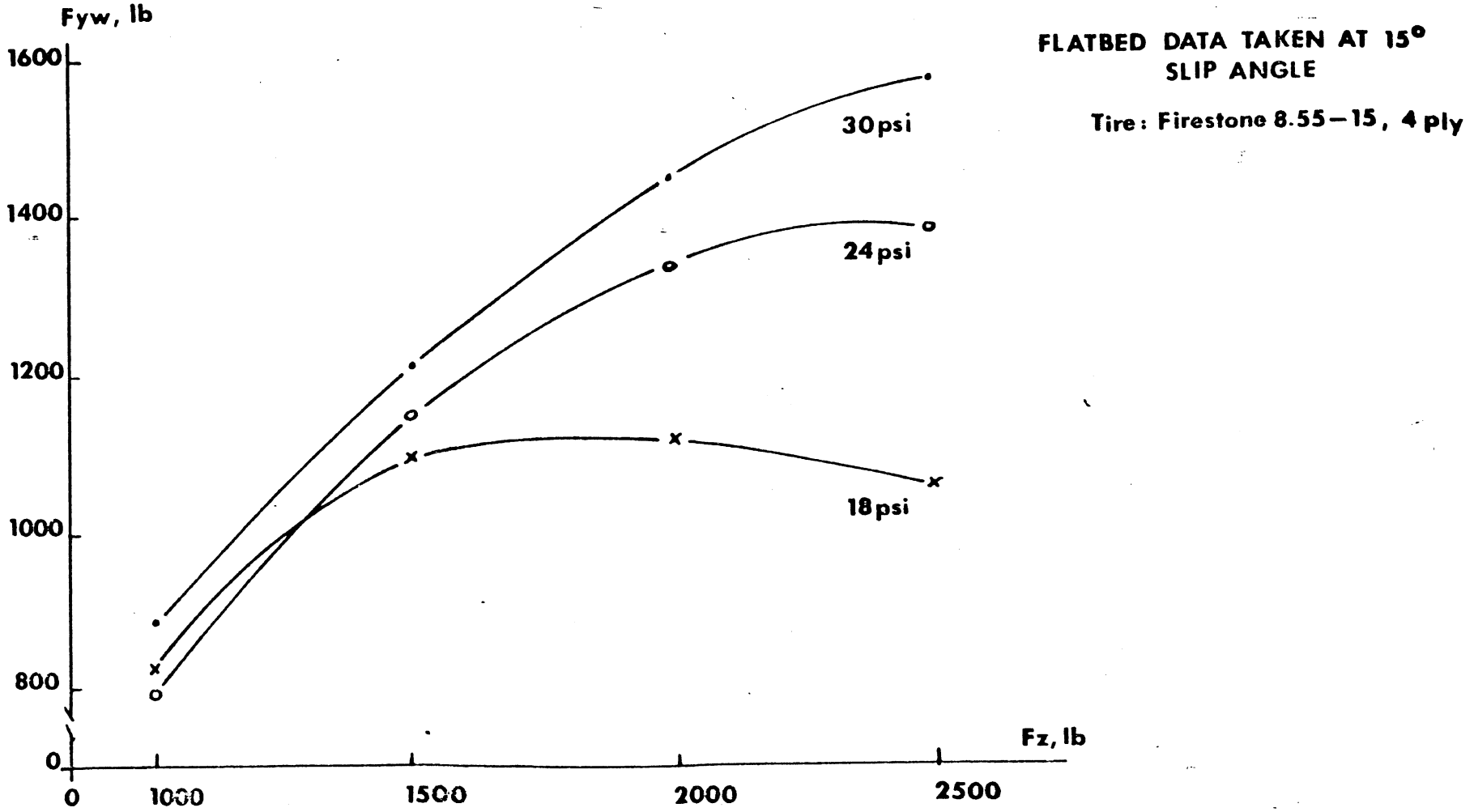

Figure 2.28 The Influence of Inflation Pressure on Maximum Lateral Force at 15° Slip Angle

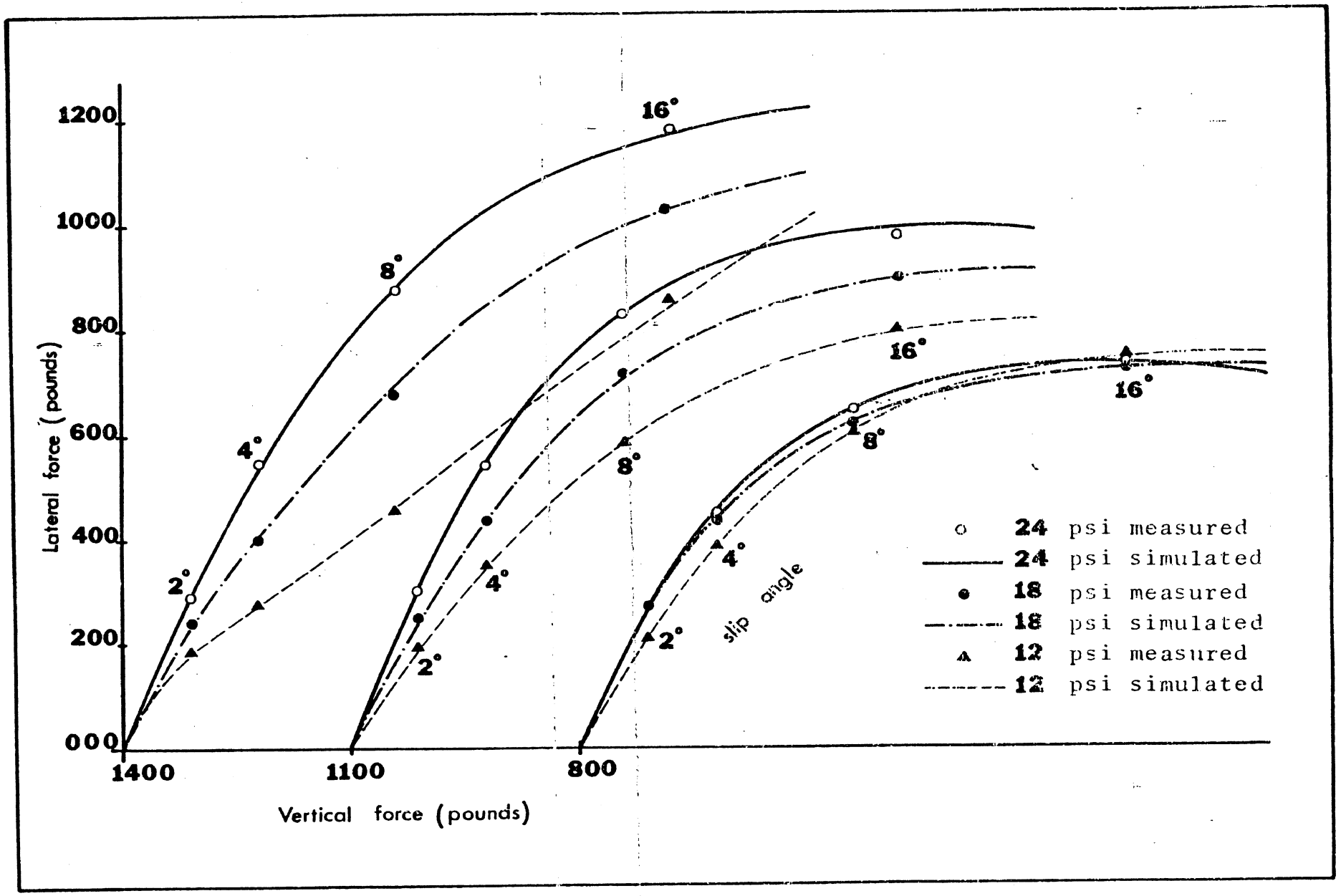

Figure 2.29 Lateral force vs. slip angle at various inflation pressures B.F. Goodrich Silvertown Belted E78-14, dry asphalt.

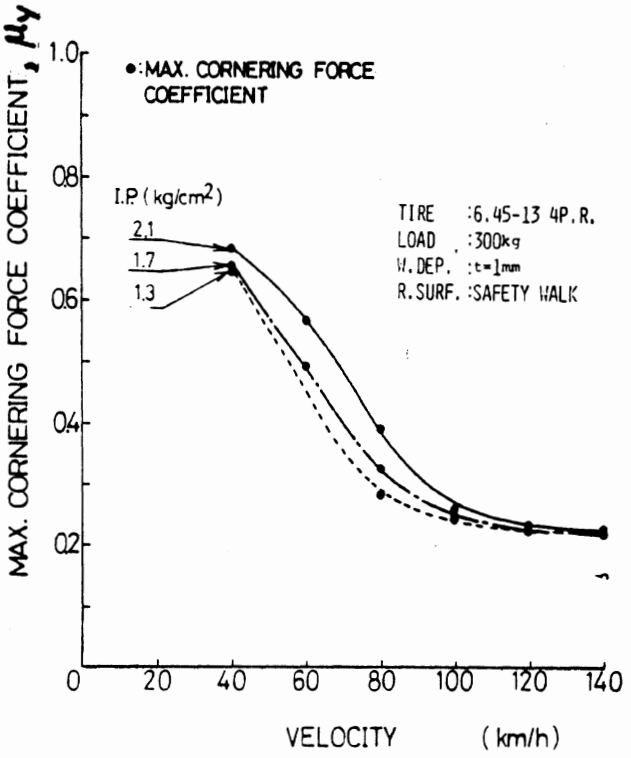

Figure 2.30 Effect of Inflation Pressure on μ_y; Bias Ply Tire.

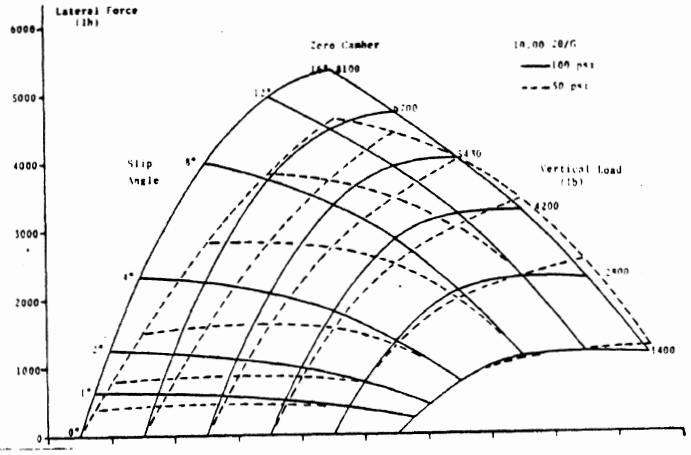

Figure 2.31 Lateral force versus slip angle and vertical load on 10.00-20/G tire at rated pressure (100 psi) and at 50 psi

taken on laboratory machines documenting this interaction are commonly presented in their non-normalized carpet plot fashion, such as in Figure 2.32 [28]. Analysis of the μ_y measures of these data show that μ_y decreases rather steeply in the range of 25% to 100% of design load, and then decreases with a reducing slope as load continues to increase. Typical reductions in μ_y for passenger car tires would appear to be as follows in Table 2.1 for the case of a dry, high friction surface [28].

Table 2.1. Typical μ_y Dependence on Load, as a Function of the Tire's Design Load.

$F_z/F_{z(\text{Design Load})}$	μ_y
.25	1.00
.50	.92
.75	.85
1.00	.79
1.25	.75

Shown in Figure 2.33 are typical F_y/F_z data, up to the μ_y saturation level, for a heavy truck tire at three different loads [8]. We see that μ_y decreases by 25% over the load range from 50% to 150% of rated load. These reductions of μ_y with load are typical for both dry and wet surface conditions.

2.3.3 Sensitivity of μ_y to Velocity. As with peak longitudinal traction, μ_p, it is known that the lateral limit, μ_y, is strongly sensitive to velocity on wetted surfaces but only slightly influenced by velocity on dry surfaces. For wetted surfaces, it is known that velocity sensitivity is highly dependent upon surface texture and tire tread pattern. As shown in Figure 2.34, four wetted surfaces and four different car tires produce a very broad array of velocity sensitivities in μ_y [37]. For the key to surfaces and tires

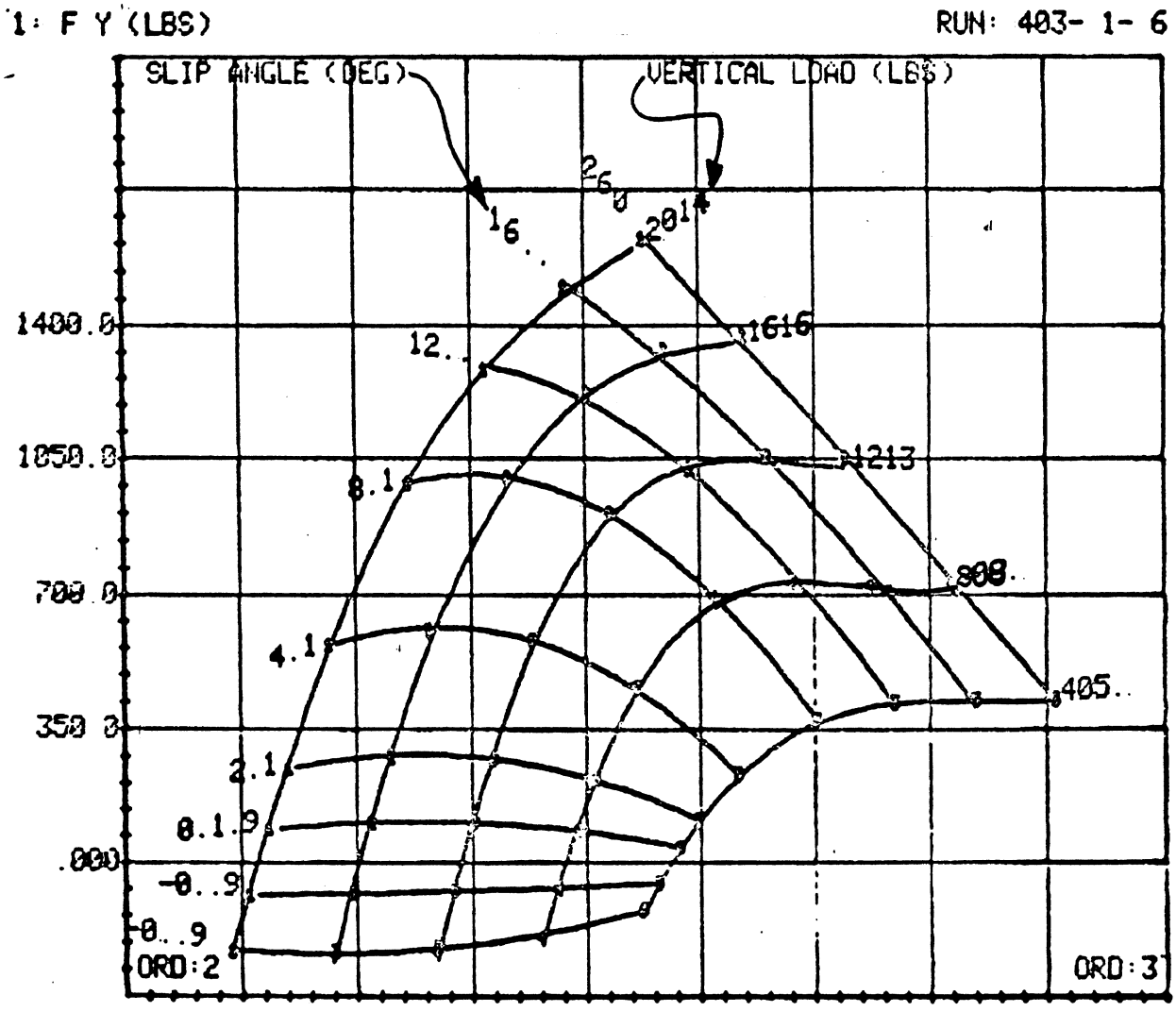

Figure 2.32 Carpet Plot Showing F_y vs α and Load.

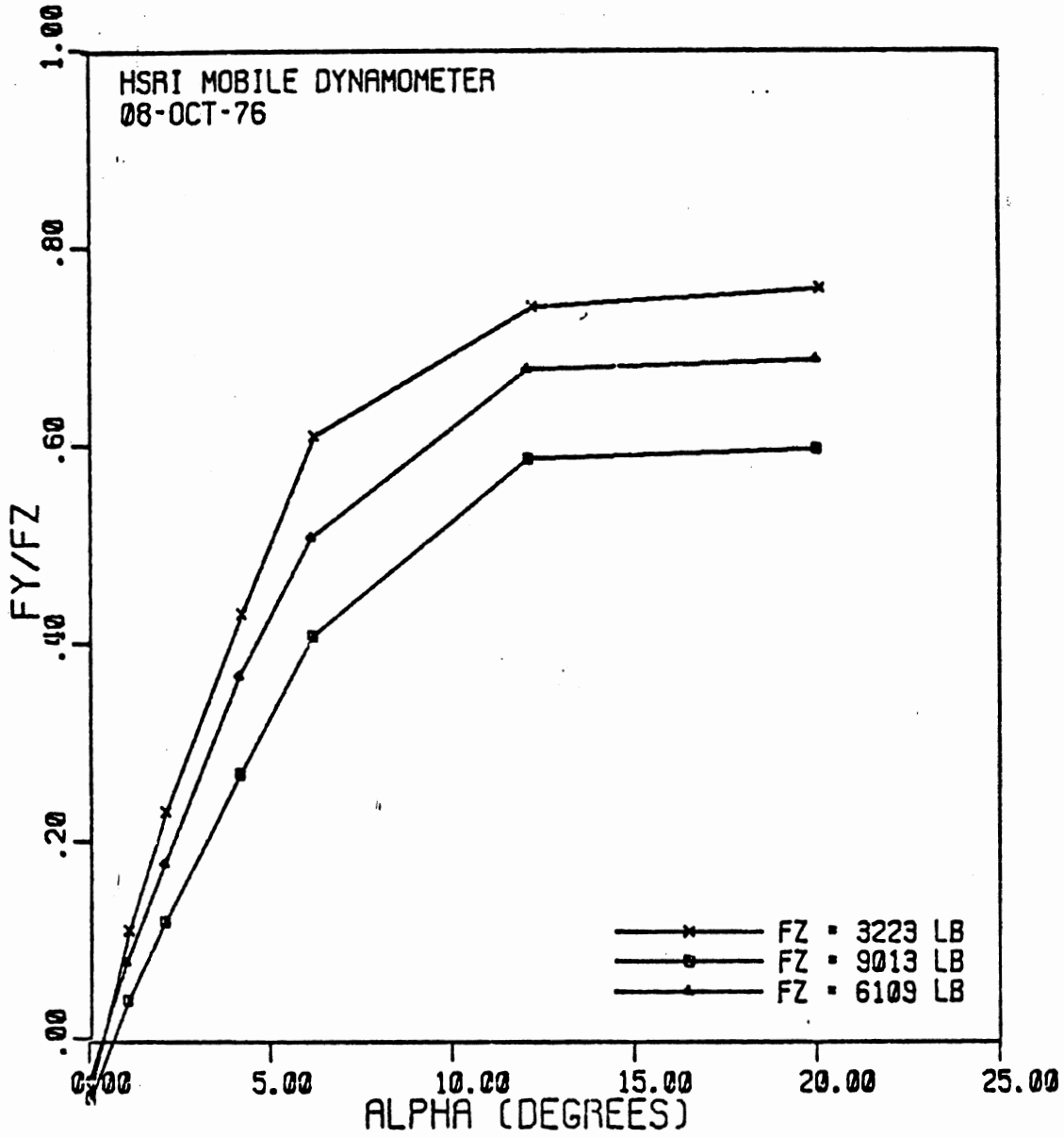

Figure 2.33 Normalized lateral force versus slip angle for nominal tire loads of 0.5, 1.0, and 1.5 times T&RA rated load. The radial, 10:00R20, load range G, Firestone Transteel Traction tires were tested on a wet Portland cement concrete surface. Nominal vehicle speed was 20 mph.

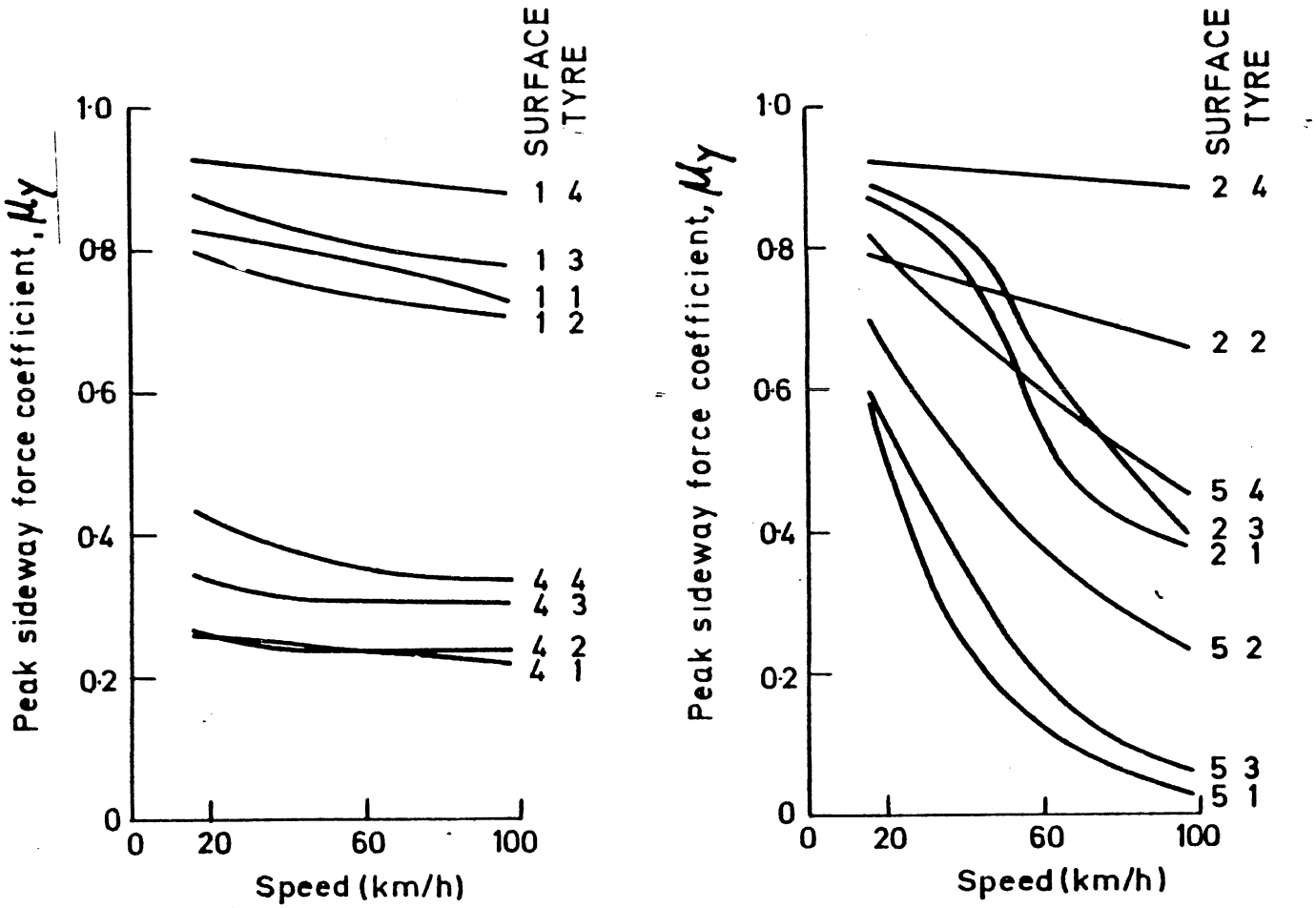

Figure 2.34 The Effect of Speed on μ_y for Different Passenger Car Tires (See Table 2.2) and Surfaces (See Table 2.3).

in this figure, see Table 2.2. It can be seen that velocity sensitivities (that is, the slope, $d\mu_y/dV$) vary by a factor of 25 to 1 among the differing tire and pavement combinations.

While less data are available for truck tires, distinctive velocity sensitivities in μ_y are known to exist. In Figures 2.35 and 2.36, typical dry and wet surface data are shown for a rough macrotexture surface and a fully-patterned tire [8]. A 20% change in μ_y on the wet surface is contrasted with a 4% change on dry over the 20- to 55-mph velocity range.

2.3.4 Sensitivity of μ_y to Surface Texture. As shown in the preceding section, μ_y is especially sensitive to the texture of the supporting pavement when the surface is wetted. As seen in Figure 2.37, surfaces with harsh (gritty) microtexture (such as No.'s 1 and 2, see Table 2.2) provide much higher values of μ_y for the wet condition than do the more polished surfaces (No.'s 3 and 4) [37]. Moreover, since μ_y is a measure of the frictional coupling limit, the friction implications of surface texture are of comparable significance to those cited earlier in relation to the longitudinal traction peak, μ_p.

It should be noted that μ_y typically occurs at a slip angle of about 20°. At this condition, most of the tread in the contact patch is experiencing a sliding velocity equal to tan 20°, or .36 times the resultant velocity. Thus, the μ_y traction peak is achieved at tread slip velocities which, while twice as high as those associated with the longitudinal peak, μ_p, are still far removed from the 100% slip condition of μ_s. Accordingly, μ_y sensitivities to friction coupling mechanisms are more similar to μ_p sensitivities than to μ_s sensitivities.

2.3.5 Sensitivity of μ_y to Water Depth. At increasing speeds, the lateral traction limit becomes increasingly sensitive to water depth. At a sufficient depth, of course, the full hydroplaning condition virtually eliminates a side force response. Shown in Figure 2.38 are data taken on a bias-ply passenger car tire covering deep water conditions up to .40 inches (10 mm) of water. We see that at

TABLE 2.2

Details of Test Surfaces

No.	Description	Texture
1	9.5 mm quartzite macadam carpet	rough, harsh
2	Fine cold asphalt	smooth, harsh
3	9.5 mm mixed aggregate macadam carpet*	rough
4	9.5 mm Bridport macadam carpet	rough, polished
5	Mastic asphalt	smooth, polished

* Aggregate is a mixture of those in 1 and 4

TABLE 2.3

Details of Test Tyres

No.	Make	Tread Pattern	Construction	Size	Resilience*	Hardness≠
1	Dunlop	Smooth	Crossed ply	5.00x16	55	63
2	Dunlop Gold Seal	Patterned	Crossed ply	5.25x16	51	58
3	Dunlop	Smooth	Crossed ply	5.00x16	38	63
4	Dunlop Gold Seal	Patterned	Crossed ply	5.25x16	31	62
5	Dunlop C41	Patterned	Crossed ply	5.90x15	31	63
6	Pirelli Cinturato	Patterned	Textile banded radial ply	165x15	36	65
7	Dunlop SP41	Patterned	Textile banded radial ply	165x15	35	60
8	Michelin 'X Stop'	Patterned	Metal banded radial ply	165x15	39	60
9	Michelin 'X Rib'	Patterned	Metal banded radial ply	5.50x16	–	–
10	Michelin 'X Rib'	Worn	Metal banded radial ply	5.50x16	–	–

* Percentage rebound measured on a modified B.S. Lupke pendulum at 20°C

≠ Measured at 20°C on Dunlop Scale

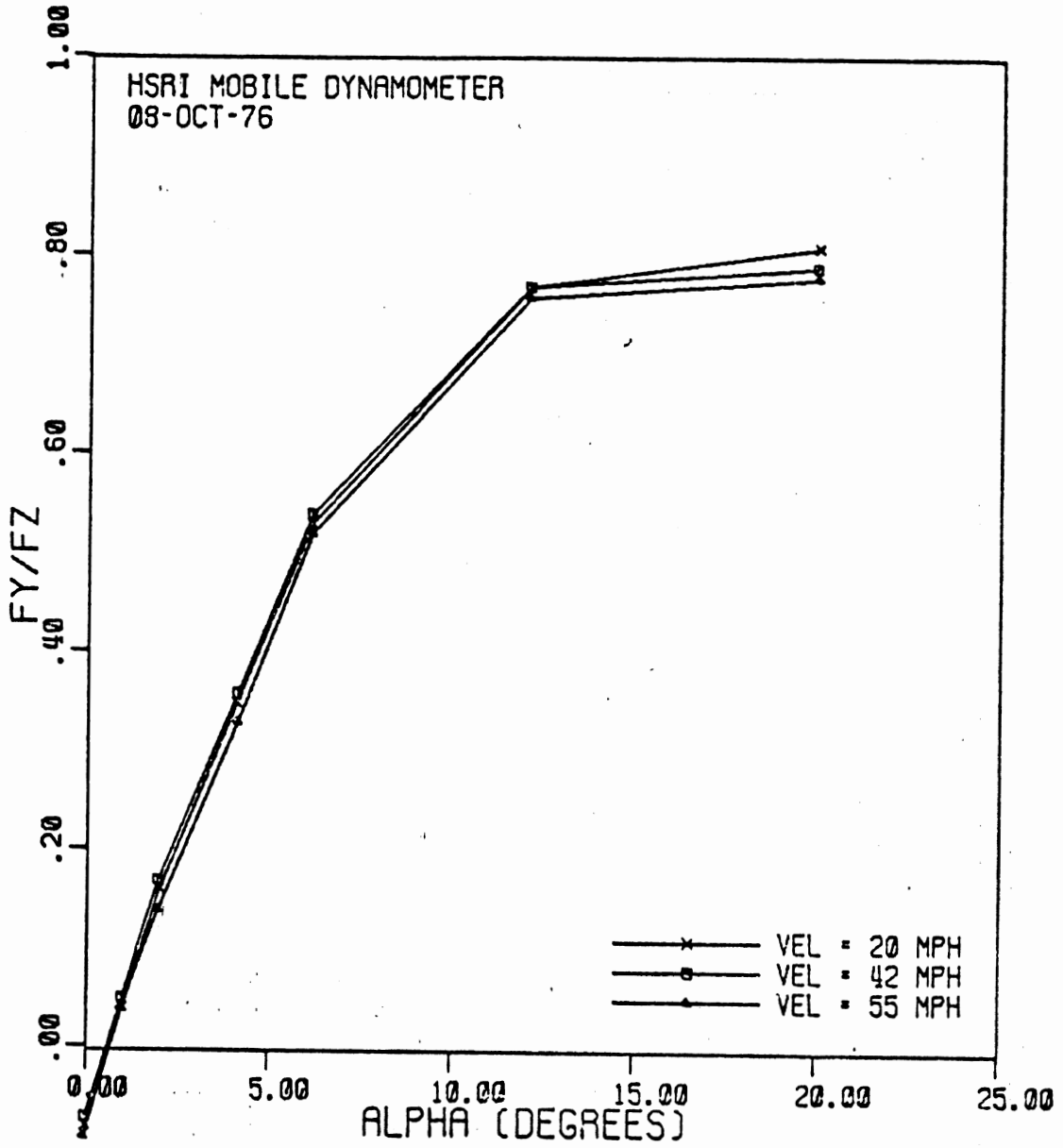

Figure 2.35 Normalized lateral force versus slip angle data at nominal vehicle speeds of 20, 40 and 55 mph. The radial, 10:00R20, load range G, Firestone Transteel tires were tested on a dry Portland cement concrete surface. Tire load was 6019 pounds.

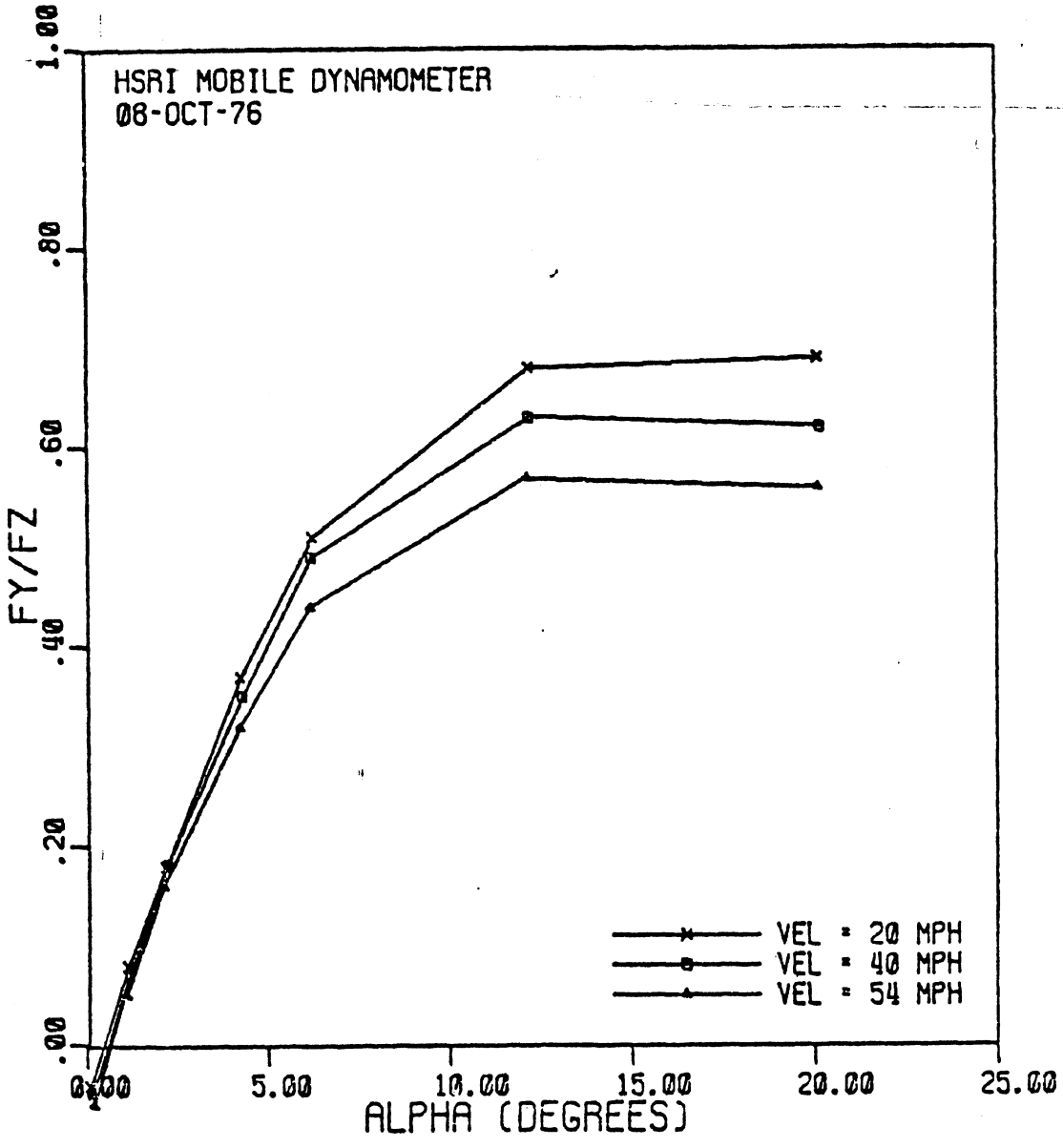

Figure 2.36 Normalized lateral force versus slip angle data at nominal vehicle speeds of 20, 40 and 55 mph. The radial, 10:00R20, load range G, Firestone Transteel Traction tires were tested on a wet Portland cement concrete surface. Tire load was 6171 pounds.

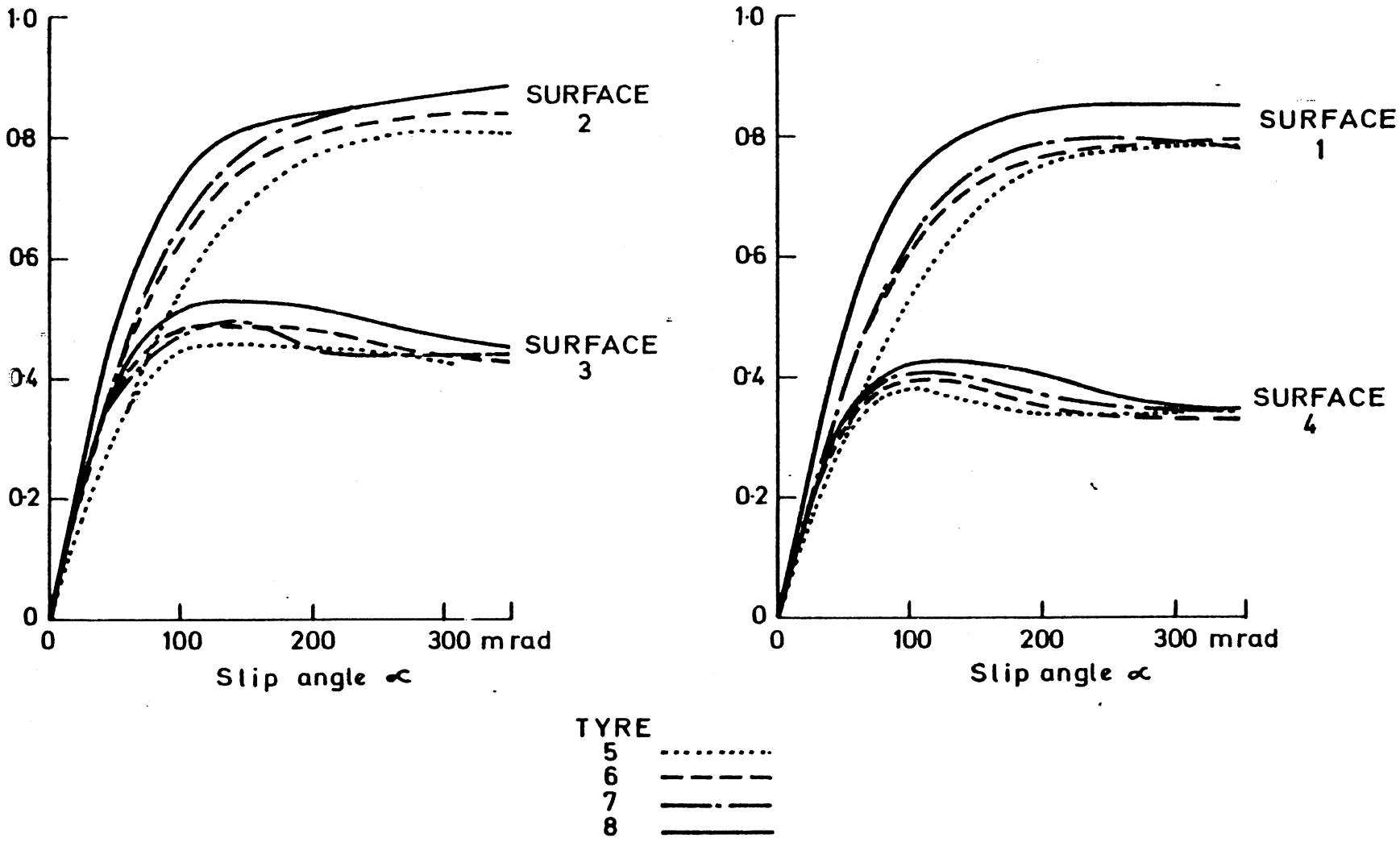

Figure 2.37 F_y vs α Performance of Differing Car Tires on Harsh (1 & 2) and Smooth (3 & 4) Textured Surface.

intermediate velocities (20 to 60 km/h) water depth is not a significant determinant of μ_y. At higher speeds, the data sort out clearly according to depth for the non-hydroplaning cases, while the μ_y values at depths which cause hydroplaning tend to run together.

Figure 2.39 shows the interaction between inflation pressure and the sensitivity of μ_y to water depth at two speeds [38]. While the influence of inflation pressure on μ_y is consistently positive at all water depths for the intermediate speed, 65 km/h, the relationship is more complex at the elevated speed.

2.3.6 Sensitivity of μ_y to Carcass Design. It is generally known that carcass construction details impose only minor influences on μ_y. As shown in Figure 2.40, passenger car tires show a narrow spread in the mean values (dark lines) of μ_y for bias-ply, bias-belted, and radial-ply carcass constructions on a dry surface [39]. Similarly, for heavy truck tires, Figure 2.41 shows a summary of F_y/F_z versus α envelopes for bias- and radial-ply tires indicating only small distinctions in the μ_y level between carcass types [8]. Available data also show very small distinctions in μ_y deriving from tire aspect ratio, cord material, or belt material [25].

On wetted surfaces, differences in μ_y which are uniquely attributable to carcass construction are small. For passenger car tires, a slight advantage has been seen for the radial construction [40], while truck tires show increased μ_y levels for the bias-ply varieties [8].

2.3.7 Sensitivity of μ_y to Tread Design. As with longitudinal traction limits, μ_y is definitely dependent upon tread pattern and depth, especially on wetted surfaces. Gross changes in tread pattern, such as shown in Figure 2.42, are seen to have a substantial interaction with water depth in determining μ_y changes with speed [38]. In each of the patterned tires of Figure 2.42 identical ratios of groove area to total contact area are provided, but large differences in μ_y are observed at the greater water depths.

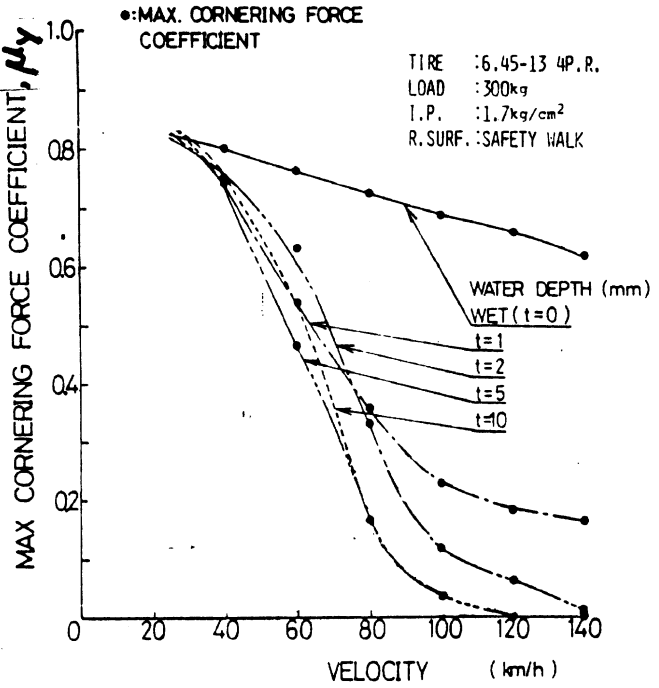

Figure 2.38 Influence of Water Depth on μ_y, as a Function of Speed.

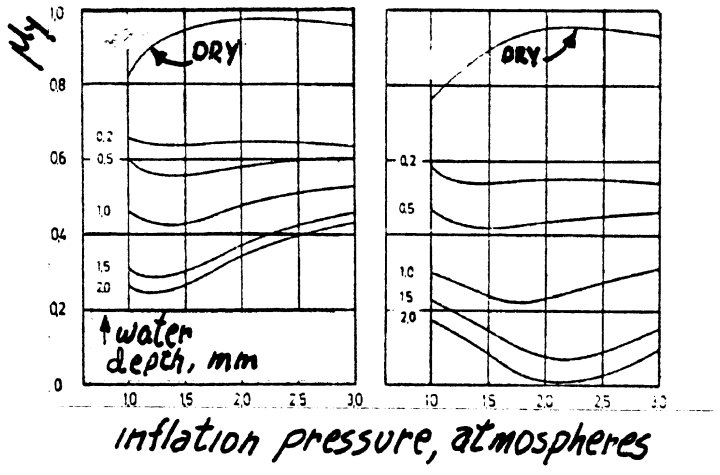

Figure 2.39 Interaction Between Water Depth and Inflation Pressure in Determining μ_y.

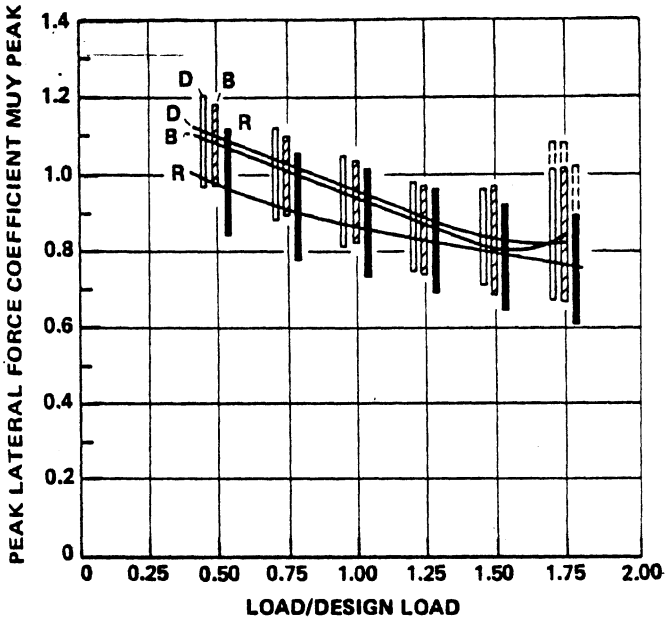

Figure 2.40 Distribution of μ_y mean values and ranges for bias ply, (D), bias belted, (B), and radial (R) passenger car tires at differing levels of normalized load.

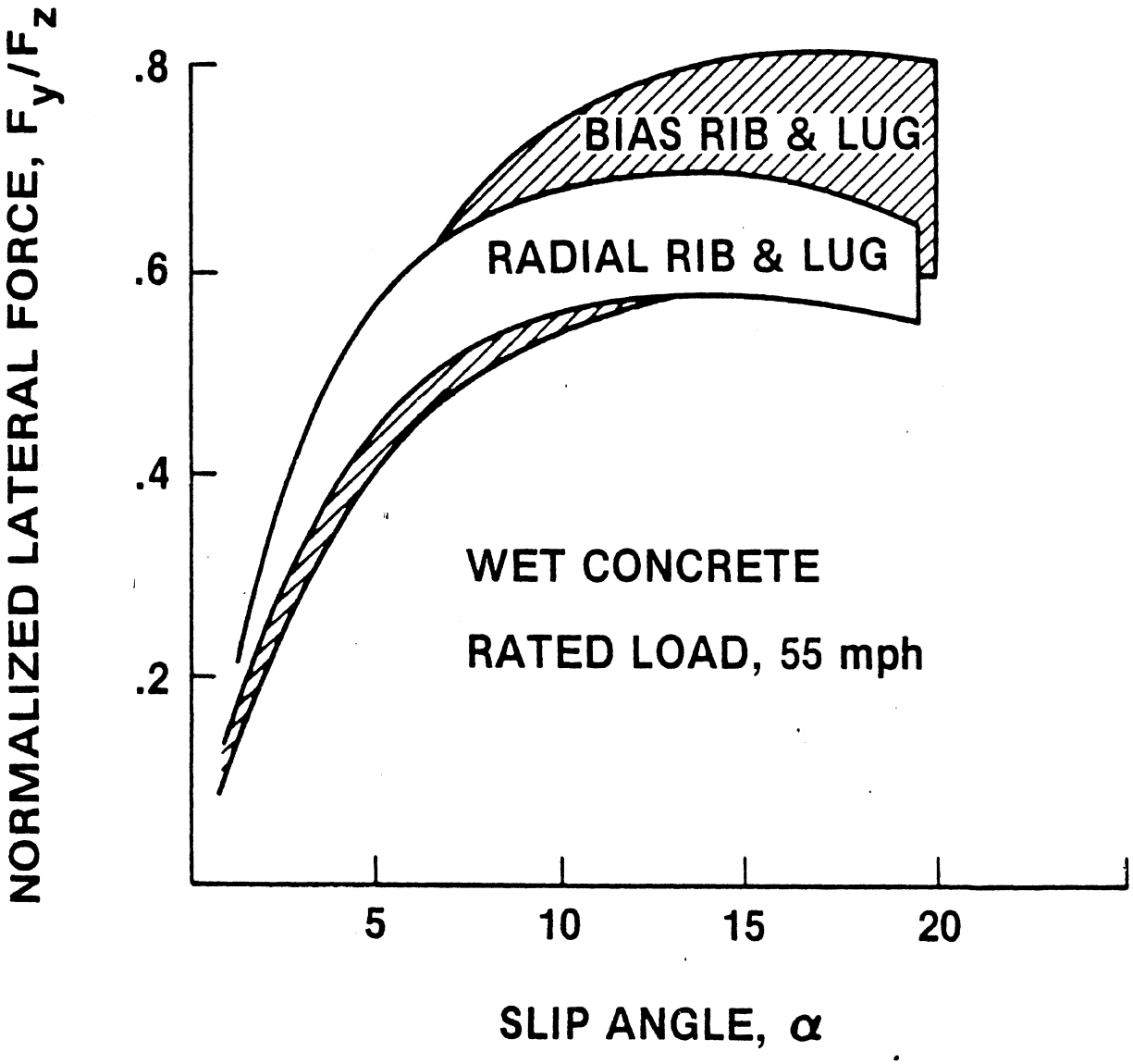

Figure 2.41 Envelopes of F_y/F_z vs α behavior for heavy truck tires on wet concrete.

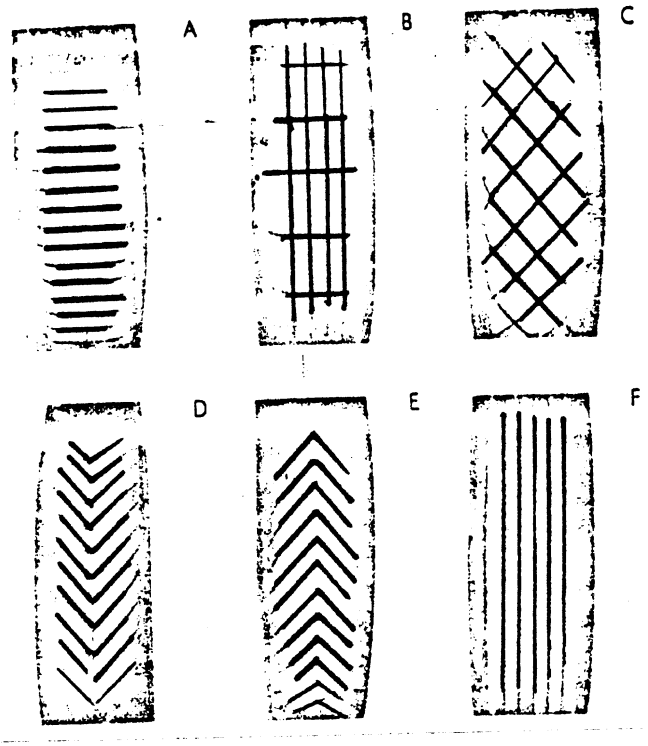

Tread Patterns

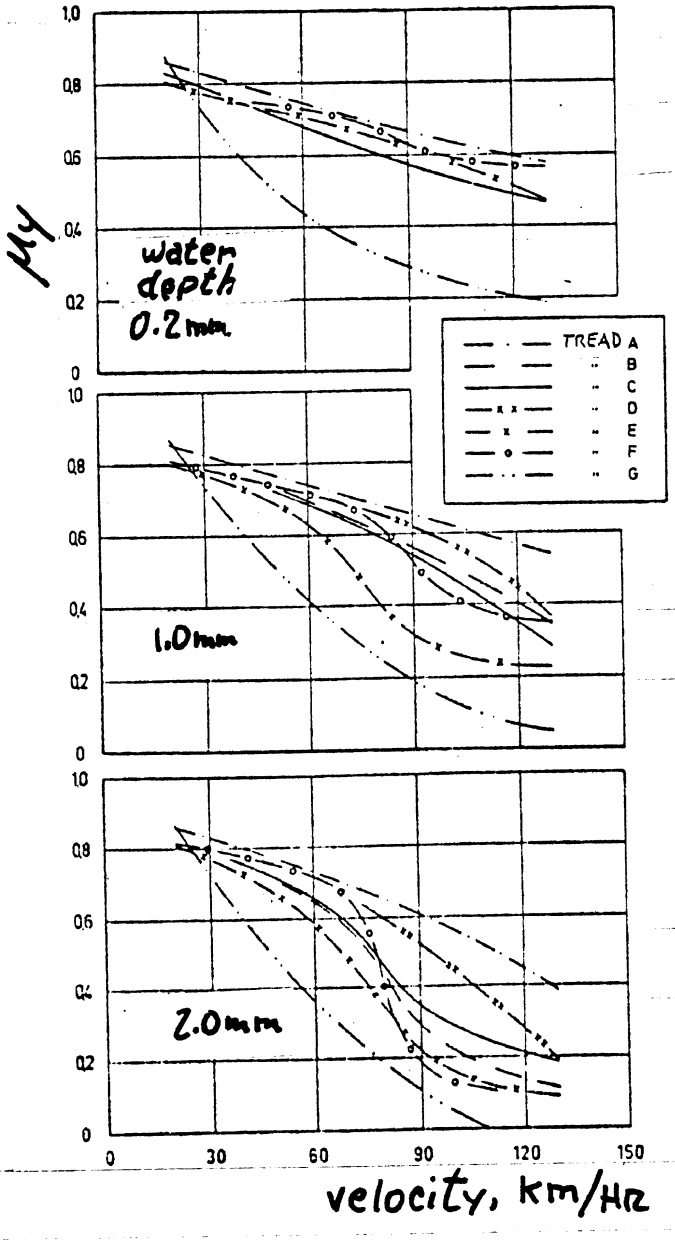

Figure 2.42 The influence of gross tread pattern layout on μ_y, at differing water depths and speeds. (For a 5.60-15 bias ply car tire).

It is known, as stated in the discussion on longitudinal traction, that tread pattern becomes significant to the wet cornering limit only when smooth-textured surfaces are present. For very coarse surfaces, the surface itself provides the means for water drainage and the minimization of hydrodynamic water pressure.

On dry surfaces it is known that the elimination of groove area improves μ_y, with completely smooth tires typically showing highest performance. An anomaly of the relationship between tread profile and μ_y is known to derive from the peculiar wearing of tires during repeated operation at elevated slip, as shown in Figure 2.43 [7]. These data are typical of the μ_y sensitivity to "shoulder wear" which, although involving only slight changes in tread profile at the outer ribs, results in a 25% increase in μ_y on a dry surface. By contrast, Figure 2.44 shows a much smaller interaction between tread depth, per se, as accrued from normal driving, and the μ_y level exhibited on a dry pavement [7].

2.3.8 Sensitivity of μ_y to Tread Compound Variations. Tread compound is known to affect μ_y by the same mechanisms and extent as were discussed for the longitudinal limits, μ_p and μ_s. The dominant property of the tread rubber appearing to influence μ_y is the hysteresis or, conversely, "resilience," feature. A large increase in the rebound measure of the resilience of tread rubber can result in as much as a 25% reduction in μ_y on a low friction wetted surface [37].

2.3.9 Significance of μ_y to Vehicle Maneuvering Performance. Clearly, μ_y is a tire property which is relevant only to the determination of the limits of steady cornering or lane change or other abrupt steering-input maneuvers. For passenger cars, the exceedance of the tire's μ_y capability leads to either a "plowout" or "spinout" type of response. The plowout response, deriving from premature exceedance of μ_y at the front tires, yields a trajectory whose curvature is less than that desired, although vehicle sideslip angle

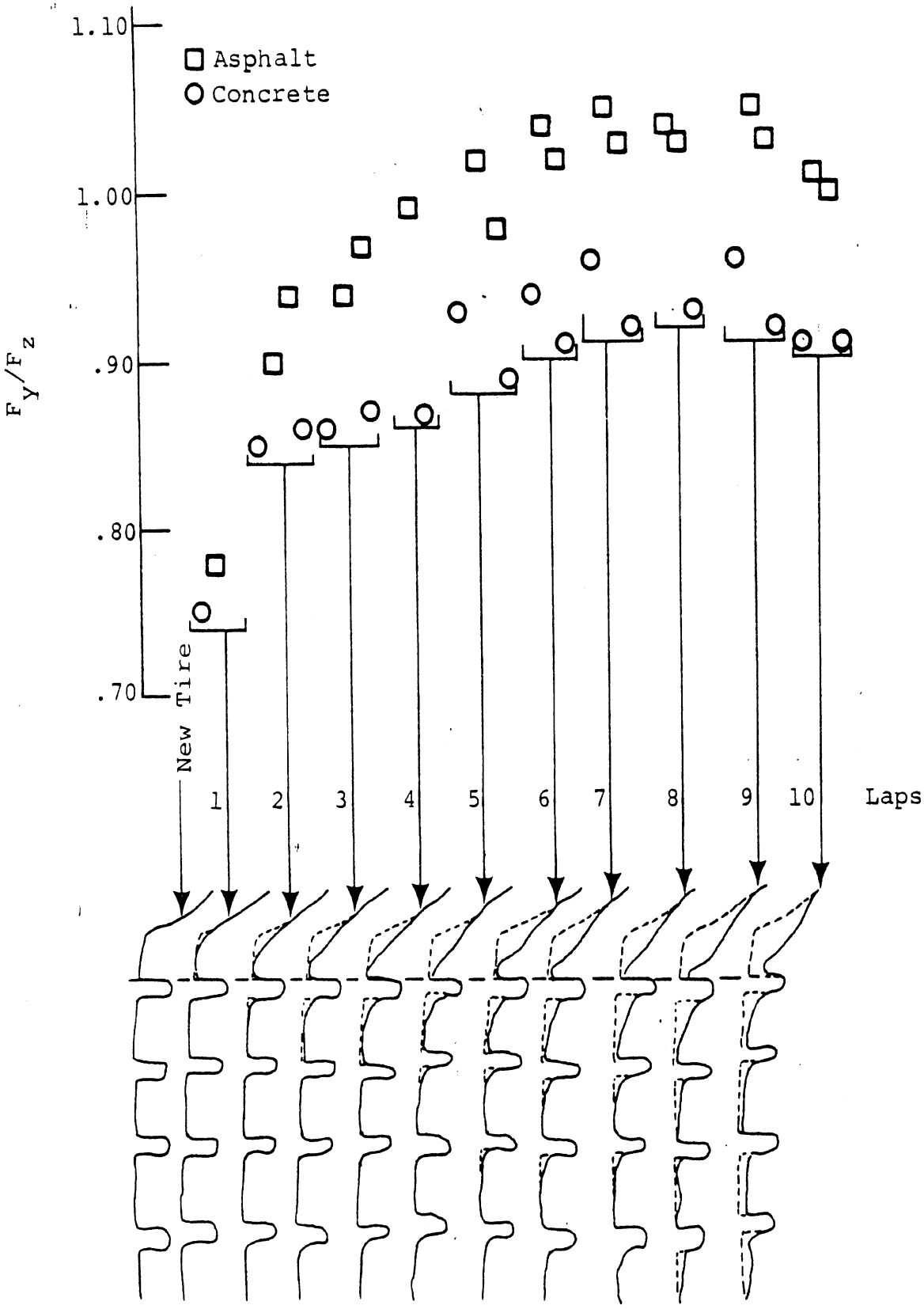

Figure 2.43 The influence of shoulder wear on the μ_y performance, on dry asphalt and concrete pavements, of a bias, belted, car tire.

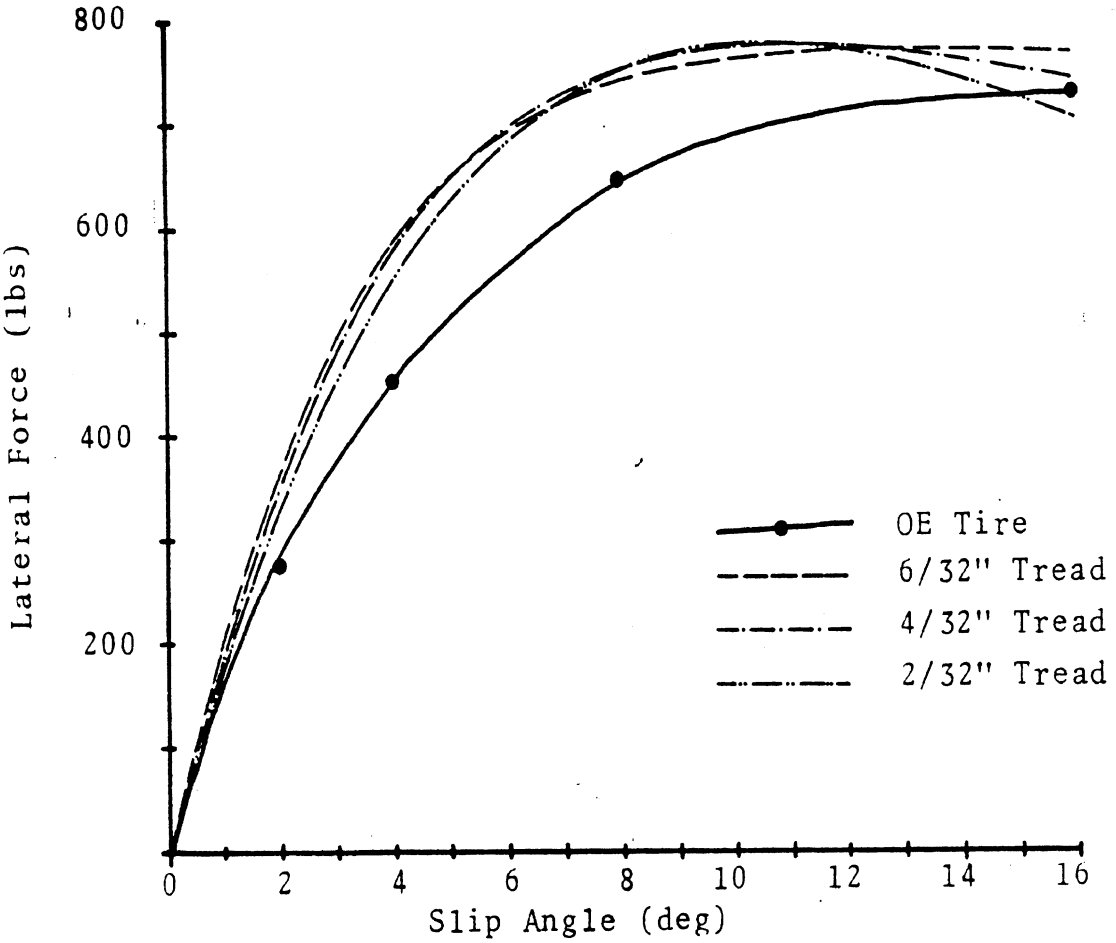

Figure 2.44 Lateral force vs. slip angle for various tread depths, B.F. Goodrich Silvertown, 800 lbs. 24 psi.

is kept small. In an actual driving situation, a plowout incident on a curved section of roadway will result in a more or less tangential departure from the road.

A spinout response derives from premature saturation of rear tires and is characterized by a divergent vehicle sideslip angle response—i.e., the vehicle attempts to rotate towards a rear-end-first orientation. When such incidents occur on the roadway, the vehicle may move in a straight line trajectory, but the loss of control over yaw orientation provides numerous possibilities for an accident—including impacts deriving from the wide swept path and from off-road impacts and rollover made possible by departure from the roadway. While the determination of the plow, or spin, character of the cornering limit on a given vehicle derives from many factors, the μ_y level at the tires determines the level of maneuvering severity at which the cornering limit will occur. Thus, maximization of μ_y ensures the largest possible range of cornering maneuvers just as maximization of the longitudinal limit, μ_p, ensures the largest range of braking maneuvers.

For heavy trucks, μ_y is perhaps an irrelevant measure, except for cases of low friction surfaces. On dry surfaces, however, the typical heavy truck or tractor-trailer will roll over before its μ_y traction limits are reached. Thus, it is generally held that only the low friction μ_y properties of truck tires are likely to be relevant to vehicle safety.

In the case of motorcycles, the μ_y limit of tire traction clearly constitutes the limitation on cornering severity. When front tire μ_y is exceeded first, the vehicle falls down or "capsizes" very rapidly. When rear tire μ_y is exceeded first, the motorcycle typically spins around to an attitude at which it capsizes. Since, again, motorcycles produce most of their side force as camber thrust, the μ_y limit on ordinary (dry) road surfaces will be reached when motorcycle roll, and thus camber, angle is in the range of 30° to 45°.

3.0 COMBINED BRAKING AND CORNERING PROPERTIES

When a tire is operated under conditions of simultaneous longitudinal and lateral slip, the respective longitudinal and lateral forces are seen to markedly depart from those values deriving under the independent conditions of slip. That is, if a given tire produced a 500-lb side force, F_y, at a given condition of lateral slip, a reduction in F_y value to only 200 lbs might result from the simultaneous application of braking up to a level of 20% longitudinal slip. Likewise, the application of simultaneous lateral slip generally tends to reduce the longitudinal force level being produced by the braking tire.

While these combined slip phenomena have been demonstrated by numerous researchers, there have not been broad studies of the sensitivities of the combined force and slip interactions to changes in operating conditions, surface characteristics and tire design variables. Thus it suffices here to cite the basic character by which the simultaneous slip conditions influence the generation of combined shear forces.

As shown in Figure 3.1, increasing levels of braking slip produce an initially sharp reduction in side force [37]. At high levels of braking slip, approaching wheel lock, F_y approaches the value $F_x \tan \alpha$, since side force prevails then only as the lateral component of a resultant shear force which opposes velocity. We see in Figure 3.1, for the case of a wet, rough macrotexture surface, that load plays no distinctive role in the combined slip interaction, per se. Also, there are only subtle differences apparent between the steel-belted radial, tire No. 8, and the cross-ply tire, No. 5. Looking at the converse interaction, Figure 3.2 shows the effect of slip angle on the longitudinal force versus longitudinal slip relationship [37]. We see that, while the locked-wheel values of F_x/F_z are not significantly

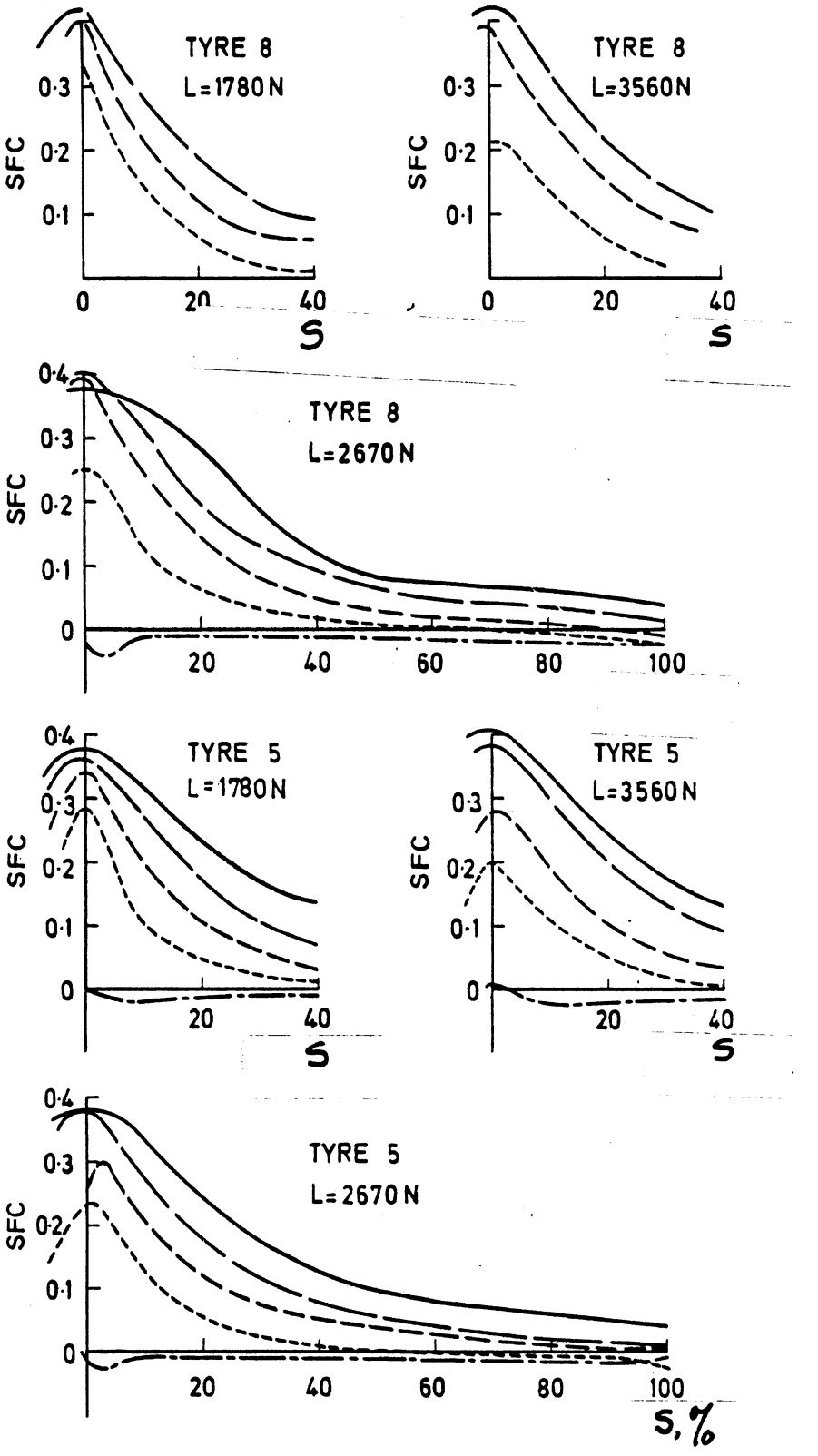

Figure 3.1 THE EFFECT OF BRAKING SLIP S ON THE SIDEWAY FORCE COEFFICIENT (SFC) (F_y/F_z)

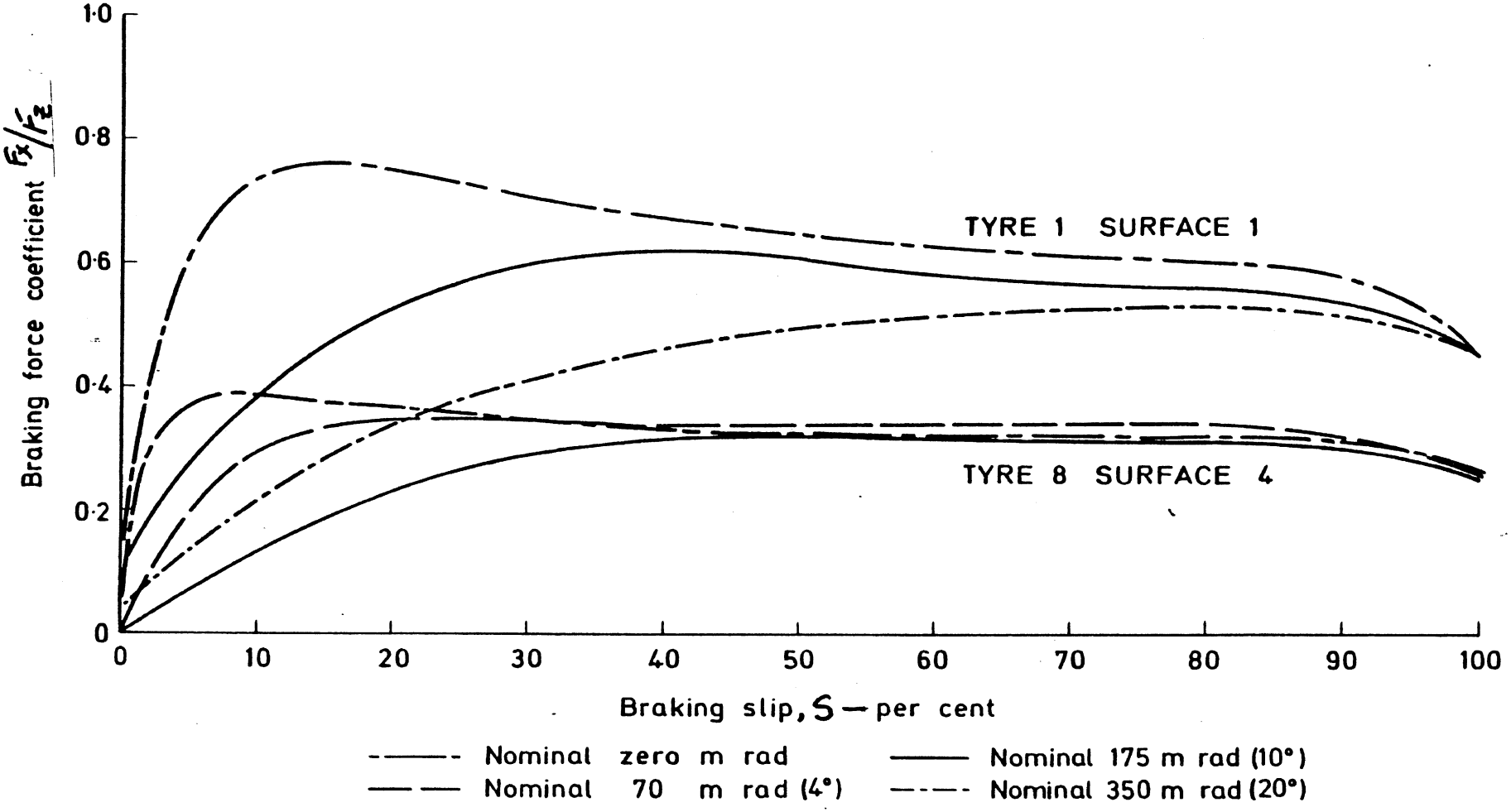

Figure 3.2 THE EFFECT OF SLIP ANGLE ON THE BFC/S RELATIONSHIP

changed by the presence of a simultaneous slip angle, the curve becomes considerably depressed with increasing α in the regime of low values of S. When wheel lockup does occur, clearly the F_x force component is related to the resultant shear force by the relation, $F_x = (F_{resultant} \times \text{cosine } \alpha)$.

Looking at both of these interactions together for bias and radial tire samples, Figure 3.3 shows the F_x and F_y responses at slip angles of 2° and 10° over the full range of S [36]. These data also incorporate a broad range of speeds, revealing that speed does not have a significant influence on the combined slip interactions, per se, although speed clearly determines the absolute level of the F_y or F_x shear forces. If the shear force data in Figure 3.3 are cross plotted, as in the example curves of Figure 3.4, we obtain the so-called "traction fields" plot (with S_y being the lateral slip variable, equal to tan α) [41]. Such a display of the combined slip interaction has led some vehicle mechanicians to postulate a "friction circle" (or ellipse) description of the limiting resultant shear force behavior of the tire. The traction field plot directly displays the "trade-off" which exists between lateral and longitudinal force production.

The only known data describing truck tire response to combined slip is shown in Figure 3.5 [42]. These data reveal the same basic character of interaction as shown for car tires, although distinctions which may be of significance to truck dynamics remain to be explored in any depth.

For the case of motorcycles, the relevant interactive condition involves combined longitudinal slip and inclination angle (rather than slip angle). A very limited amount of work is known to have been done, producing data as shown in Figure 3.6 [43]. Here we see a normalized side force level, F_y/F_{y_0}, which ratios the actual side force to that value which prevails at S=0. The data display the F_y fall off with S for differing motorcycle tires operating at an inclination angle of 20°, as overlaid, for contrast, on the range of F_y data

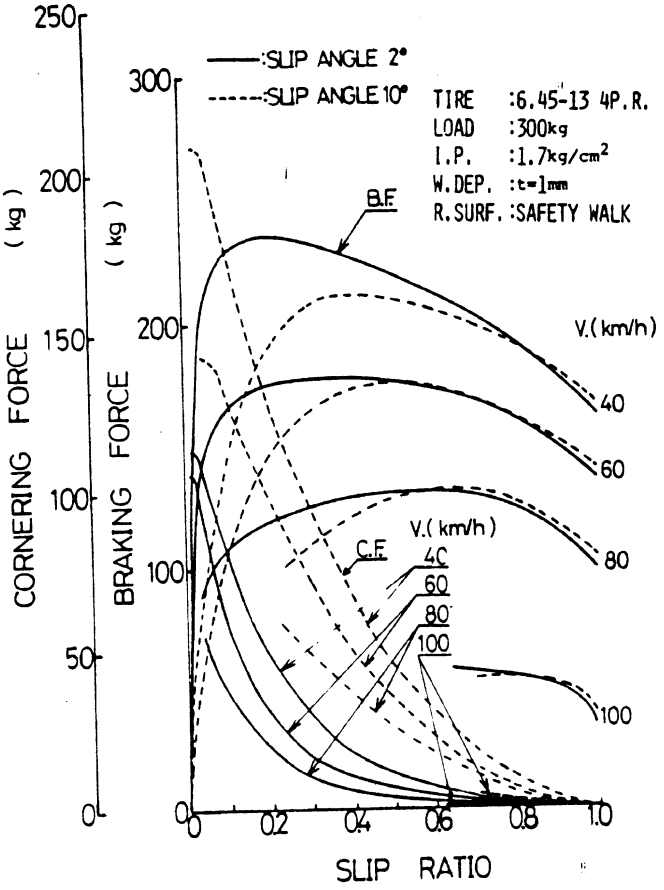

Figure 3.3a Relation between cornering force, braking force and slip ratio at slip angle 2° and 10°, cross-ply tire

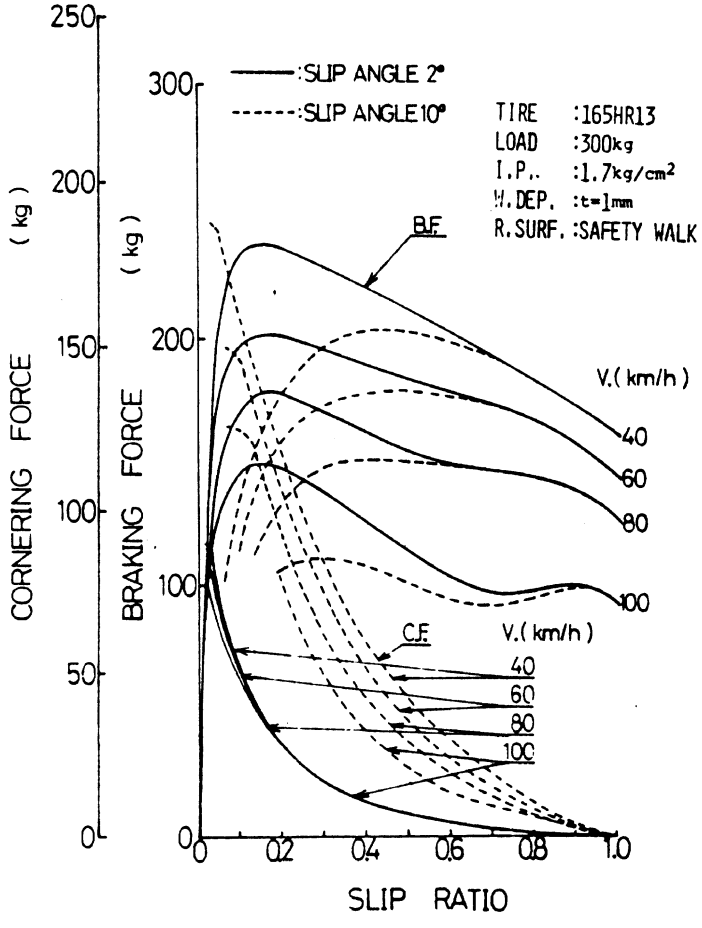

Figure 3.3b Relation between cornering force, braking force and slip ratio at slip angle 2° & 10°, radial-ply tire

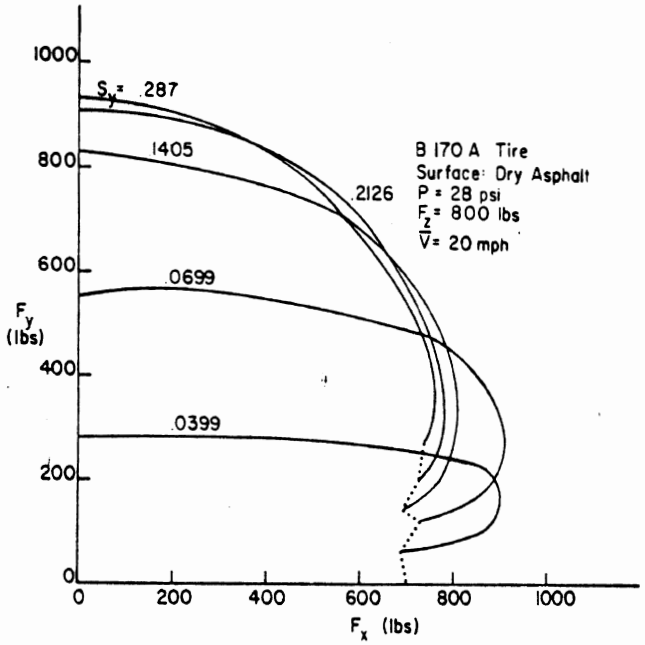

Figure 3.4 Lateral force versus longitudinal force at constant values of lateral slip.

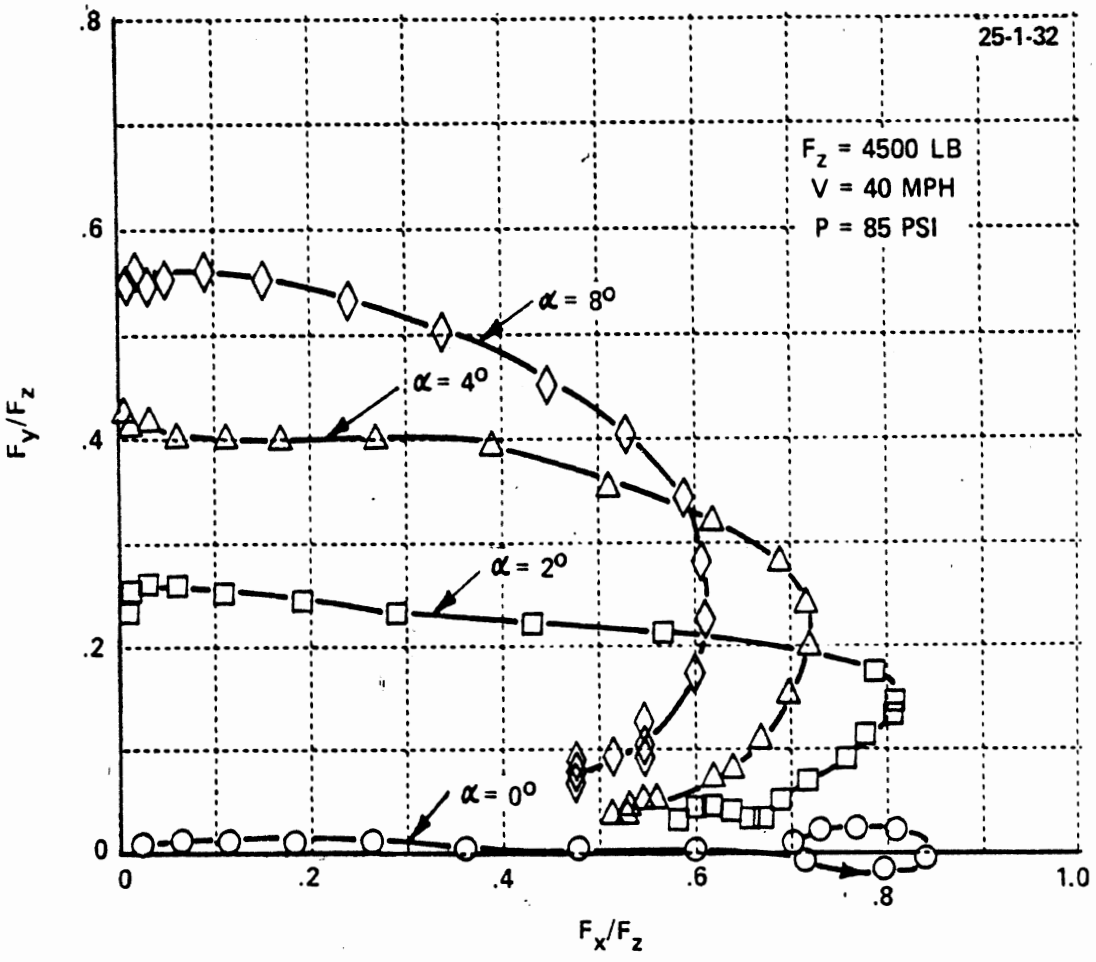

Figure 3.5 TRACTION FIELD (FY/FZ VS FX/FZ) OF 10.00-20 (F) TRUCK TIRE

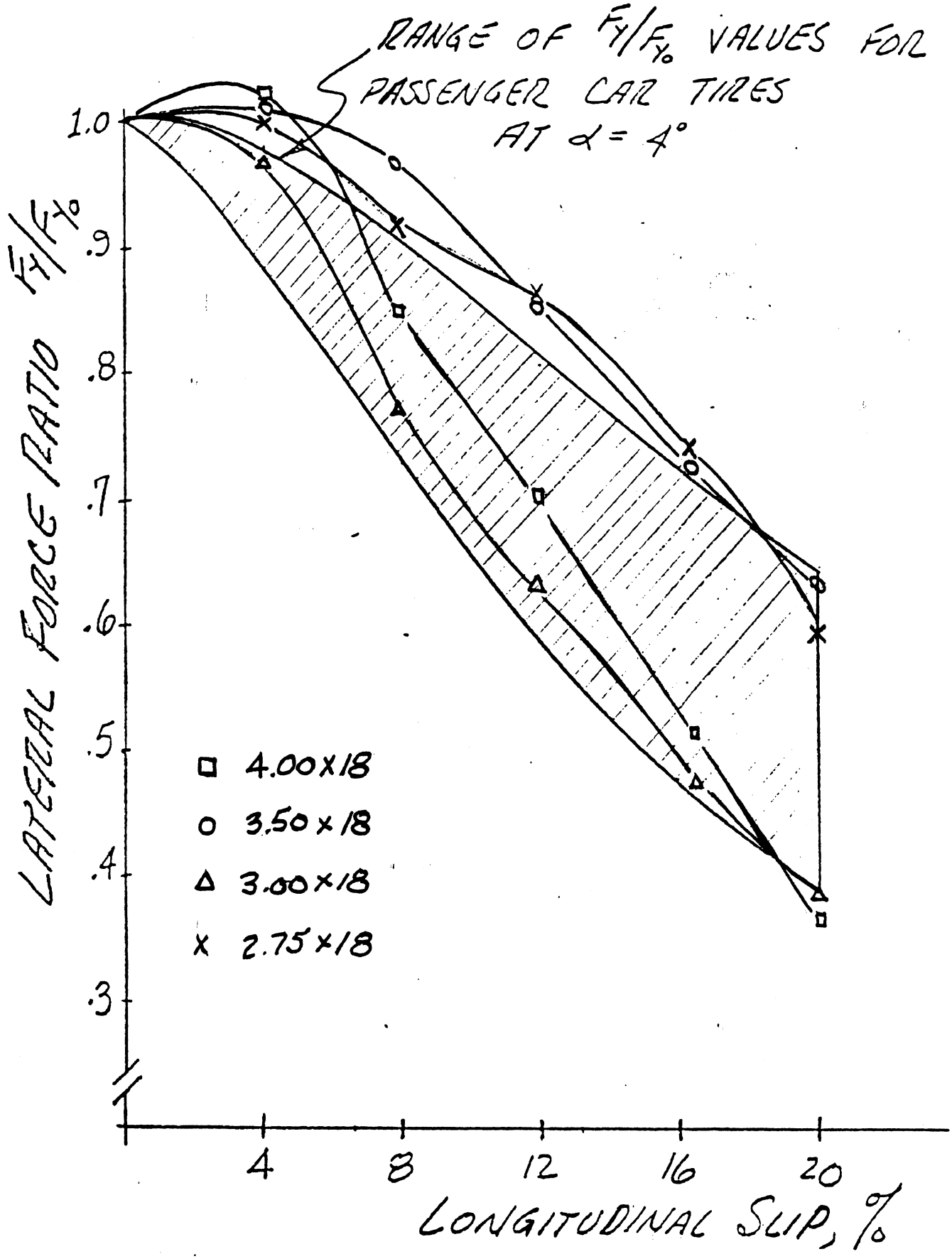

Figure 3.6 Fall-off in F_y/F_{y_0} with slip for four different motorcycle tires at $\gamma = 20°$ compared to envelope of car tire responses measured at $\alpha = 4°$. Motorcycle tires all operated at a nominal static (motorcycle plus rider) load.

exhibited by various car tires operating at a slip angle of 4°. These data show that, for the conditions examined, the motorcycle tire loses side force as a result of increasing braking slip at a rate comparable to that exhibited by the typical car tire, even though one involves a camber thrust mechanism and the other involves side force due to slip angle.

One can meaningfully interpret the combined slip interactions of the tire in the context of vehicle braking-in-a-turn behavior. When brakes are applied to a vehicle in an initially steady turn, the increasing level of tire longitudinal slip produces a loss in tire side force which characteristically serves to perturb the path and/or yaw orientation of the vehicle. By another view, if a large steering input is applied while the vehicle is braking, both the braking performance and the cornering performance stand to be degraded in comparison to the performances expected with independent inputs of steering or braking.

Research [44] has shown that minimal degradation in the stopping capability of passenger cars accrues from simultaneous cornering in the vicinity of 0.3 g lateral acceleration. On the other hand, as the limit stopping level is approached, the directional or yaw response can become degraded to the point of total loss of control. The nature of the control loss will depend upon the order in which front and rear tires approach the wheel-lock condition. For vehicles which produce a sufficiently high level of front braking that front wheels lockup first, the attending loss in front tire side force will render the vehicle unsteerable, resulting in an essentially straight-line vehicle path. When rear wheel lockup is approached first, the imminent loss of control incident will be a spinout. On tractor-semitrailers, the overbraking of the tractor's rear wheels will result in the jackknife response of the combination. In such cases, the spinout of the tractor takes place very quickly, causing it to rotate about the fifth-wheel coupling until the cab finally collides with the side structure of the trailer. In the case of motorcycles, the lockup

of the front tire eliminates the side force mechanism which begets roll stability. The result is an extremely rapid capsize, or rollover. Lockup of the motorcycle rear tire, of course, renders the vehicle yaw unstable.

The significance of yaw disturbances occurring when less than limit level braking is applied is not well established. Although numerous research studies [e.g., 44, 45] have endeavored to quantify and evaluate the sublimit yaw responses to braking in a turn, the current state is one of debate and speculation. Although objective measures of these response characteristics have been developed, their significance as regards the driver's challenge in maintaining control is unknown.

4.0 TRACTION OR MOBILITY ON DEFORMABLE SURFACES

When the pneumatic tire is operated over snow or soil, interaction mechanisms prevail which typically degrade the tire's traction force potential relative to that prevailing on uncontaminated paved surfaces. While various fields of research related to this area have progressed for some time, the state of knowledge pertaining to highway vehicles and typical on-road conditions is rather sparse. For both agricultural and military tire applications, research has centered upon the cases of deep snow and soil of infinite depth. Highway vehicles, on the other hand, typically encounter shallow snow as an overlay on pavement or a shallow layer of unstable soil existing over a "hard pan" or relatively rigid strata—such as in unpaved driveways or truck marshaling yards.

For the military and agricultural cases (or for highway tires which happen to be in deep snow or uncompacted soil), "flotation" is a relevant issue pertaining to tire design. In these applications, it has been seen that tire diameter and tread width are principal determinants of the rolling resistance trends in soil, as shown in Figure 4.1 [47]. These relationships are pertinent since the net tractive force of any tire on a deformable surface is determined heavily by the rolling resistance deriving principally from "sinkage" of the tire into the surface material. Thus, flotation is a quality which minimizes rolling resistance.

The sinkage of a tire into an uncompacted soil is determined, of course, by the magnitude of the vertical stresses which are produced in the soil. Since pressure existing at the tire contact directly determines stresses within the soil, it is clear that sinkage is reduced when the inflation pressure of a tire is reduced so as to yield a larger loading surface area. This favorable action explains the advantages of so-called "low pressure tires" on soft ground. Additionally, the deflation of even the more conventional profile tire has

proved so advantageous to mobility that certain military vehicles have been designed with central tire inflation systems. Such arrangements permit deflation and refilling of tires "on the run" so as to maximize mobility on degraded soil conditions and still recover stability properties for high-speed movement. As shown in the data of Figure 4.2, one such vehicle exhibits a 50% increase in its maximum "drawbar pull" measure as a result of tire deflation from 35 psi to 7 psi [48].

As might be imagined, there are a broad range of soil and snow conditions which serve to influence the tractive capabilities of a given tire. As shown in Figure 4.3, a tire of typical construction for use on farm tractors produces traction and rolling resistance coefficients which vary widely over a set of soil conditions [49]. In these data, the "rolling resistance" value pertains to the resistance of a non-driven wheel which is towed through the soil while the "traction" value indicates the net value of F_x available for drawing a load. It can be seen that, for silt and soil slurry conditions, a four-wheeled vehicle with only two wheels driving would become immobile if outfitted with this same typical tractor tire at all wheel positions.

An associated field of interest focusing upon sinkage has derived from the use of military aircraft on unpaved forward field areas. In such cases, the drag or rolling resistance properties of aircraft tires have been studied to establish constraints on aircraft take-off limitations due to soft soil [50].

Regarding the importance of tread pattern to mobility in deep snow or soft ground, it is widely accepted that tread design is a secondary effect and, in any case, does not significantly influence traction due to an improved interaction between tread and soil (snow) [47]. Rather, in deep snow and soil situations the interaction between tire and surface material primarily involves friction coupling between either the tread rubber and the medium material, or within the layers of soil or snow itself.

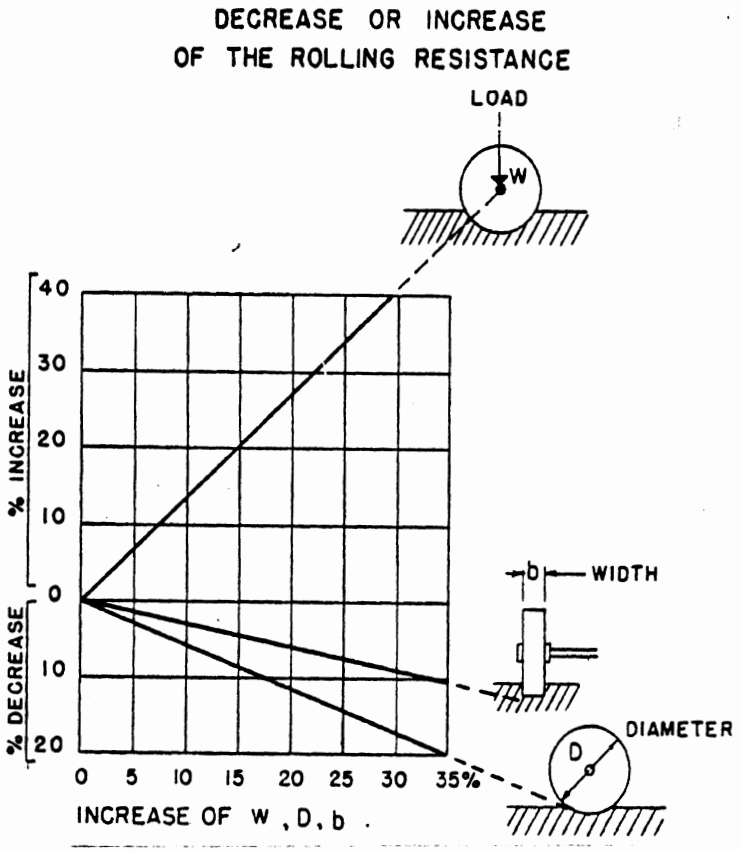

Figure 4.1 Influence of tire width, diameter and load on rolling resistance in soil.

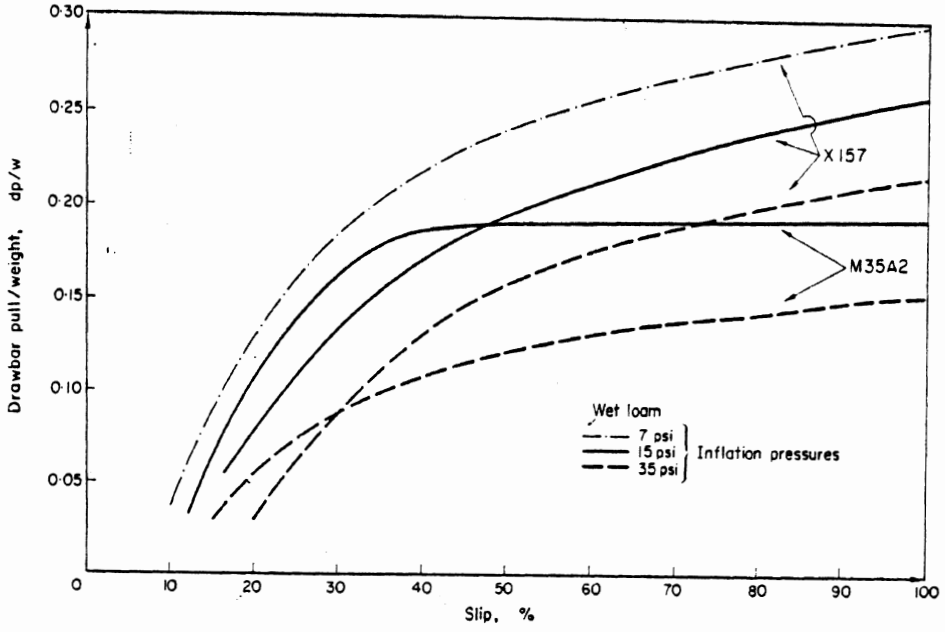

Figure 4.2 Influence of tire inflation pressure on the drawbar pull/weight performance of two military vehicles.

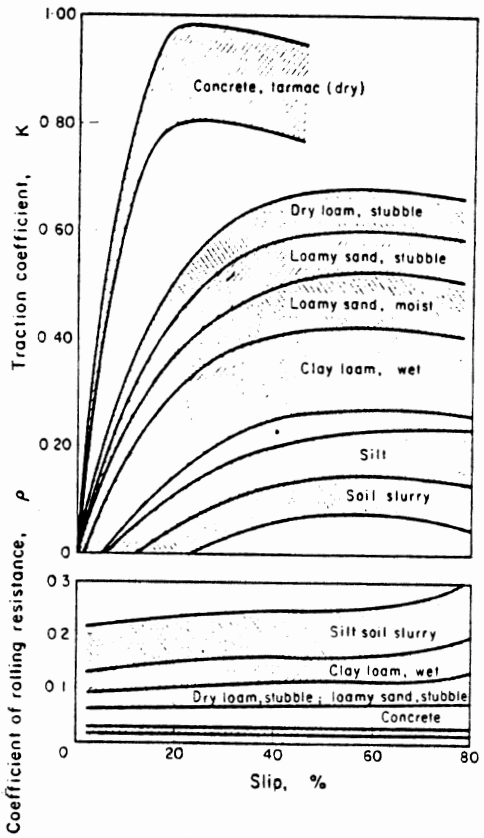

Figure 4.3 Coefficient of traction and rolling resistance under different soil conditions.

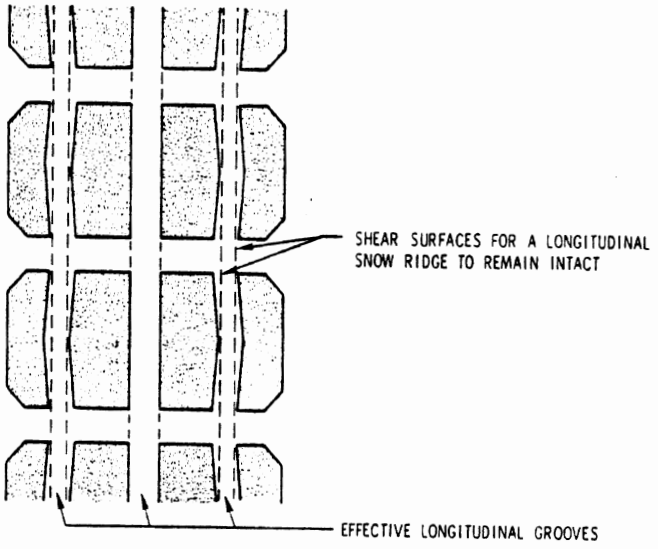

Figure 4.4 Tread pattern with effective longitudinal grooves.

Considering now the more common deformable surface situations encountered by highway vehicles, we find that tread pattern and other characteristics of the tire play significant roles in determining mobility characteristics. Looking first at carcass construction influences, we can isolate at least four features affecting mobility properties: the differences in contact pressure in the footprint such as it produces varied sinkage, the overall dimensions of the contact patch, the self-cleaning characteristics of the tread, and the squirm motions which take place in the tread due to carcass deflections. Footprint pressure is known to be significantly nonuniform in the contact patch of a pneumatic tire. With bias-ply tires, zones of higher pressure exist, especially along the outer circumferential rib positions. With belted bias-ply tires, more uniform distributions are obtained; and with radial tires, the least variation in contact pressure is seen. Because of nonuniform compaction of snow or soil beneath the tire, the resulting shear strength of the surface material will vary much more over the contact area of a bias-ply tire than with a radial tire. The net effect of these differences in compaction could favor either tire, depending upon details of the surface conditions. Presumably, situations exist in which the elevated pressures at the shoulder area of a bias-ply tire, for example, could cause it to penetrate and interlock with densely packed snow, while a radial tire might be incapable of such penetration.

The larger footprint area of the radial tire is, by itself, an advantage because more tread is contacting the surface material whose shear strength ultimately determines the maximum traction force.

Concerning the cleaning properties of the tire, radials typically offer an advantage. Less snow or soil is retained in tires whose tread grooves are larger—as are radials, since their more stable belting system is capable of supporting a more open tread without excessive wear rates. The less surface material that is retained, of course, the higher the friction potential since more tread blocks will be capable of penetrating and "connecting with" the soil or snow mass.

Another advantage of the more stable tread support features of radials is the low level of squirm such as causes snow and soil ridges to shear laterally, tending to reduce traction potential. Thus, although some surface conditions may be an exception, radial constructions tend to offer generally improved levels of mobility [51].

Concerning tread pattern, it is accepted that a patterned tire will offer advantages only when the snow or soil is sufficiently uncompacted that penetration by the tread edges can take place. (For unlubricating, highly-compacted surfaces, a bald tire will produce higher traction levels than a patterned tire.) When light to moderate compaction exists, it appears that both longitudinal and lateral grooves assist in enhancing traction. The longitudinal groove must, of course, possess some "throw" or zig-zag geometry so that snow or soil shear stress is generated. Shearing then takes place either along vertical planes, across the free exposed edges of the zig-zag (see Fig. 4.4), or at the base of the ridge of surface material penetrating into the groove [51].

Cross grooves provide for shearing of surface material only at the base of the penetrating ridge. Since the shear strength of either snow or soil will depend upon the degree of compaction, the relative degree of initial compaction before tire contact is relevant, as is the depth of the tread grooves. Thus tire sinkage beyond the dimension of one tread depth results in enhanced traction, at least from the mechanism of further snow compaction within the groove. When tread sinkage is less than groove depth, the degree of compaction existing prior to tire contact determines the shear strength which will prevail.

Tread sinkage into a relatively compacted medium is determined by the ratio of groove width to groove spacing. The greater the groove width to spacing ratio, the greater will be contact pressures on the rib elements and thus the greater will be the penetration, as well as the effective area of snow or soil in shear.

Accordingly, a certain openness of snow-type treads is essential both to the self-cleaning and to the snow mass penetration mechanisms. There are also considerations related to the characteristic shear failure patterns of snow that lead to observations about optimum groove widths. As diagrammed in Figure 4.5, a certain inefficiency in traction force production is accrued when either a narrower- or wider-than-optimum groove width prevails. When the tire operates with slip, however, another optimum would be defined than that suggested in Figure 4.5 [51]. It is not known whether snow-tire treads have been designed to afford an overall optimum performance given the detailed mechanics of snow shear failure.

At the outer sidewall area of the tread, traction force gains can also be made due to the shear strength of snow or soil ridges penetrating sidewall grooves and by friction mechanisms at the outer surfaces. Reduced normal forces in this region, however, reduce the traction effectiveness of sidewall grooves, although substantial gains can be made relative to the small degree of tread void which is added by sidewall grooves.

As a general comment on the matter of traction on deformable surfaces, it must be noted that the very complex mechanisms of shear force production render the performance of a given tire highly dependent upon the prevailing properties of the snow or soil. Regarding snow, it is known that among its relevant mechanical properties are the shear strength, the compressive and shear force-displacement characteristics, and the coefficients of friction for (1) the micro-interference mechanism at the snow/rubber interface, (2) the sliding snow/snow interface, and (3) for the sliding snow/rubber interface. All these properties, including snow depth (plus density, temperature, moisture content, and grain structure) combine to determine the extent of tire penetration as well as the magnitude and relative importance of the various traction mechanisms [51]. Further, these properties are highly variable, even in the course of a single day, such that experimental efforts in this area have been typically hampered by non-repeatability and by lack of generality. Similar statements can be

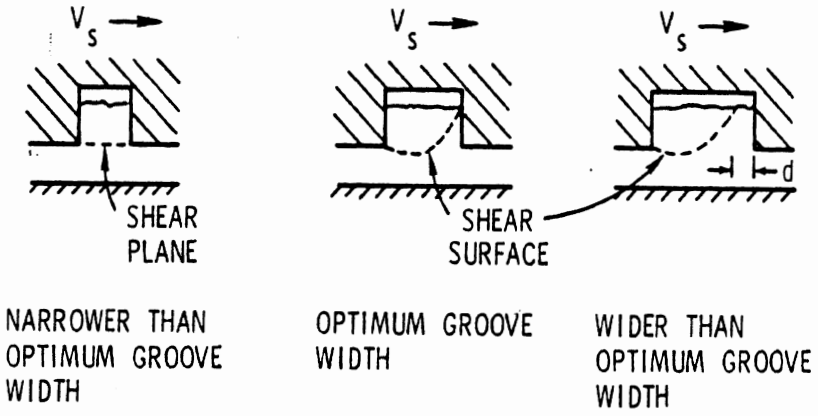

Figure 4.5 Optimizing the width of effective cross grooves for a pure rolling tire.

made for the case of soft soils and for the peculiar problems which resist major advances in tire design so as to enhance mobility in general.

REFERENCES

1. Society of Automotive Engineers, Inc. Vehicle Dynamics Terminology, SAE J670c. January 1973.

2. Tielking, J.T., Fancher, P.S., and Wild, R.E. "Mechanical Properties of Truck Tires." SAE Paper No. 730183, January 1973.

3. Ervin, R.D., MacAdam, C.C., and Fancher, P.S. The Longitudinal Traction Characteristics of Truck Tires as Measured on Dry Pavements. Highway Safety Res. Inst., Univ. of Michigan, Report No. UM-HSRI-PF-75-3, February 1975.

4. Mechanics of Pneumatic Tires. S.K. Clark (Ed.), NBS Monograph 122, U.S. Department of Commerce, Washington, D.C., November 1971.

5. Ervin, R.D., et al. Effects of Tire Properties on Truck and Bus Handling. Final Report, Contract No. DOT-HS-4-00943, Highway Safety Res. Inst., Univ. of Michigan, Report No. UM-HSRI-76-11, December 1976.

6. Bond, R., Lees, G., and Williams, A.R. "An Approach Towards the Understanding and Design of the Pavement's Textural Characteristics Required for Optimum Performance of the Tyre." The Physics of Tire Traction: Theory and Experiment. D.F. Hays and A.L. Browne (Eds.), General Motors Research Laboratories, 1974.

7. Bernard, J.E., et al. Vehicle-In-Use Limit Performance and Tire Factors: The Tire In Use. Final Report, Contract No. DOT-HS-031-3-693, Highway Safety Res. Inst., Univ. of Michigan, Report No. UM-HSRI-PF-75-1, March 1975.

8. Noise and Traction Characteristics of Bias-Ply and Radial Tires for Heavy Duty Trucks. G.R. Thurman and W.A. Leasure, Jr. (Eds.), Final Report, Joint DOT/MVMA Study, October 1977.

9. Yeager, Robert W. "Tire Hydroplaning: Testing, Analysis, and Design." The Physics of Tire Traction: Theory and Experiment. D.F. Hays and A.L. Browne (Eds.), General Motors Research Laboratories, 1974.

10. Ervin, R.D. and Winkler, C.B. Braking Efficiency Test Technique. Final Report, Contract No. DOT-HS-031-3-765, Highway Safety Res. Inst., Univ. of Michigan, Report No. UM-HSRI-PF-74-13, December 1974.

11. Kelley, J.D. and Speyer, A.G. "Effect of Tire Construction Variables on Passenger Tire Wet Traction." Transportation Research Record 621, Transportation Research Board, 1977.

12. Dijks, A. "Influence of Tread Depth on Wet Skid Resistance of Tires." Transportation Research Record 621, Transportation Research Board, 1977.

13. Beaton, J.L. "Providing Skid Resistant Pavements." Transportation Research Record 622, Transportation Research Board, 1977.

14. Meades, J.K. The Effect of Tyre Construction on Braking Force Coefficients. Road Research Laboratory, Crowthorne, England, RRL Report No. LR-224, 1969.

15. DeVinney, W.E. "Factors Affecting Tire Traction." SAE Paper No. 670461, 1967.

16. Besse, Jean-Pierre. Water Film Thickness Effects on the Friction Between Tire and Pavement. Report No. S51, NCHRP Project 1-12(2) "Locked Wheel Pavement Skid Tester Correlation and Calibration Techniques," The Pennsylvania State University, June 1972.

17. Staughton, G.C. and Williams, T. Tyre Performance in Wet Surface Conditions. Road Research Laboratory, Crowthorne, England, RRL Report No. LR-355, 1970.

18. Kienle, R.N. "The Role of the Tread Pattern--A Blend of the Simple and Complex." The Physics of Tire Traction: Theory and Experiment. D.F. Hays and A.L. Browne (Eds.), General Motors Research Laboratories, 1974.

19. Veith, A.G. "Tire Wet Traction Performance: The Influence of Tread Pattern." Transportation Research Record 621, Transportation Research Board, 1977.

20. Peterson, R.F., Jr., Eckert, C.F., and Carr, C.I. "Tread Compound Effects in Tire Traction." The Physics of Tire Traction: Theory and Experiment. D.F. Hays and A.L. Browne (Eds.), General Motors Research Laboratories, 1974.

21. Fancher, P.S. and MacAdam, C.C. "Computer Analysis of Antilock System Performance in the Braking of Commercial Vehicles." Paper presented at a Conference on Braking of Road Vehicles, The Inst. of Mechanical Engineers, Loughborough, England, 1975.

22. Nordeen, D.L., Rasmussen, R.E., and Bidwell, J.B. Tire Properties Affecting Vehicle Ride and Handling. General Motors Technical Center, Engineering Publication 3759, July 1968.

23. Schuring, D.J. and Roland, R.D. "Radial Ply Tires—How Different Are They in the Low Lateral Acceleration Regime." SAE Paper No. 750404, February 1975.

24. Bidwell, J.B. "Car-Tire Relationships." Presented at Akron Rubber Group Winter Meeting, November 4, 1965.

25. Roland, R.D., Rice, Dell'Amico, F. The Influence of Tire Properties on Passenger Vehicle Handling. Vol. II, Technical Report, Final Report, Contract DOT-HS-053-3-727, Calspan Corp., Report No. ZM-5350-K-2, June 1974.

26. Nordstrom, O. and Formgren, C. Side Force Characteristics of Passenger Car Tyres. Difference Between Tyres of the Same Type and Manufacture, and Difference Between Tyres of Various Manufacture. The National Swedish Road and Traffic Research Institute, Stockholm, Report No. 8, 1972.

27. Peterson, K.G. and Rasmussen, R.E. "Mechanical Properties of Radial Tires." SAE Paper No. 730500, May 1973.

28. Roland, R.D. and Kunkel, D.T. The Influence of Tire Properties on Passenger Vehicle Handling. Vol. V, Measured Tire Performance Data. Final Report, Contract DOT-HS-053-3-727, Calspan Corp., Report No. ZM-5350-K-5, June 1974.

29. Nordeen, D.L. and Cortese, A.D. "Small Differences in Tire Properties = Large Differences in Vehicle Handling." SAE Journal 71(7), 1963, pp. 83-90.

30. Bundorf, R.T. and Leffert, R.L. The Cornering Compliance Concept for Description of Directional Control (Handling) Properties. General Motors Engineering Staff, #2771, 1971.

31. Milliken, W.F., Jr. High-Camber Tire Tests on Calspan Tire Research Facility. Calspan Technical Report, Buffalo, N.Y., November 1975.

32. Bartol, J.A., Livers, G.D., and Miennert, R. Requirements Analysis and Feasibility Studies for an Experimental Safety Motorcycle. AMF, Inc., Final Report, Contract DOT-HS-4-00816, July 1975.

33. Davisson, J.A. "Design and Application of Commercial Type Tires." Fifteenth L. Ray Buckendale Lecture, SAE No. SP-344, Society of Automotive Engineers, January 1969.

34. Leffert, R.L., Riede, P.M., and Rasmussen, R.E. "Understanding Tire Intermix Through the Cornering Compliance Concept." SAE Paper No. 741104, October 1974.

35. Dunlap, D.F. et al. Influence of Combined Highway Grade and Horizontal Alignment on Skidding. Final Report, NCHRP Project 1-14, Highway Safety Res. Inst., Univ. of Michigan, Report No. UM-HSRI-PF-74-1, September 1974.

36. Sakai, H., Kanaya, O., and Okayama, T. "The Effect of Hydroplaning on the Dynamic Characteristics of Car, Truck, and Bus Tires." SAE Paper No. 780195, Feb.-March 1978.

37. Holmes, K.E. and Stone, R.D. Tyre Forces as Functions of Cornering and Braking Slip on Wet Road Surfaces. Road Research Laboratory, Crowthorne, England, Report No. LR-254, 1969.

38. Gengenbach, W. "Experimentelle Untersuchung von Reifen auf nasser Fahrbahn (Experimental Investigation of Tires on a Wet Roadway, Part 3: Further Test Results)." Automobil-technische Zeitschrift, Vol. 70, No. 9, 1968, pp. 310-316.

39. Schuring, D.J., Tapia, G.A., and Gusakov, I. "Influence of Tire Design Parameters on Tire Force and Moment Characteristics." SAE Paper No. 760732, October 1976.

40. Kelly, J.D., Jr. "Factors Affecting Passenger Tire Traction on the Wet Road." SAE Paper No. 680138, 1968.

41. Segel, L. "Tire Traction on Dry, Uncontaminated Surfaces." The Physics of Tire Traction: Theory and Experiment, D.F. Hays and A.L. Browne (Eds.), General Motors Research Laboratories, 1974.

42. Bird, K.D. and Schuring, D.J. "Truck Tire Testing on TIRF." Proceedings of a Symposium on Commercial Vehicle Braking and Handling, Highway Safety Res. Inst., Univ. of Michigan, May 5-7, 1975, pp. 3-39.

43. Ervin, R. D., MacAdam, C.C., and Watanabe, Y. Motorcycle Braking Performance. Final Report, Contract DOT-HS-5-01264, Highway Safety Research Inst., Univ. of Michigan, Report No. UM-HSRI-76-30, December 1976.

44. Ervin, R.D., Campbell, J.D., Sayers, M., and Bunch, H. Improved Passenger Car Braking Performance. Final Report, Contract No. DOT-HS-6-01368, Highway Safety Res. Inst., Univ. of Michigan, Report No. UM-HSRI-78-12, March 1978.

45. Ervin, R.D., et al. Vehicle Handling Performance. Final Report, Contract No. DOT-HS-031-1-159, Highway Safety Res. Institute, Univ. of Michigan, November 1972.

46. Rice, R.S. and Davis, J.A. Vehicle Directional Control During Braking-in-a-Turn. Final Report, Contract No. DOT-HS-4-00971, July 1975.

47. Bekker, M.G. Theory of Land Locomotion. The Mechanics of Vehicle Mobility. University of Michigan Press, Ann Arbor, 1956.

48. Czako, T.F. "The Influence of the Inflation Pressure on Cross-Country Performance." Journal of Terramechanics, Vol. 11, Nos. 3 & 4, 1974.

49. Sohne, W. "Agricultural Engineering and Terramechanics." Journal of Terramechanics, Vol. 6, No. 4, 1969.

50. Kraft, D.C. "Flotation Performance of Aircraft Tires on Soil Runways." Journal of Terramechanics, Vol. 6, No. 2, 1969.

51. Browne, A.L. "Tire Traction on Snow-Covered Pavements." The Physics of Tire Traction: Theory and Experiment. D.H. Hays and A.L. Browne (Eds.), General Motors Research Laboratories, 1974.

52. Murphy R.W. A Procedure for Evaluating Vehicle Braking Performance. Final Report, Contract No. DOT-HS-031-051, Highway Safety Res. Inst., Univ. of Michigan, October 1971.